

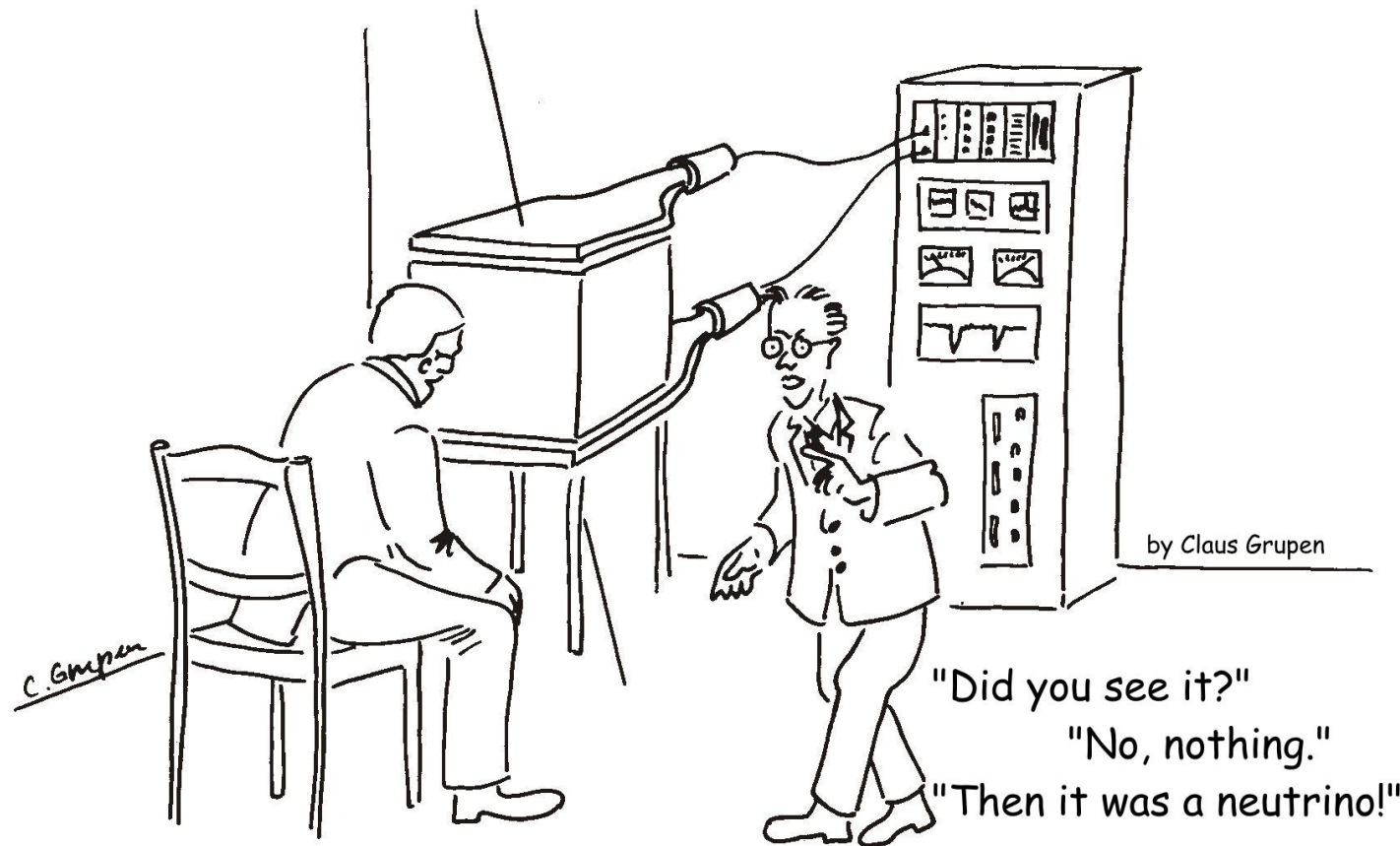
FIFTH CERN-FERMILAB HADRON COLLIDER PHYSICS SUMMER SCHOOL

August 16-27, 2010

PARTICLE IDENTIFICATION OLAV ULLALAND (CERN)

Mainly nuts and bolts
and how they could fit
together.

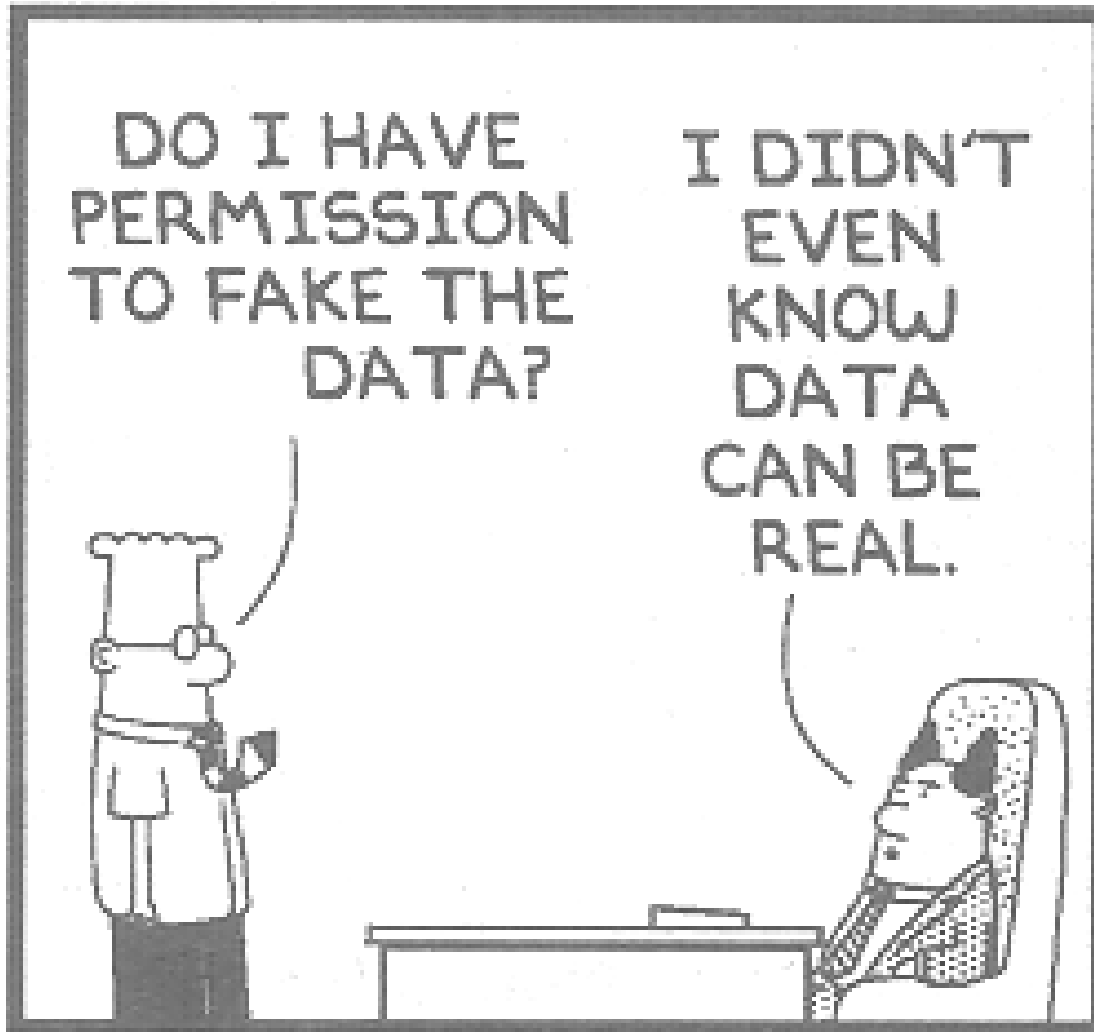




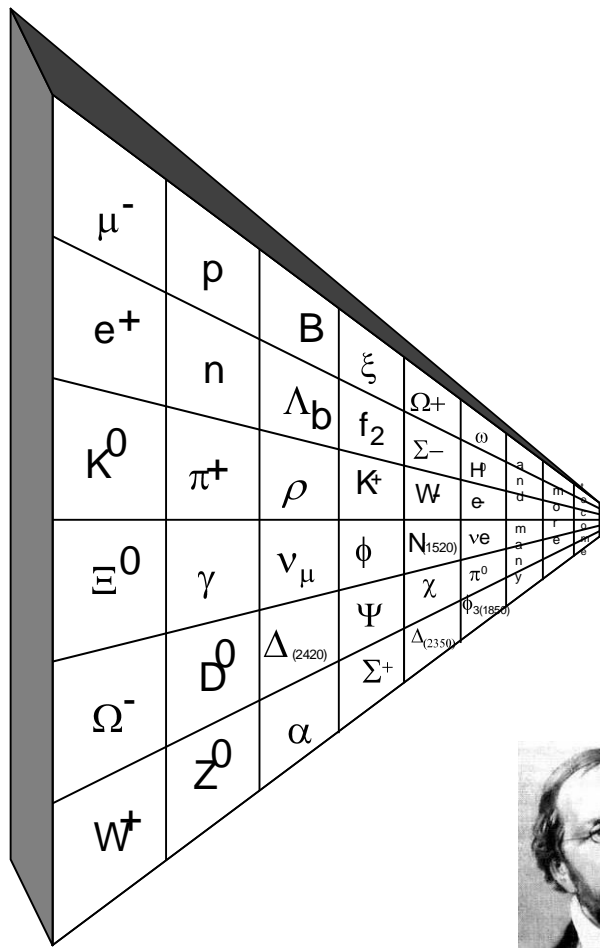
We will focus on charged particle identification as the detection and identification of neutral particles is covered in the **Calorimeter** lectures by **Jane Nachtman**. For particle **Tracking** see lecture of **Michael Hildreth** and **Statistics and Systematics** was given by **Roger Barlow**.

References and acknowledgements are normally given whenever appropriate.

8-11-10 ©2010 Scott Adams, Inc./Dist. by UFS, Inc.



We will also have a look at where the real data is coming from and why.



We will not be concerned by all the charged particles which are around.
We will just concentrate on those which have a lifetime long enough for us to observe them.
That is:

$e, \mu, \pi, K, p.$

Main topics: _____

- Time-of-Flight
- Cherenkov
- Transition radiation
- and a little
 - Muon
 - dE/dX



The Pigeon Hole Principle.

If you have fewer pigeon holes than pigeons and you put every pigeon in a pigeon hole, then there must result at least one pigeon hole with more than one pigeon.

It is surprising how useful this can be as a proof strategy.

First stated in 1834 by **Peter Dirichlet** (1805-1859)

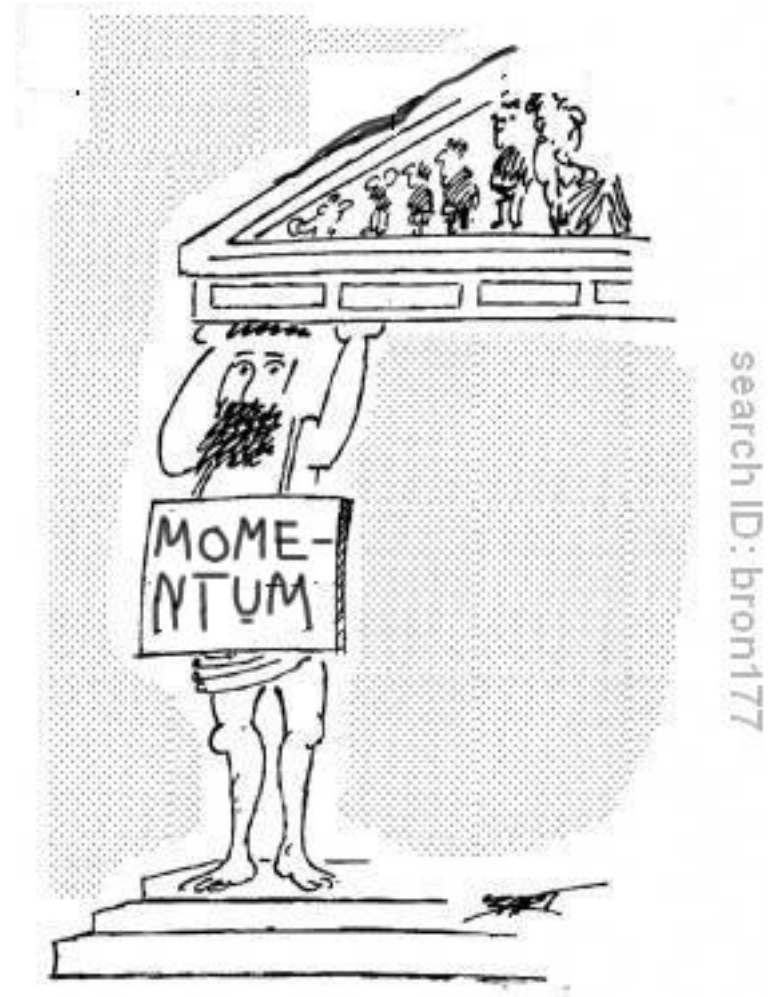
He got instant fame, not for this, but since his first publication concerned the famous Fermat's Last Theorem. The theorem claimed that for $n > 2$ there are no non-zero integers x, y, z such that $x^n + y^n = z^n$.

J J O'Connor and E F Robertson

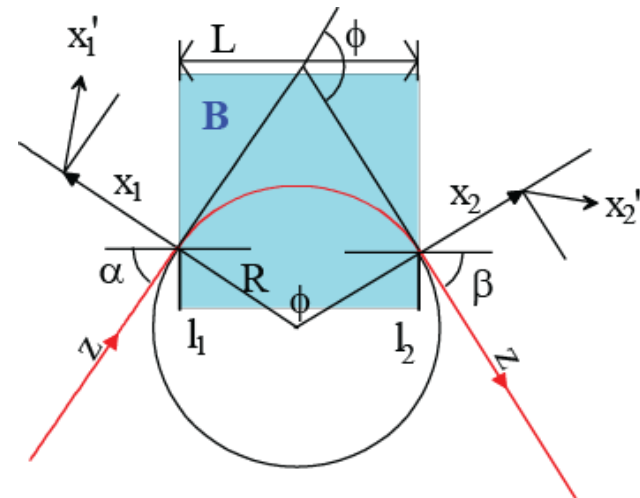
Particle Identification Detectors are normally not stand-alone detectors.

As a rule, they require that the momentum of the particle is measured by other means.

And - of course - by measuring the momentum, the track is defined.



search ID: bron177

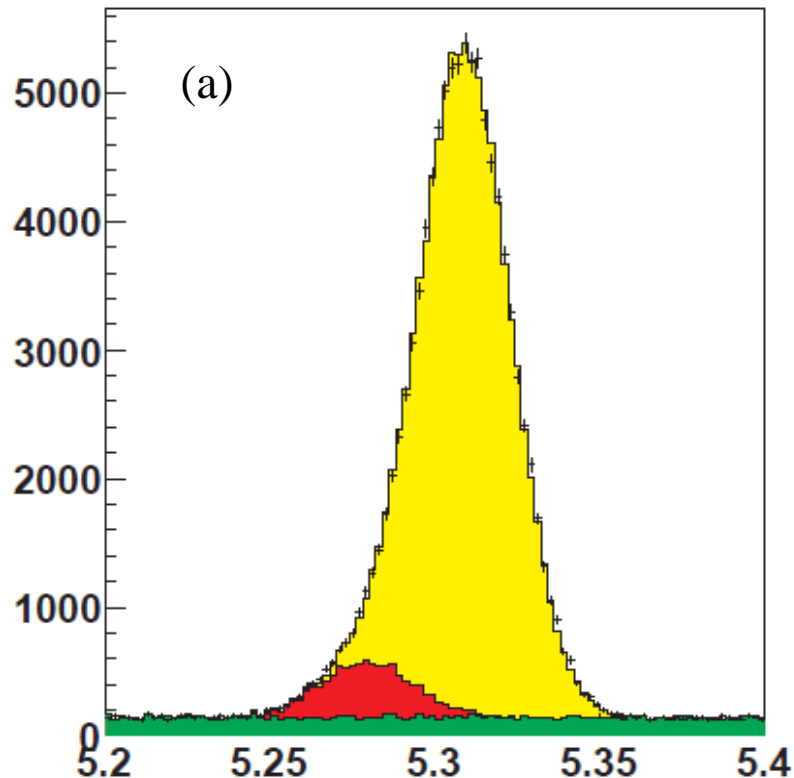


"Other means" is usually called a magnet and if:

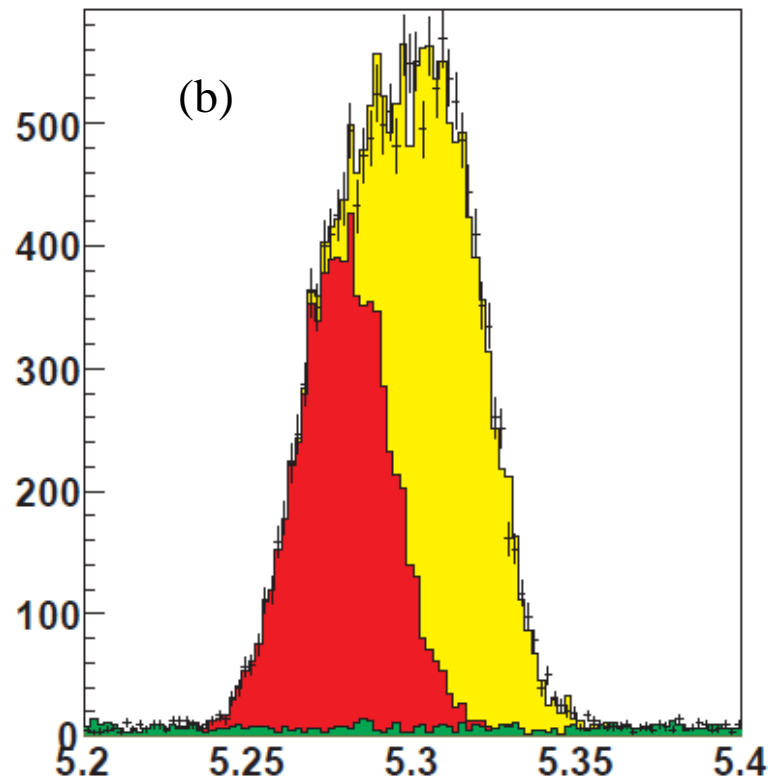
$$\alpha = \beta \text{ then } \phi \cong 0.03 \frac{BL}{p} \frac{\text{kG m}}{\text{GeV}/c}$$

Why bother? _____

**No
Particle Identification**



**With
Particle Identification**



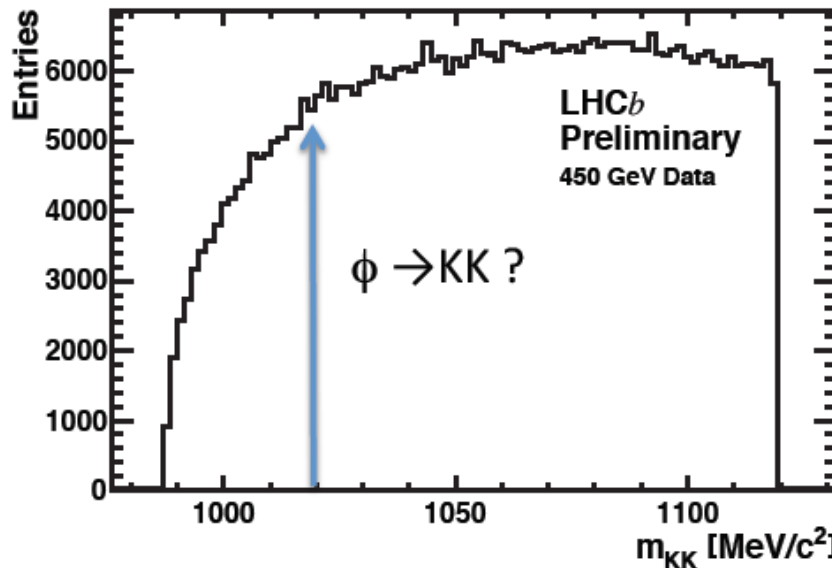
The invariant mass spectrum in units of GeV/c for selected $B \rightarrow D^0 K$ candidates, (a) before and (b) after information from the RICH detectors is introduced.

Genuine $B \rightarrow D^0 K$ candidates are shown in red while misidentified $B \rightarrow D^0 \pi$ candidates are shown in yellow. Combinatoric events are shown in green.

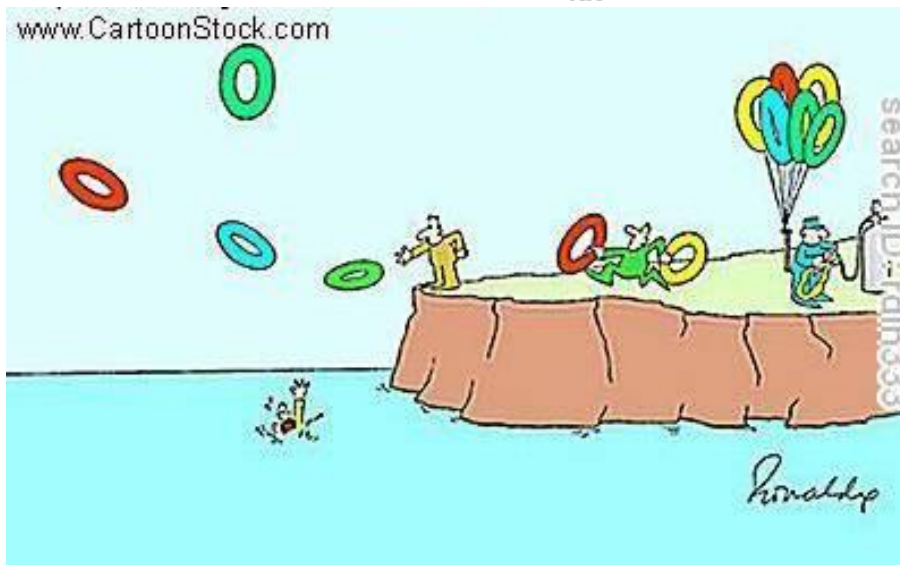
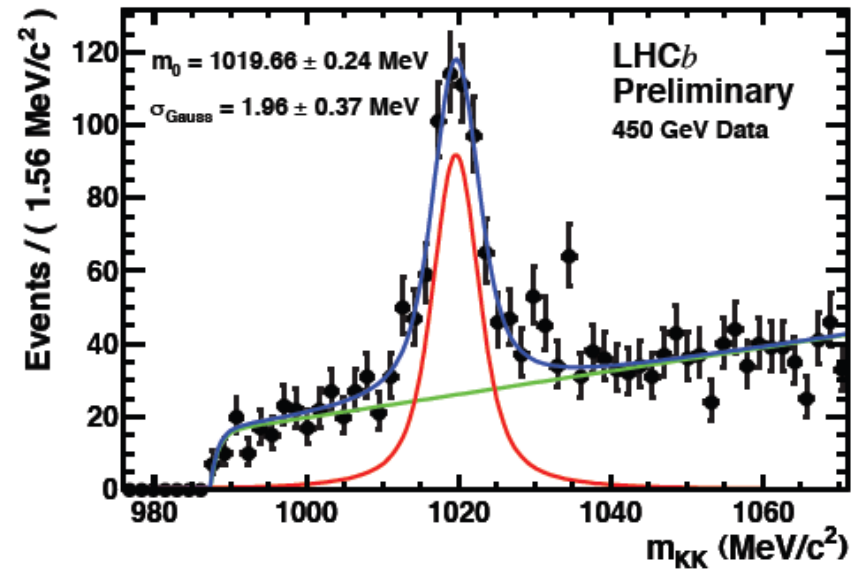
PID,

or the physics signal could be drowned in combinatory background.

No Particle Identification

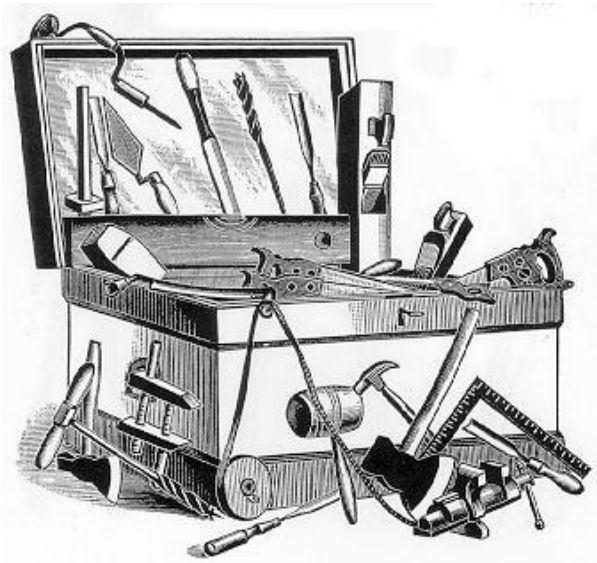


With Particle Identification



But the right tool might
be required.

The tools.



Cherenkov radiation: Prompt signal, measure photon emission angle, calculate β .

Detector: photon detector 150 to 1000 nm.

Transition radiation: Prompt signal, measure photon energy, calculate γ .

Detector: (normally) X-ray >1 keV

Time-of-Flight: measure time and flight path, calculate β .

Detector: Any detector that can detect charged particles.

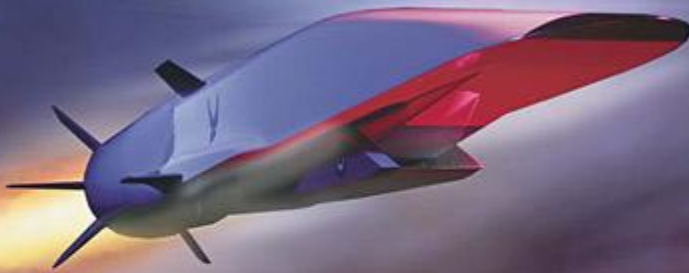
dE/dX: measure (small) energy deposit

Detector: Any detector that can detect charged particles.

Muon: measure whatever survives in the muon filter.

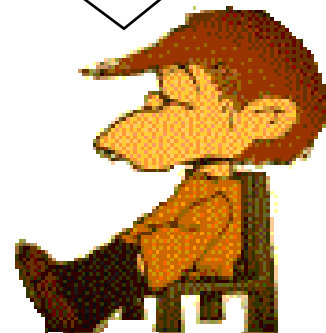
Detector: Any detector that can detect charged particles.

Particle Identification by **Time of Flight** measurement.



Scramjet Missile Sets Record for Mach 5 Flight Time

Awesome! maybe



With Time-of-Flight to Nobel Prize.

VOLUME 33, NUMBER 23

PHYSICAL REVIEW LETTERS

2 DECEMBER 1974

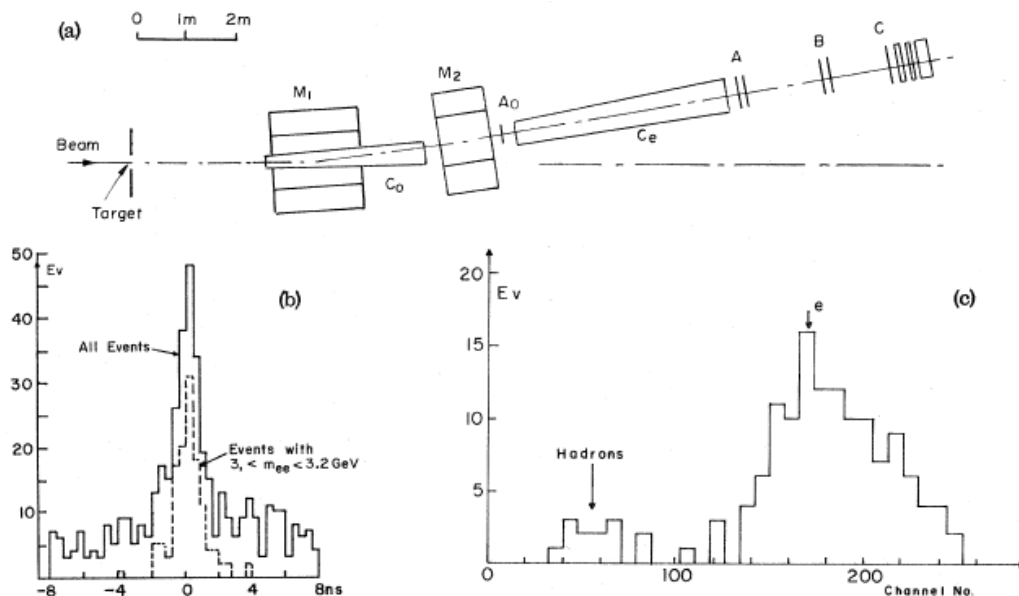


Fig. 1. (a) Simplified side view of one of the spectrometer arms. (b) Time-of-flight spectrum of e^+e^- pairs and of those events with $3.0 < m < 3.2 \text{ GeV}$. (c) Pulse-height spectrum of e^- (same for e^+) of the e^+e^- pair.

During the experiment, the time-of-flight of each of the hodoscopes and the Čerenkov counters, the pulse heights of the Čerenkov counters and of the lead-glass and shower counters, the single rates of all the counters together with the wire chamber signals, were recorded and continuously displayed on a storage/display scope.

Nobel Lecture, 11 December, 1976

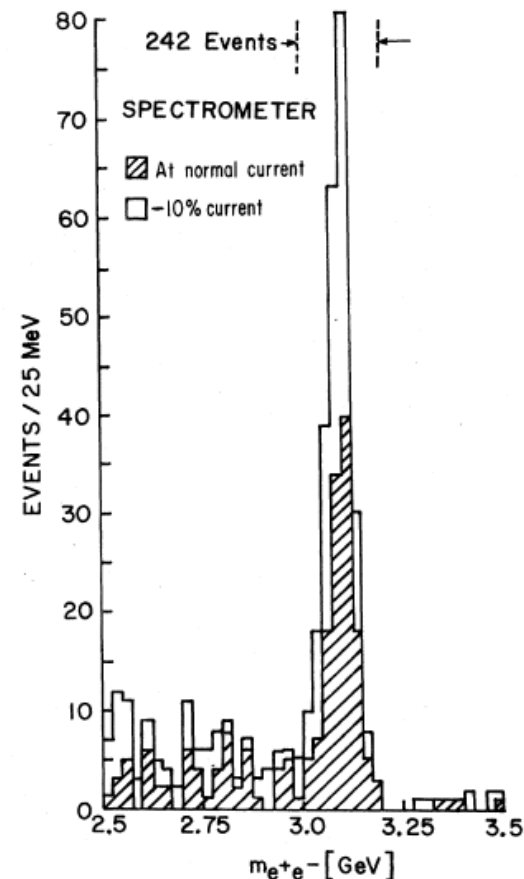
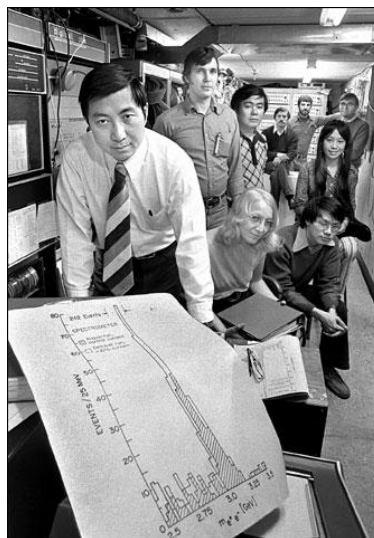
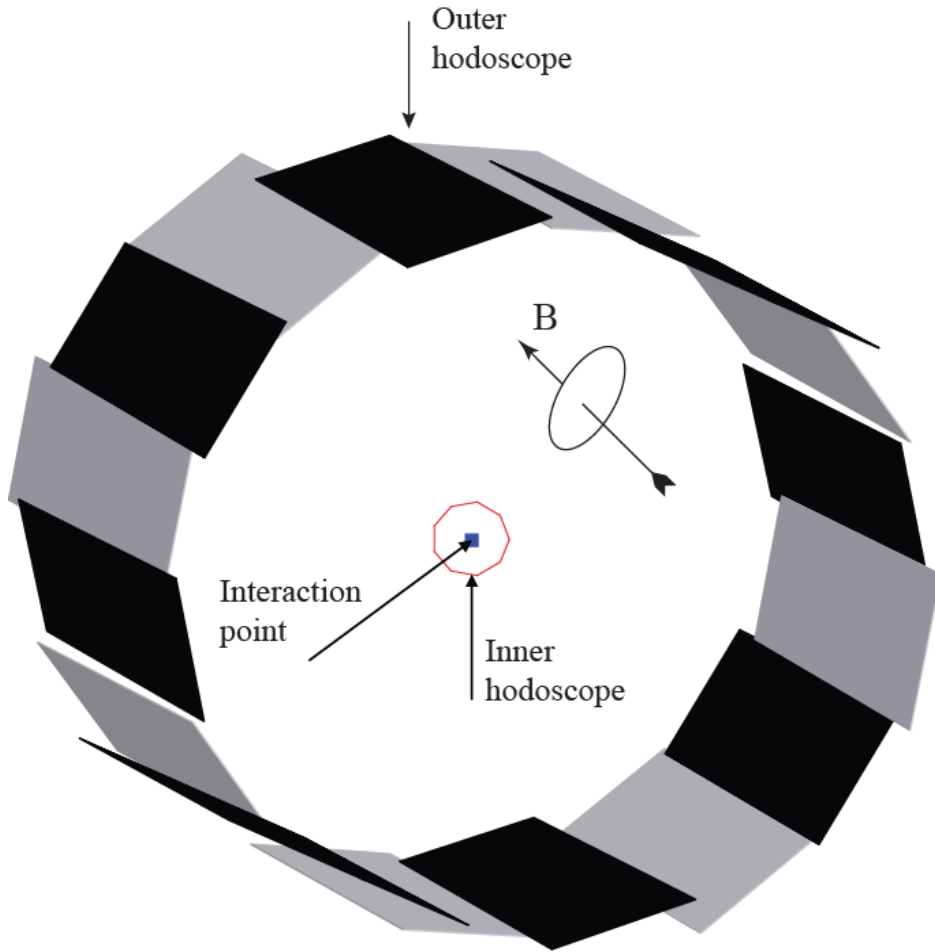


FIG. 2. Mass spectrum showing the existence of J . Results from two spectrometer settings are plotted showing that the peak is independent of spectrometer currents. The run at reduced current was taken two months later than the normal run.

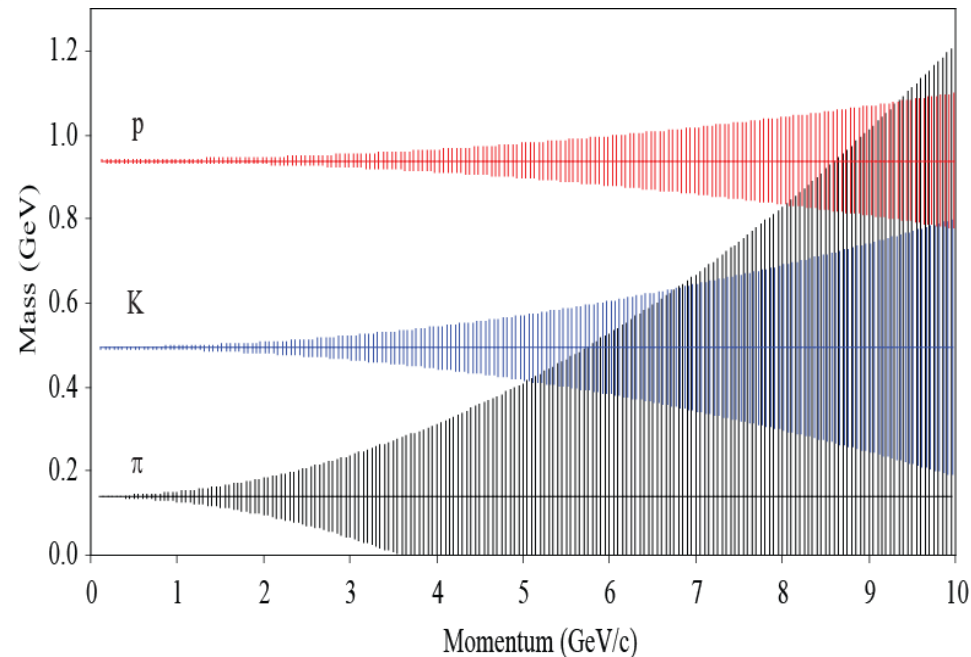
Time-of-Flight Measurements. _____



$$m_i^2 = \frac{p_i^2}{l^2} [t_i - l][t_i + l]$$

$$\left(\frac{\Delta m}{m}\right)^2 = \left(\frac{\Delta p}{p}\right)^2 + \gamma^4 \left[\left(\frac{\Delta t}{t}\right)^2 + \left(\frac{\Delta l}{l}\right)^2 \right]$$

$\Delta p/p = 4 \cdot 10^{-3}$
 $l = 10\text{m}, \Delta l/l = 10^{-4}$
 $\Delta t = 50\text{ps}.$
 The bars are 1σ .



When considering how many σ 's are required, it can be helpful to remember that (almost) all secondary particles are π (and have a momentum around 2 GeV/c) and then we have to dig out something interesting with a K or a p. Or - not confusing the π -issue with whatever the K or p is doing in the data set.

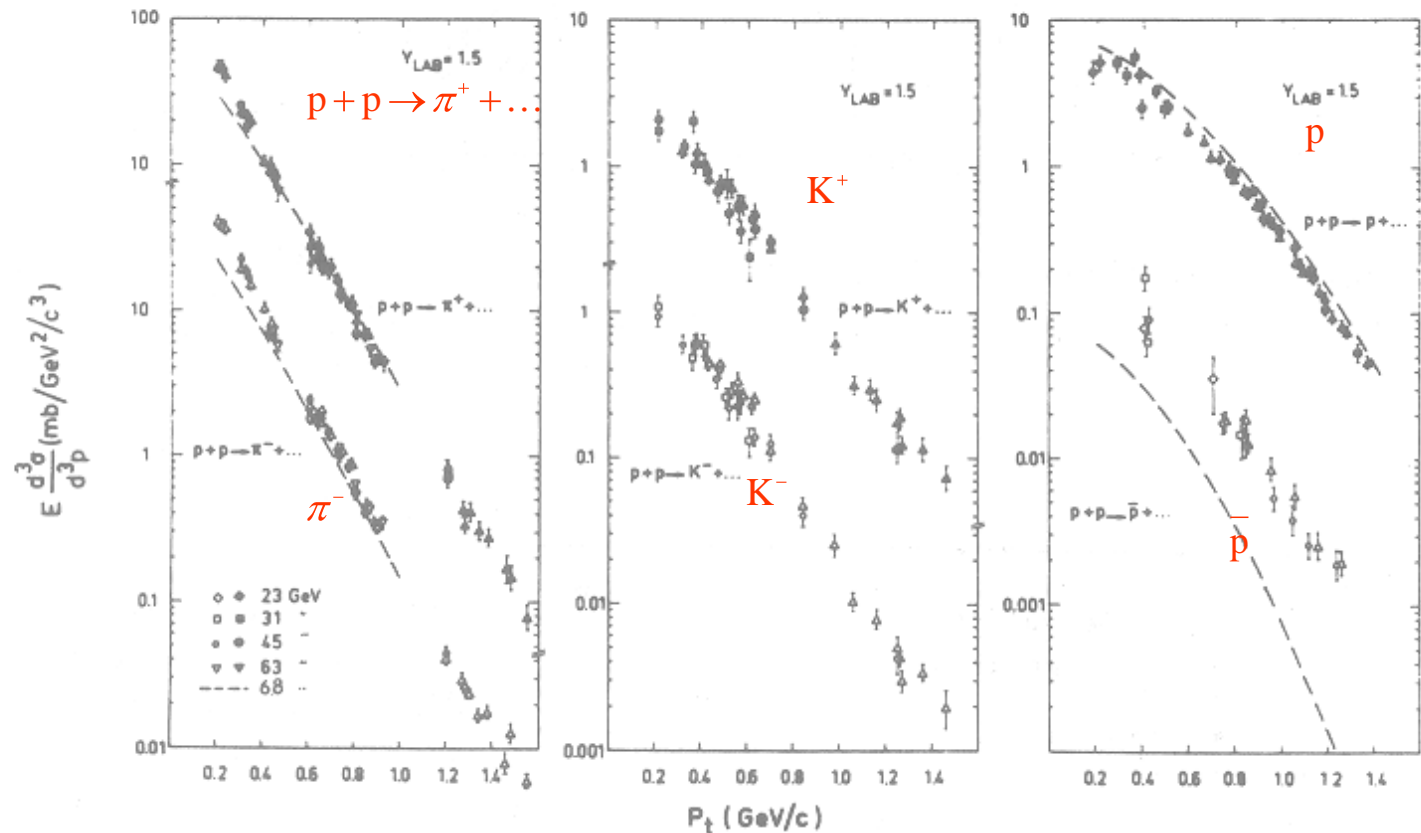


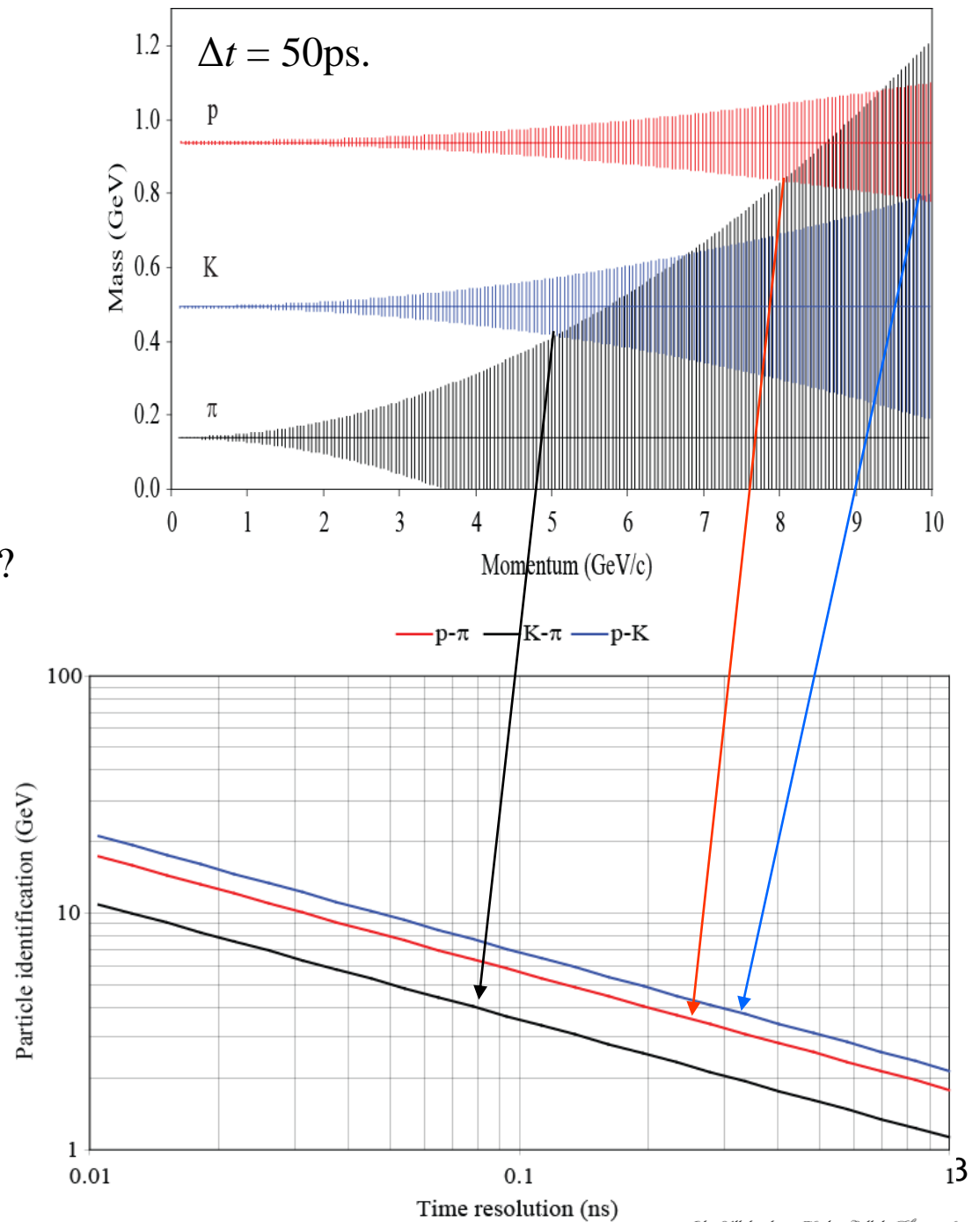
Fig. 8 - The invariant cross sections for π^+ , π^- , K^+ , K^- , p and \bar{p} production plotted versus P_t at $Y_{LAB} = 1.5$.

Assuming a spectrometer with the following characteristics:

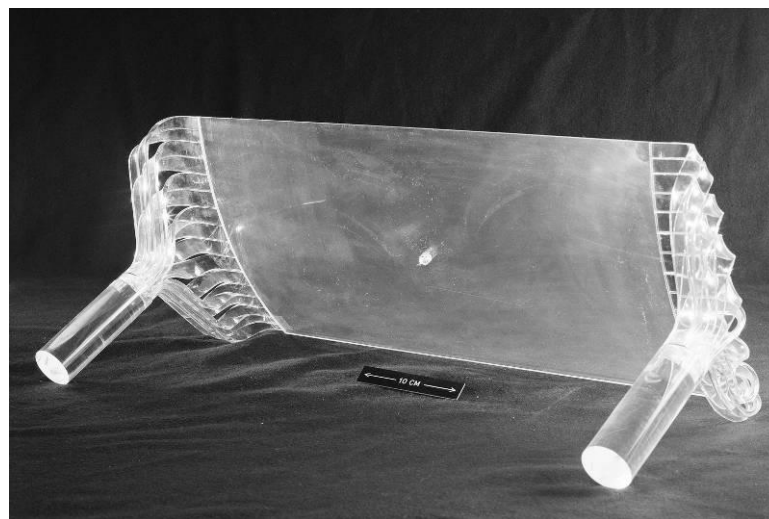
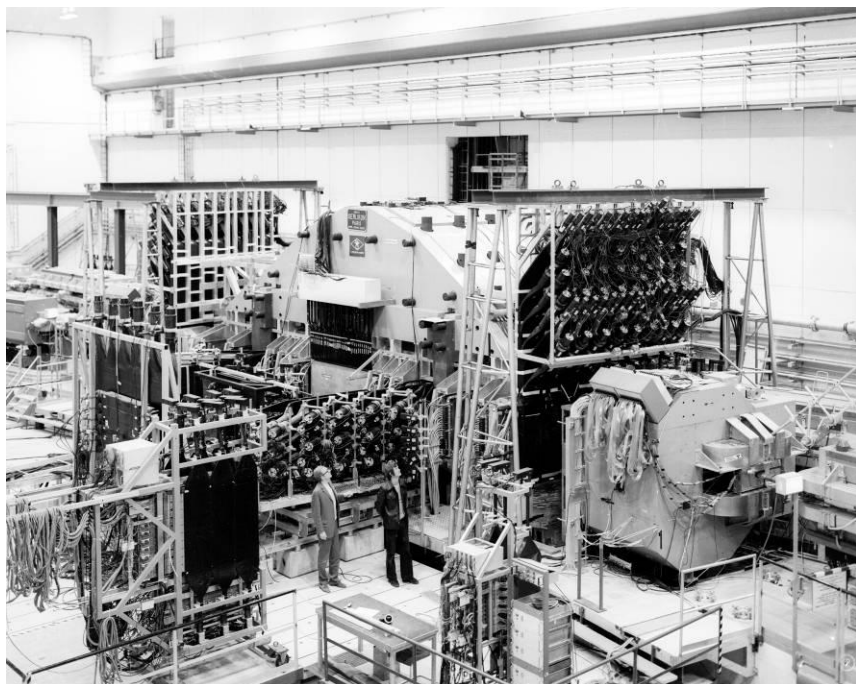
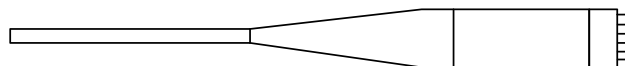
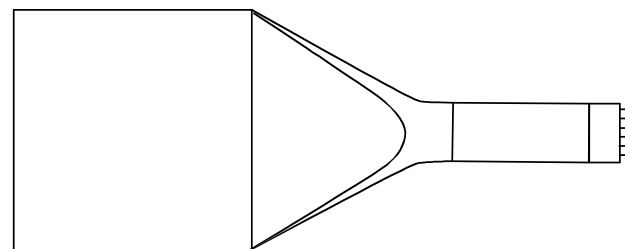
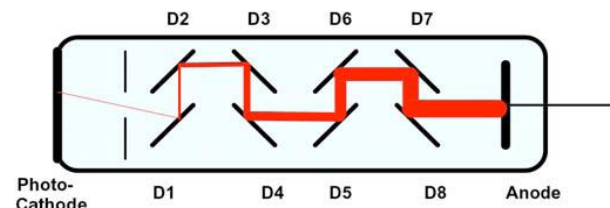
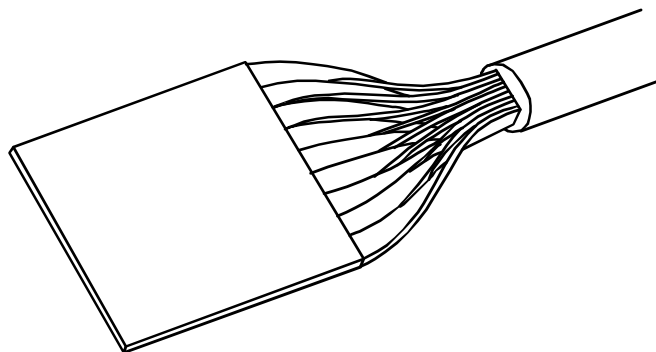
$$\Delta p/p = 4 \cdot 10^{-3}$$

$$l = 10\text{m}, \Delta l/l = 10^{-4}$$

What time resolution is required to do a particle identification up to X GeV/c?



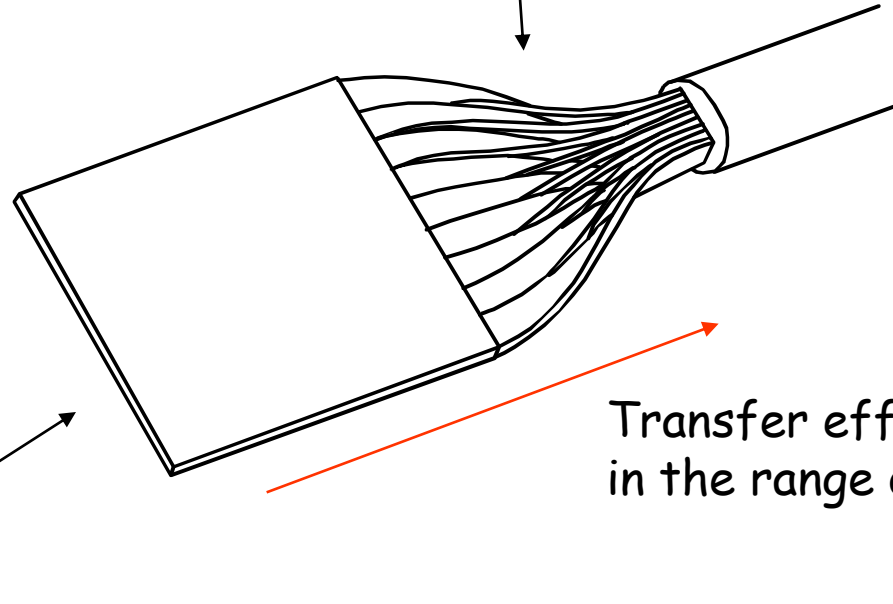
Have a closer look at the old workhorse.



Winston Cone is a nonimaging off-axis parabola of revolution which will maximise the collection of incoming rays.

(This is not a Winston cone).

Transient time spread is in the range of 1 ns. Read-out in both ends. After pulses.



Transfer efficiency in the range of 2×10^{-3}

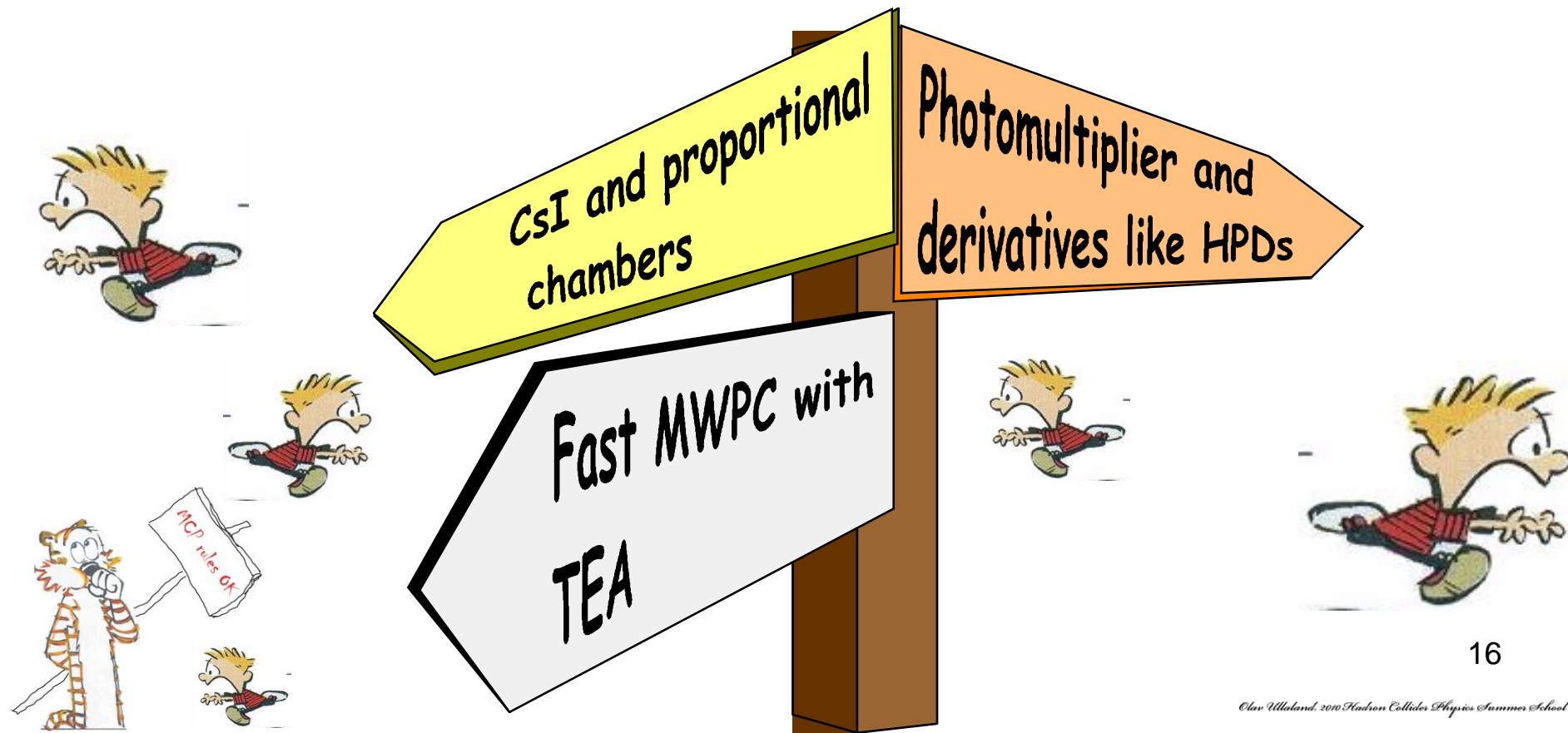
dE/dx_{\min} for a plastic scintillator is about $2 \text{ MeV cm}^2/\text{g}$, or about $2 \cdot 10^4$ photons/cm. This number of photons will be greatly reduced due to:
the attenuation length of the material,
the losses out from the material.



the rule of thumb

Time resolution of the order of 50 ps is reported (for reasonable large detectors).

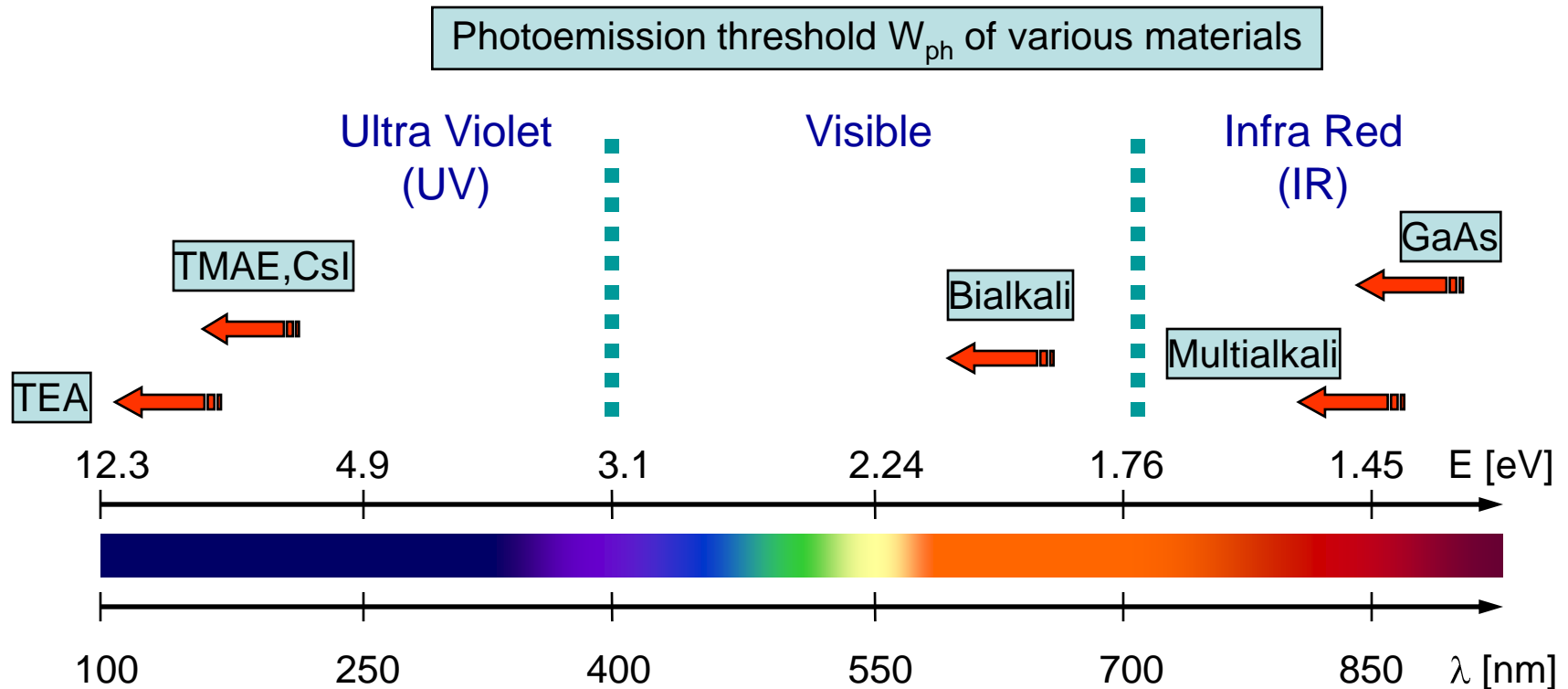
The choice of photon detector.



Photon detectors

Main types of photon detectors:

- gas-based
- vacuum-based
- solid-state
- hybrid



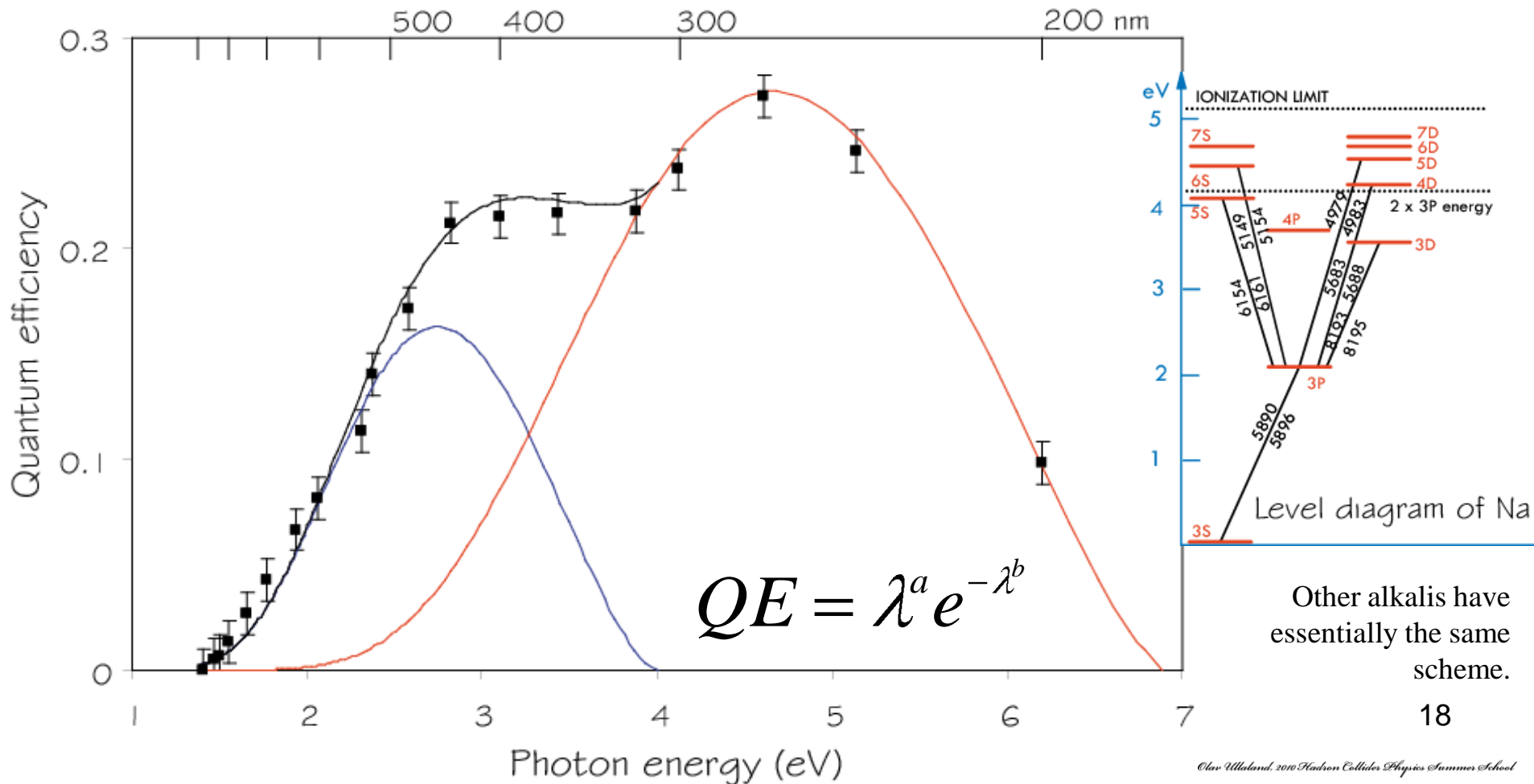
S-20 (Sb-Na₂-K-Cs) tri-alkaline photo cathode with quartz window.

Ionisation potential

Alkali		bi-alkali	
Cs	3.894 eV	Sb	8.64
K	4.341		
Na	5.139		

Photo-electric work function

Cs	2.1 eV
K	2.3
Na	2.8
Sb	4.8



How to know when the signal was there.
Time slewing and other evil things.

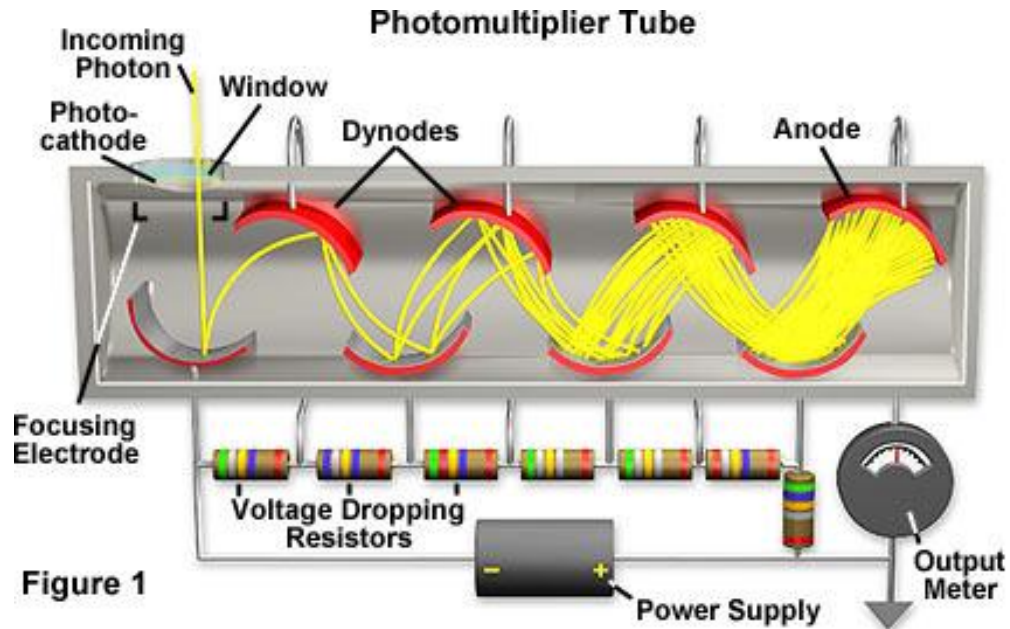
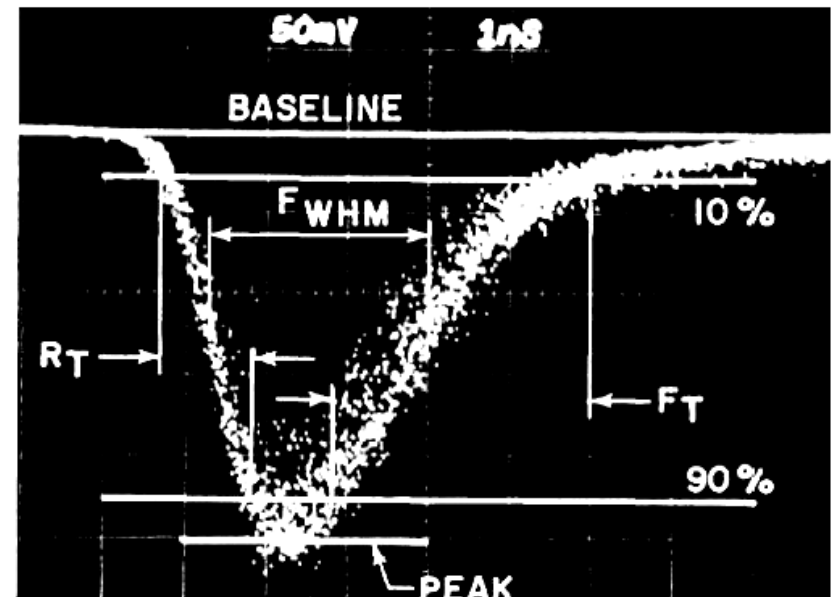
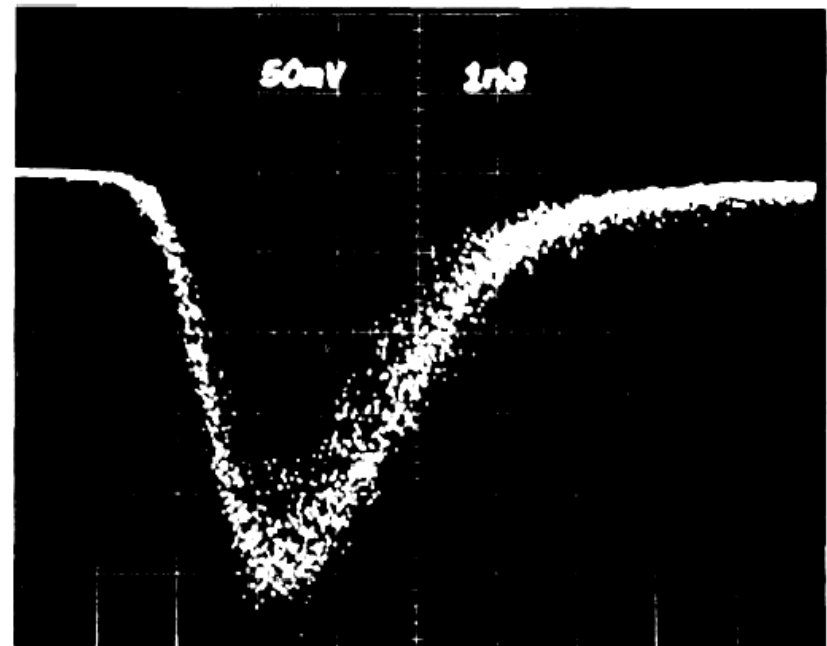
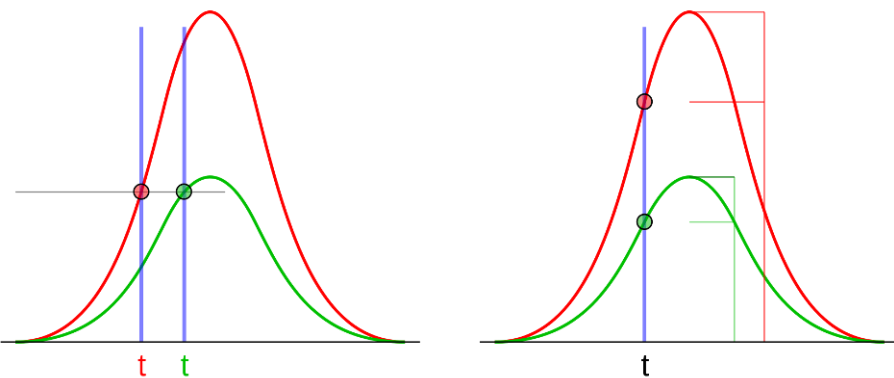


Figure 1

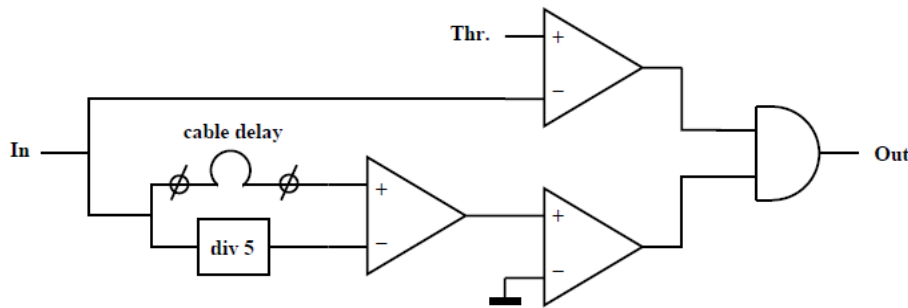


Thanks to Hamamatsu and Burle.



Comparison of threshold triggering (left) and constant fraction triggering (right)

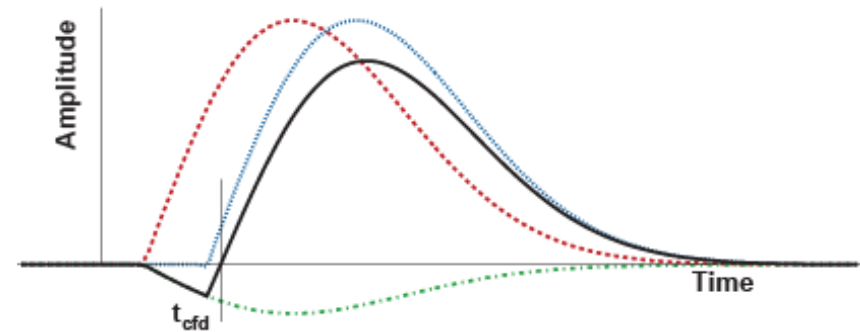
http://en.wikipedia.org/wiki/Constant_fraction_discriminator



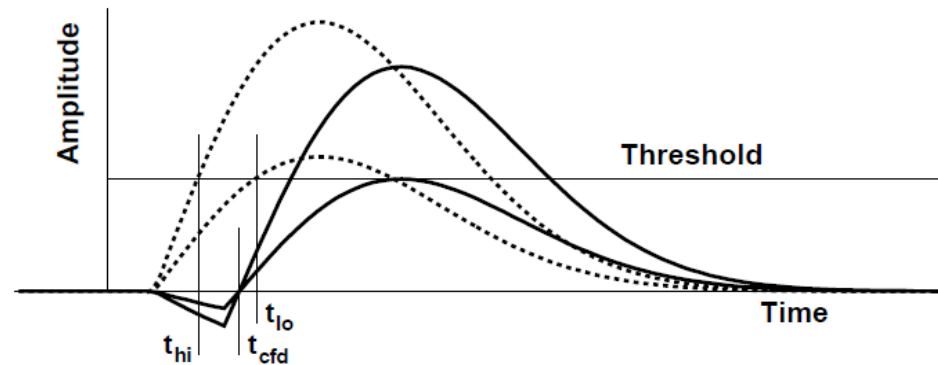
Basic functional diagram of a constant fraction discriminator.

Martin Gerardus van Beuzekom, Identifying fast hadrons with silicon detectors (2006) Dissertaties - Rijksuniversiteit Groningen
See also:
Wolfgang Becker, Advanced time-correlated single photon counting techniques, Springer Berlin Heidelberg (January 14, 2010)

Constant Fraction Discriminator.



Operation of the cfd. The input pulse (**dashed curve**) is delayed (**dotted**) and added to an attenuated inverted pulse (**dash-dot**) yielding a bipolar pulse (**solid curve**). The output of the cfd fires when the bipolar pulse changes polarity which is indicated by time t_{cfd} .



The moment at which the threshold discriminator fires depends on the amplitude of the pulse. If the cable delay of the cfd is too short, the cfd fires too early (t_{cfd}). For small input pulses, the timing is determined by the threshold discriminator and not by the cfd part.

Corrections for time slewing can also be done by measuring the apparent charge of the signal.

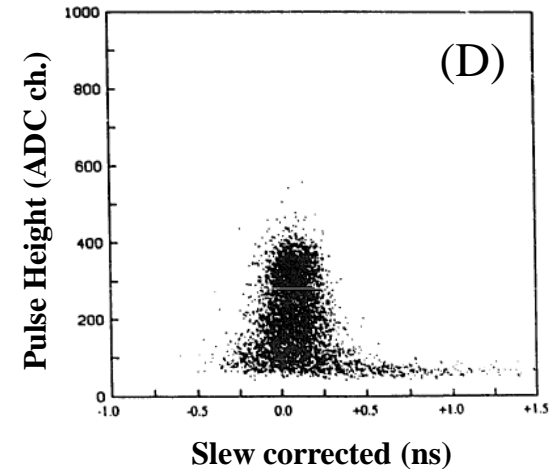
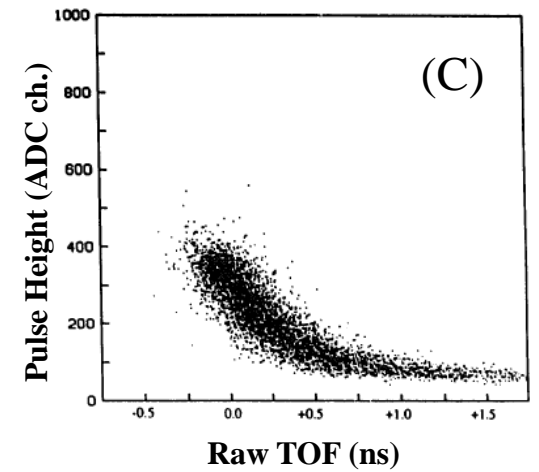
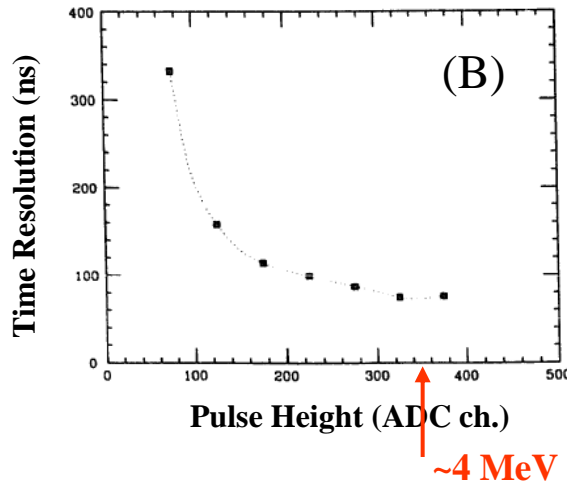
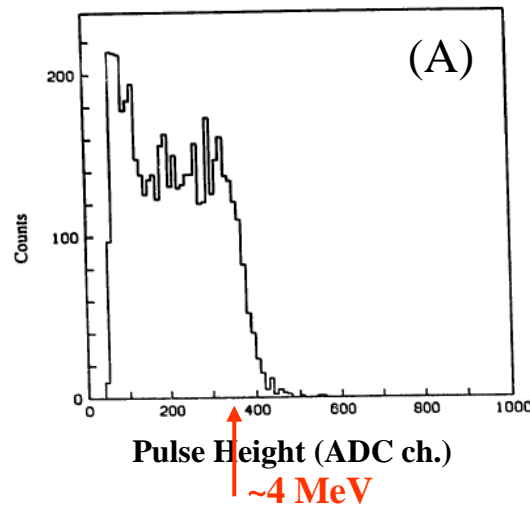
Slew-correction time, t_{cor} , is defined as:

$$t_{cor} = t + \frac{A_0}{\sqrt{ADC}}$$

where the constant A_0 is normally evaluated for each PMT and ADC is the signal pulse height.

→ σ : 55 ps

In a similar approach, Time-over-Threshold (ToT), can be used for time slewing correction.



(A) Pulse height distribution of one PM.

(B) Rms time resolution as a function of pulse height . ADC channel 350 corresponds to an energy deposit of about 4 MeV.

(C) Scatter plot of TOF(T-S1) and pulse height before slew correction.

(D) Scatter plot of TOF(T-S1) and pulse height after slew correction.

The **clock** issue.

It is challenging to issue a high frequency clock to a large distributed system without falling into traps of slewing, power requirements, length of strips across the cell

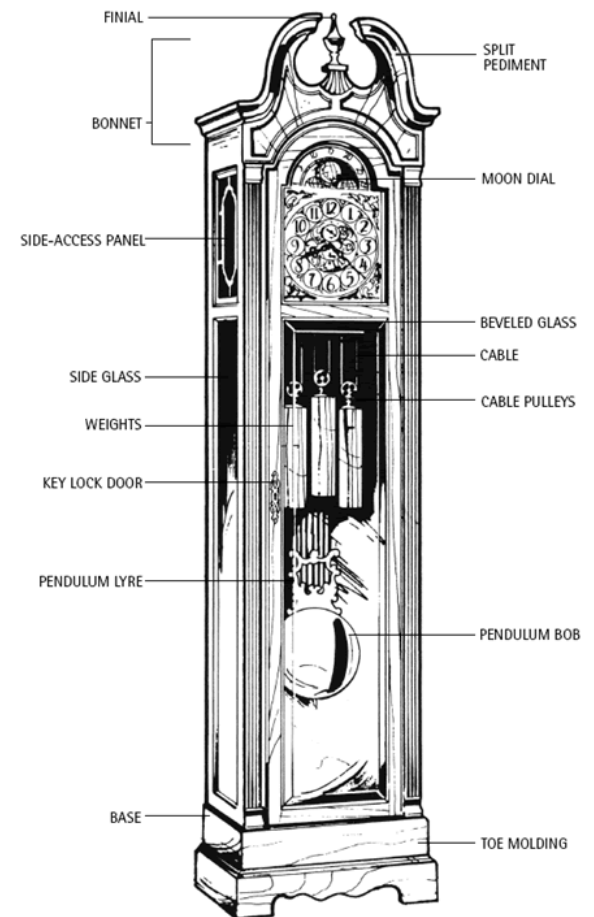


We will use the proposed NA62 experiment at CERN as an example.

For more information see:

<http://na62.web.cern.ch/NA62/>

http://na62.web.cern.ch/NA62/Documents/Chapter_3-3_GTK_V1.4.3.pdf

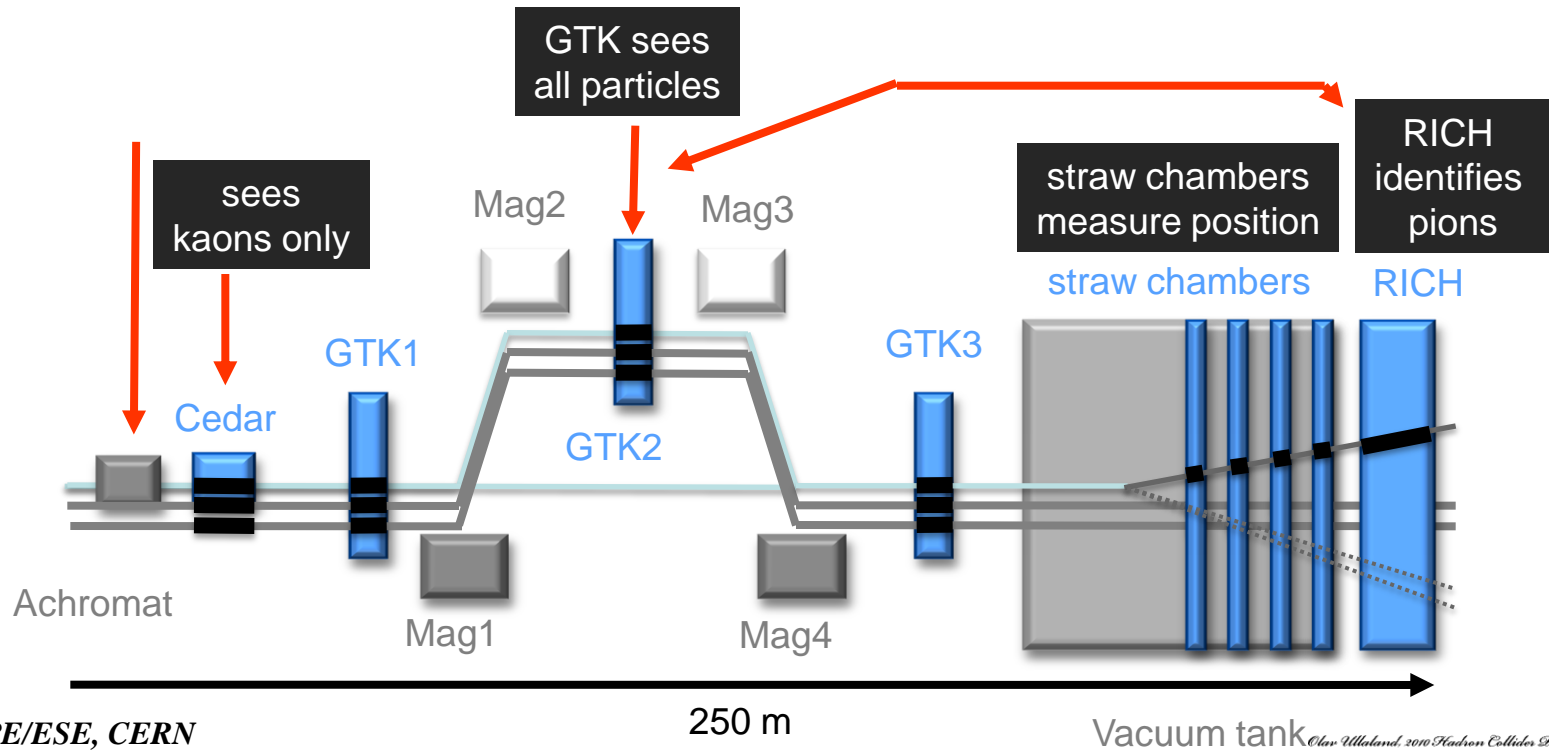


The aim of NA62:

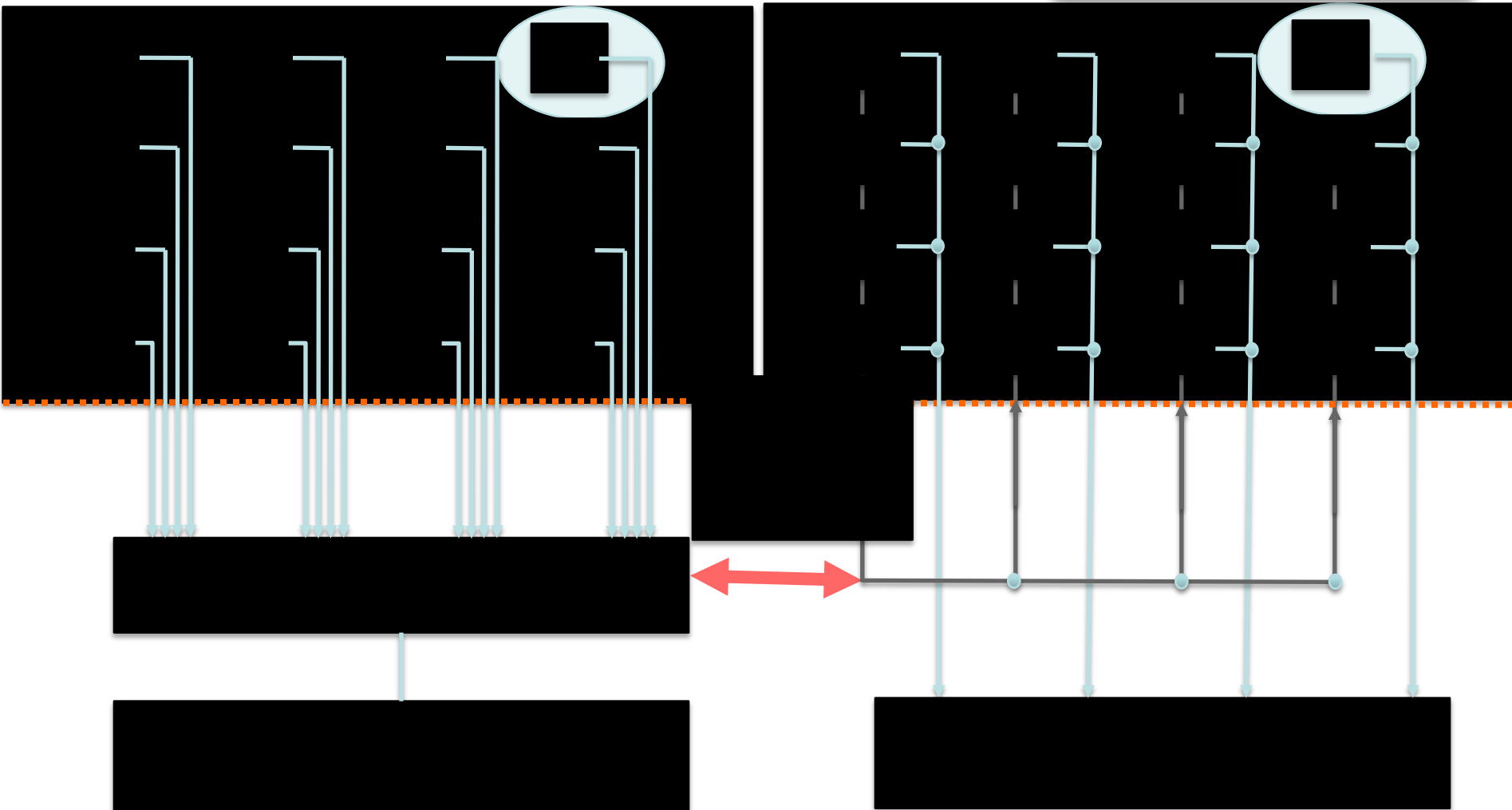
$$K^+ \rightarrow \pi^+ \nu \bar{\nu}$$

to extract a 10%
measurement of
the CKM parameter $|V_{td}|$.

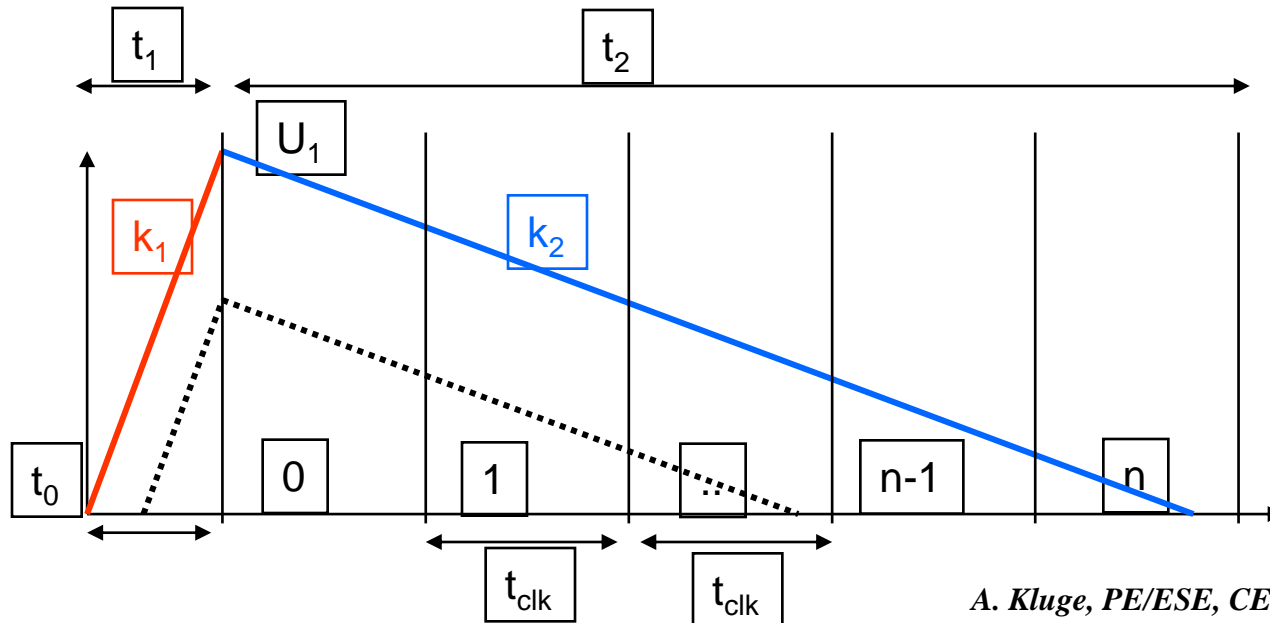
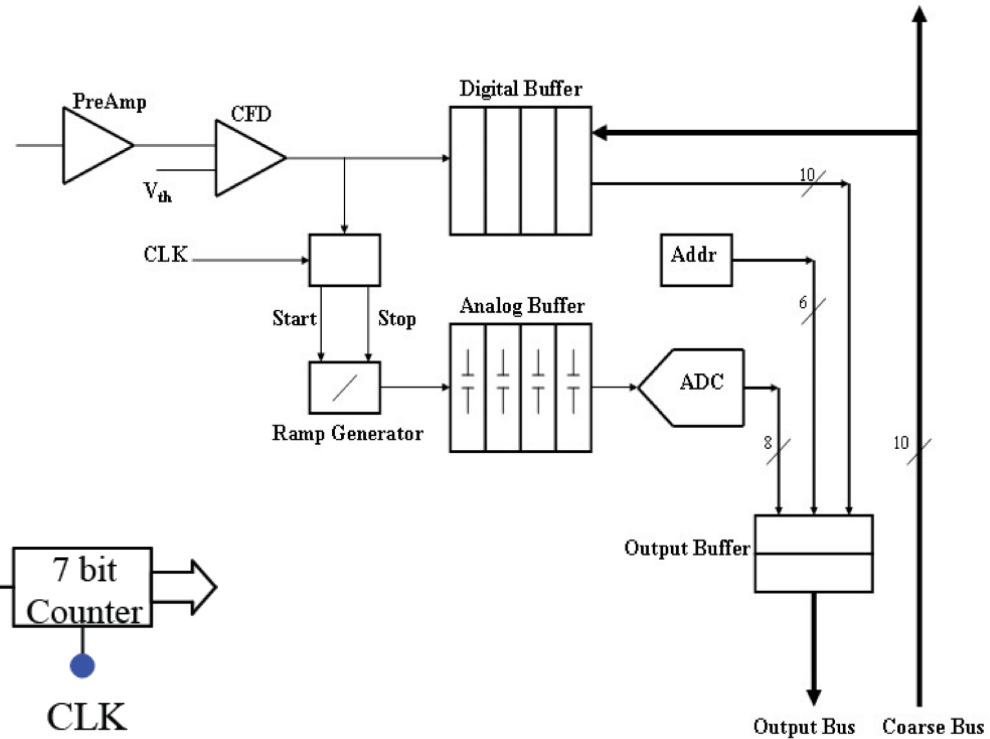
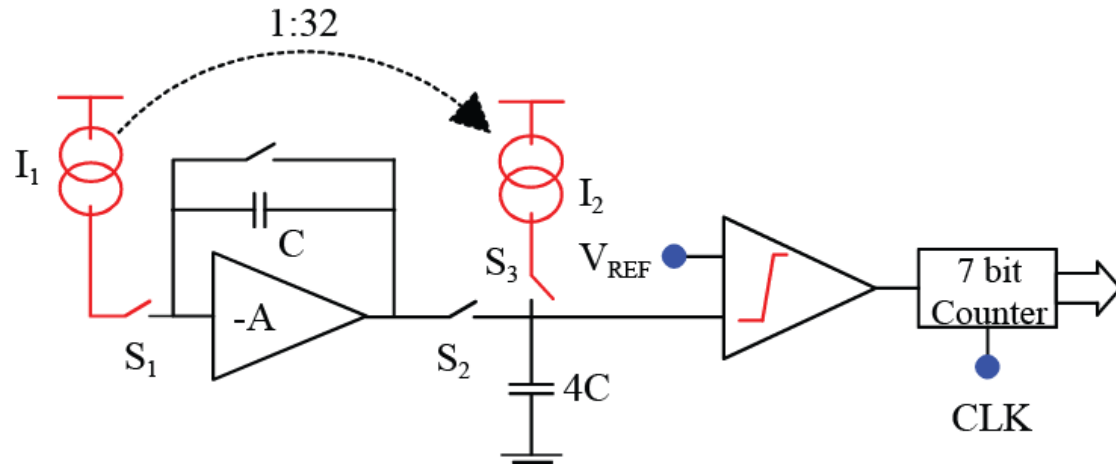
beam: hadrons, only 6% kaons	0.06
only 20% of charged kaon decay in the vacuum tank	0.20
out of which only 10^{-11} decays are of interest	10^{-11}
decay into one pion, one neutrino and one anti-neutrino	
total probability	1.2×10^{-13}



amplifier
discriminator/
time-walk-
compensator
buffering
TDC



Wilkinson Time to Digital Converter (dual slope)

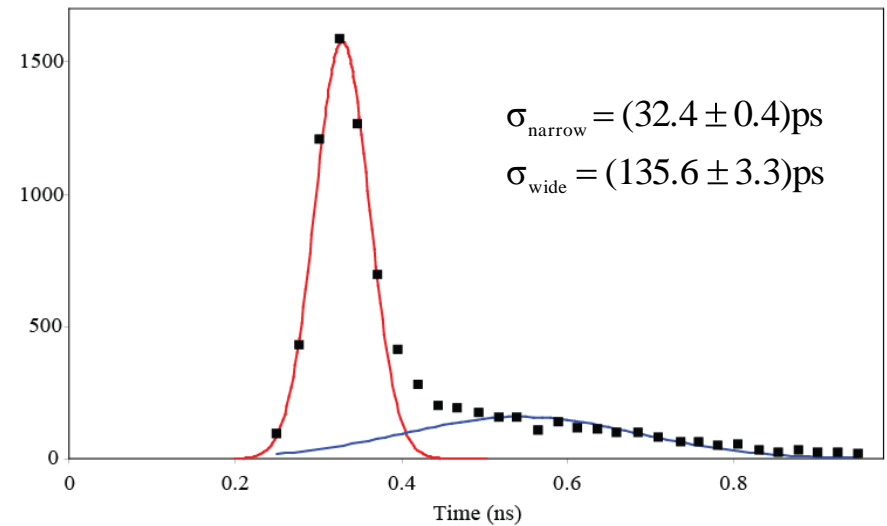
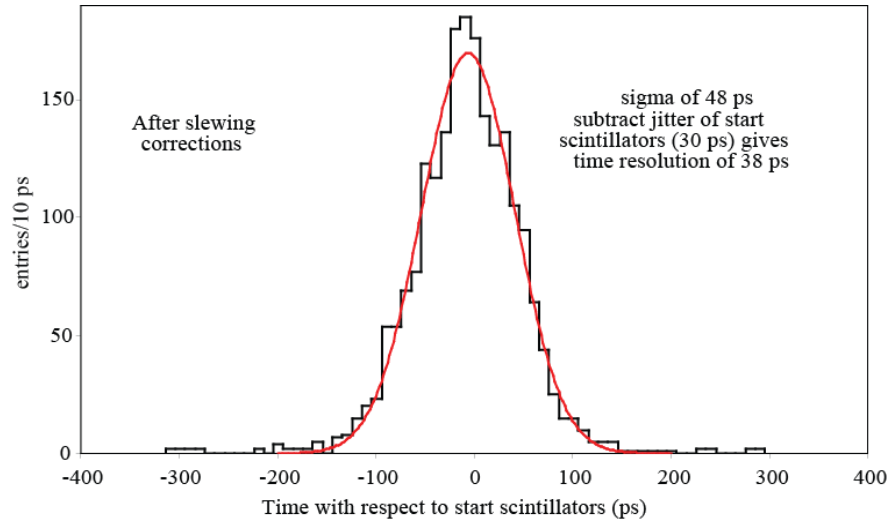
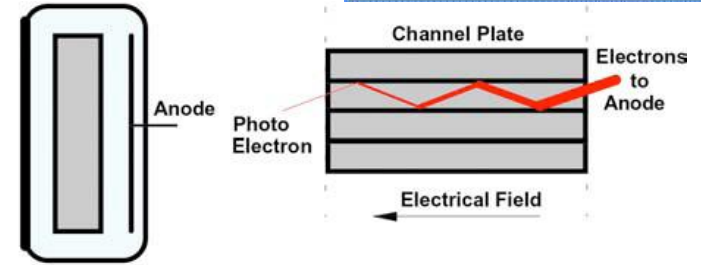
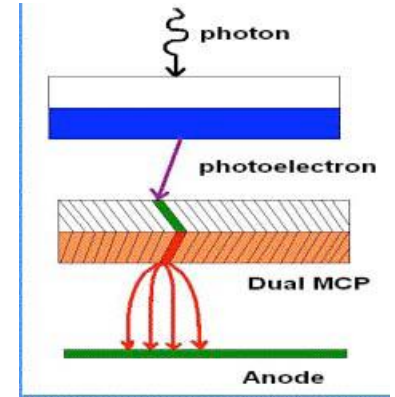
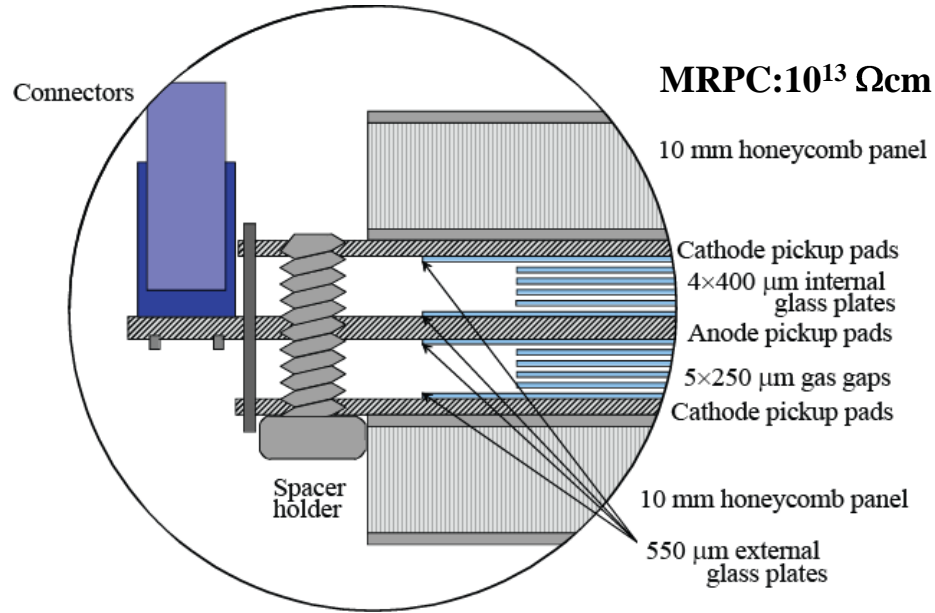


and then:

$$t_0 = n \cdot t_{clk} \cdot \frac{k_2}{k_1}$$

Related solutions with Delay Locked Loop and Phase Locked Loop

Two very different approaches to an especially good time resolution.

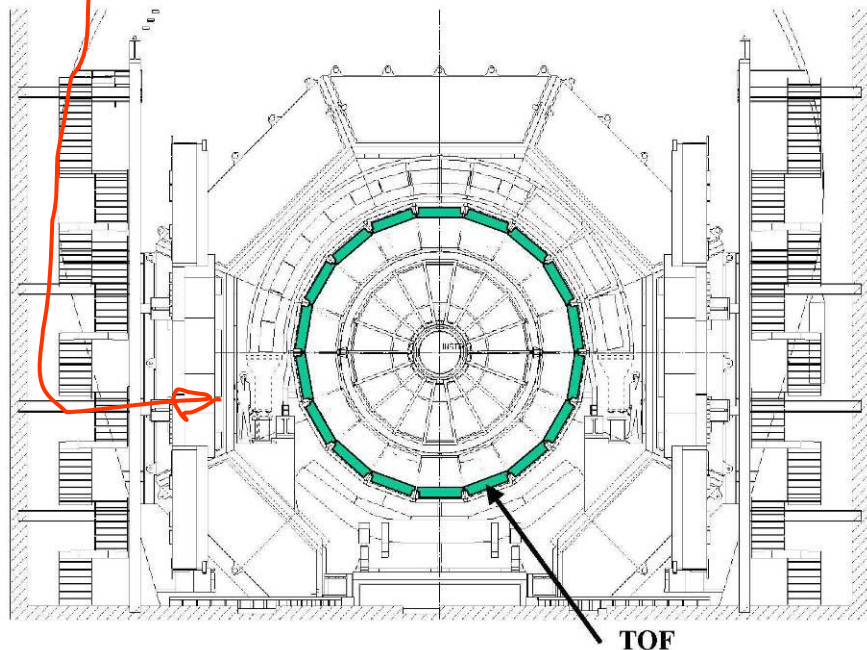


26

One thing is to have a signal, another thing is to know where the signal is.
Some things to look (out) for.

Will follow B. Zagreev at ACAT2002, 24 June 2002 <http://acat02.sinp.msu.ru/>

ALICE Time-of-Flight detector
R=3.7 m S=100 m² N=160000

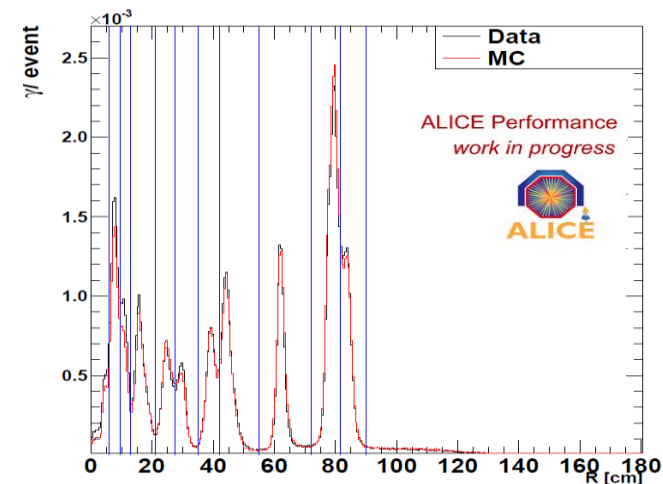


- ☐ Tracking (Kalman filtering)
- ☐ Matching
- ☐ Time measurements
- ☐ Particle identification

- High multiplicity $dN/dY \approx 8000$ primaries (12000 particles in TOF angular acceptance)
45(35)% of them reach TOF, but they produce a lot of secondaries

- High background
total number of fired pads ~ 25000
occupancy $= 25000 / 160000 = 16\%$
but only 25% of them are fired by particles having track measured by TPC
- Big gap between tracking detector (TPC) and TOF

big track deviation due to multiple scattering



Combinatorial algorithm for t_0 calculation.

1. Consider a very small subset (n) of primary
Let $l_1 \dots l_n, p_1 \dots p_n, t_1 \dots t_n$ - be length, momentum
and time of flight of corresponding tracks.

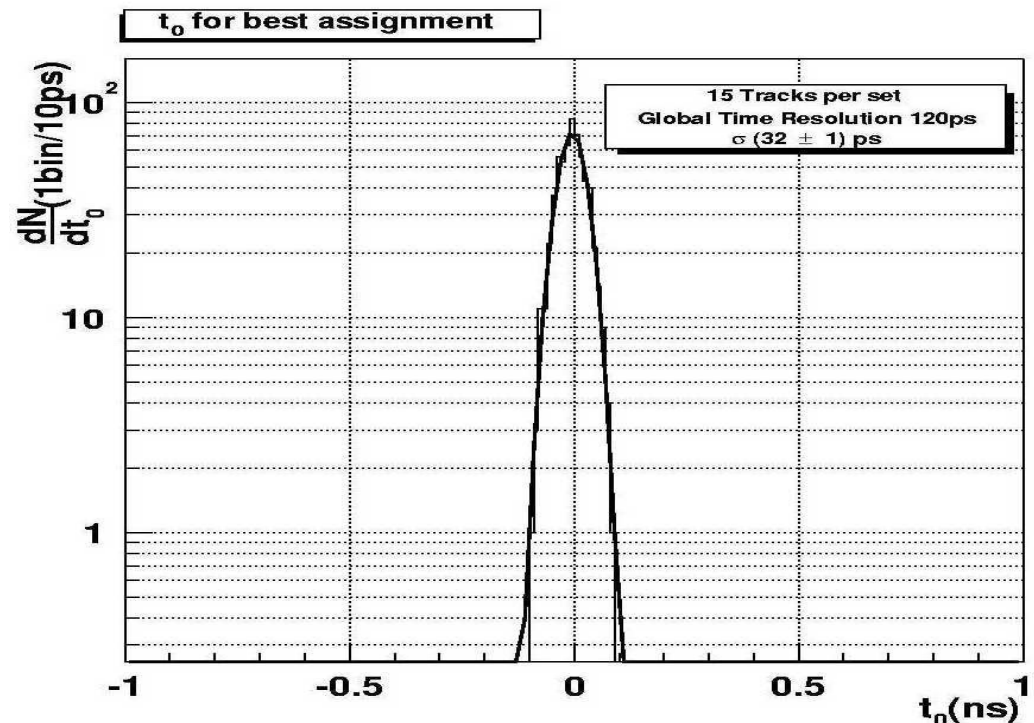
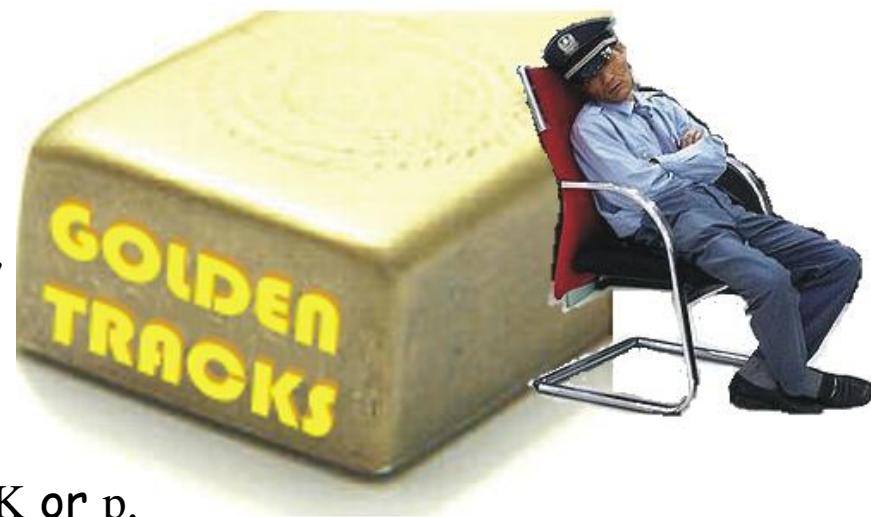
Now we can calculate the velocity (v_i) of
particle i by assuming that the particle is π , K or p.

2. Then we can calculate time zero:

$$\langle t_i^0 \rangle = \left\langle \frac{l_i}{v_i} \sum_{\pi, K, p} -t_i \right\rangle$$

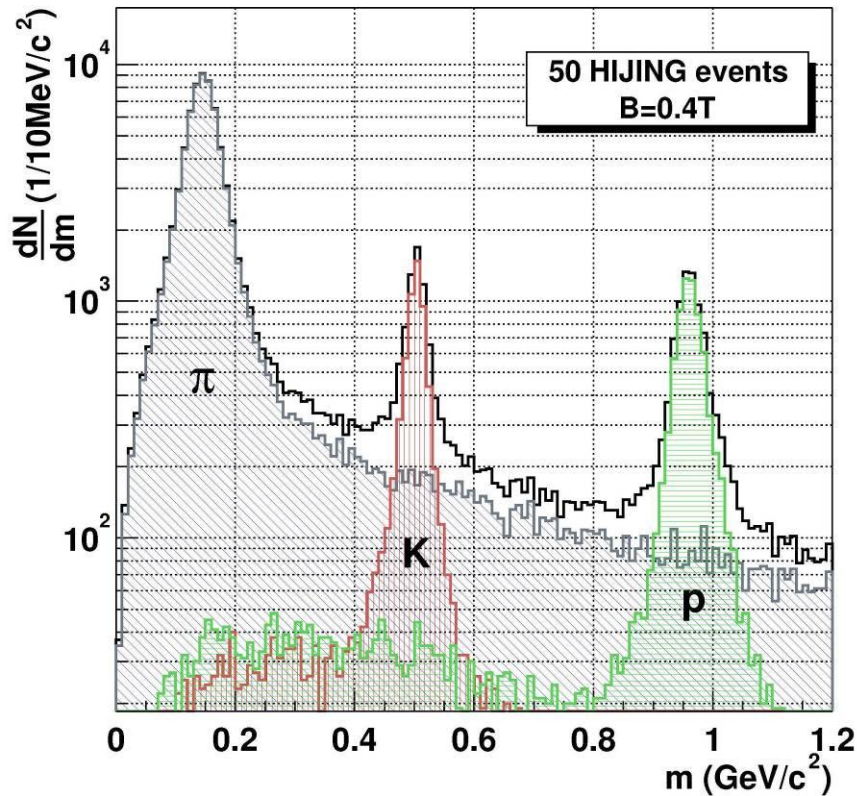
3. We chose configuration C with
minimal

$$\chi^2(C) \approx \sum_i \{t_i^0(C) - \langle t_i^0 \rangle(C)\}^2$$

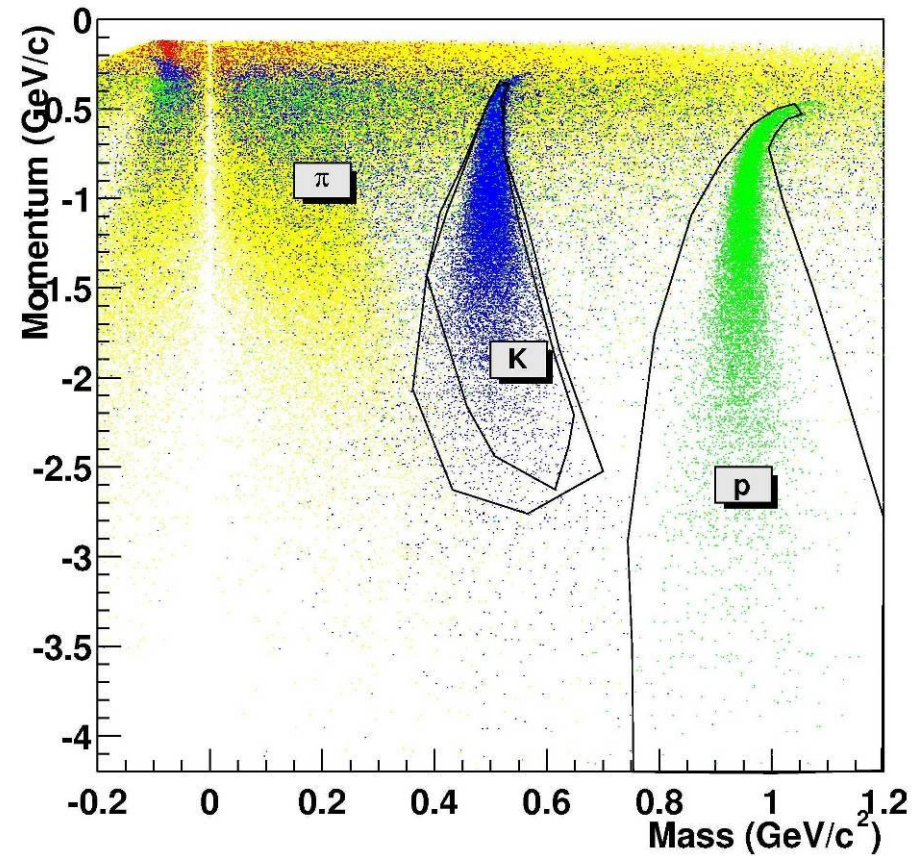


Which gives, with simulated events, particle identification with simple 1D or 2D cuts:

$$m = p \sqrt{c^2 t^2 / l^2 - 1}$$

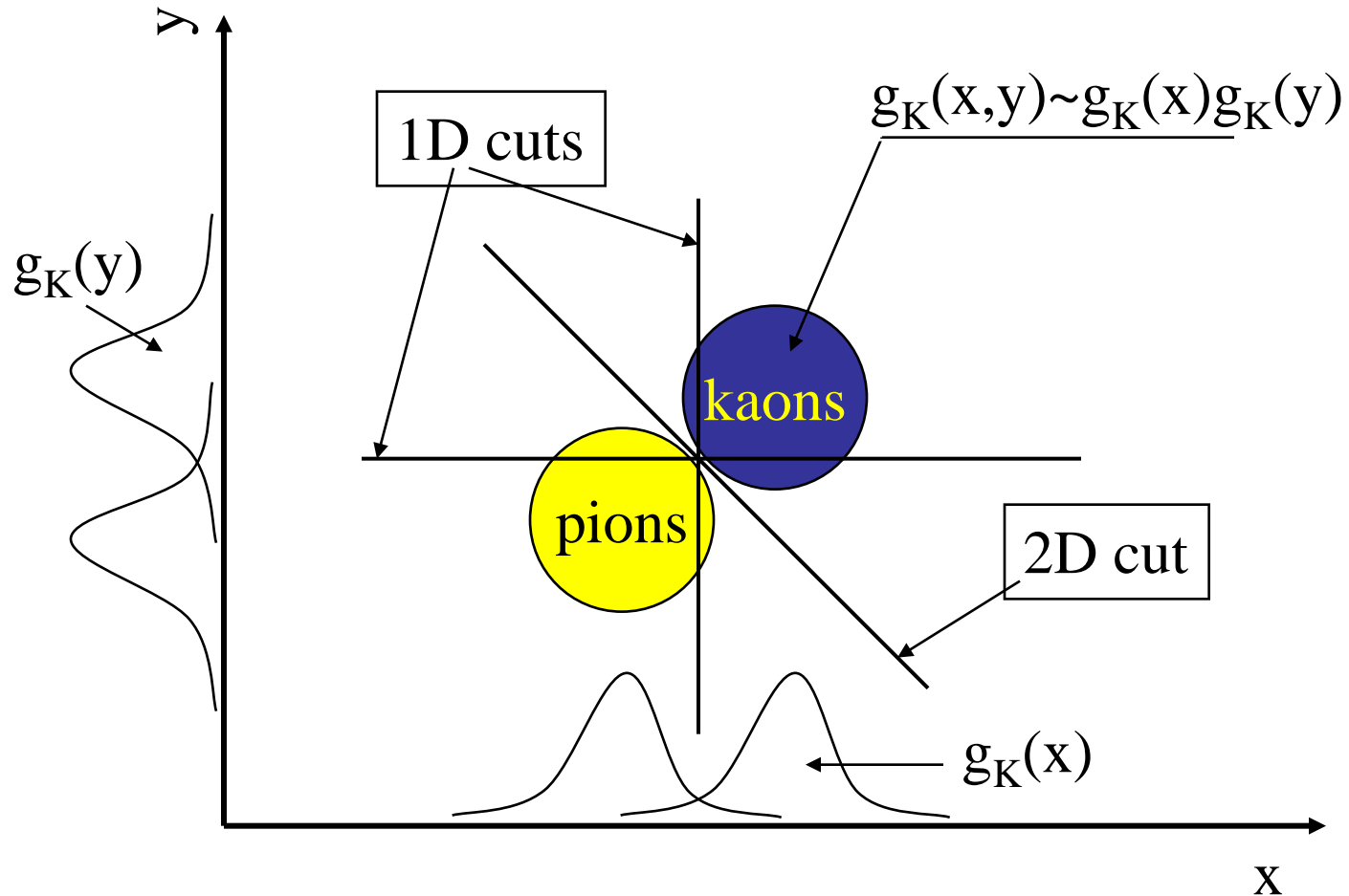


$$m = \pm p \sqrt{c^2 t^2 / l^2 - 1}$$



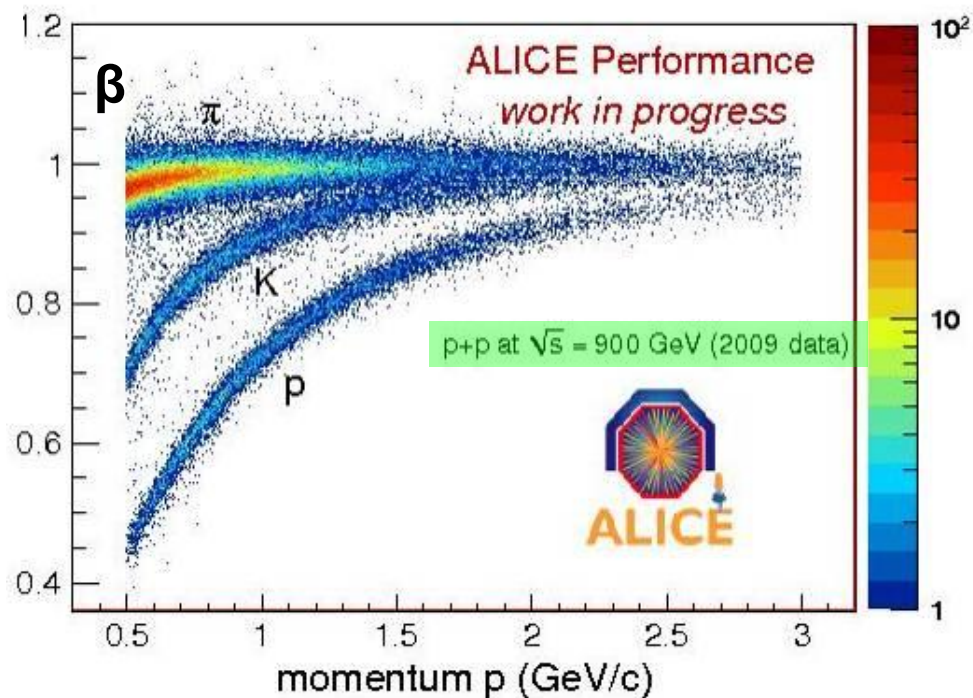
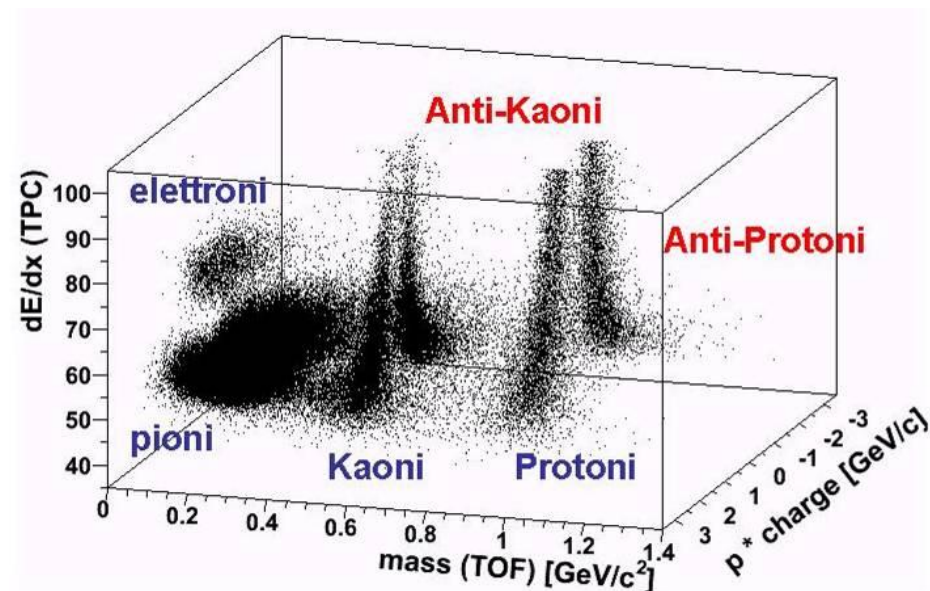
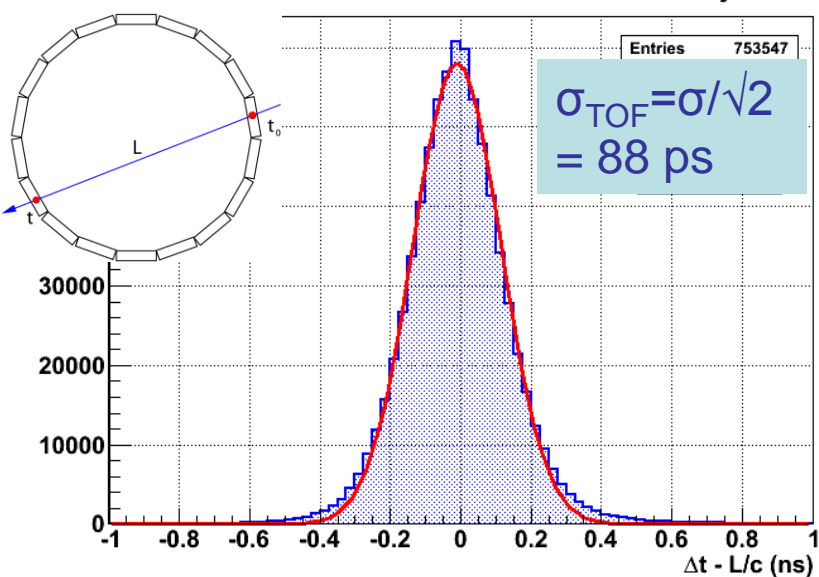
Neural network and Probability approach will of course also be used.

If you have **Detector X** and your friend has **Detector y** recording data of the same event:



With real data:

ALICE-TOF resolution measured with cosmic rays



That was all
planned for this lecture



When the messenger goes faster than the message:



Particle Identification with **Cherenkov Radiation**.

Observation of Antiprotons*

OWEN CHAMBERLAIN, EMILIO SEGRÈ, CLYDE WIEGAND,
AND THOMAS YPSILANTIS

Radiation Laboratory, Department of Physics, University of
California, Berkeley, California

(Received October 24, 1955)

The most legendary
experiment built on
PID with Cherenkov
radiation.

OWEN CHAMBERLAIN
The early antiproton work
Nobel Lecture, December 11, 1959

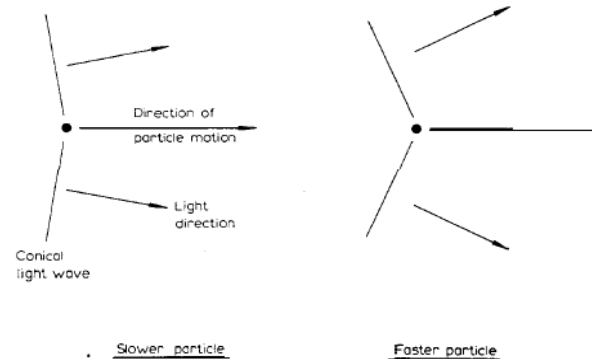
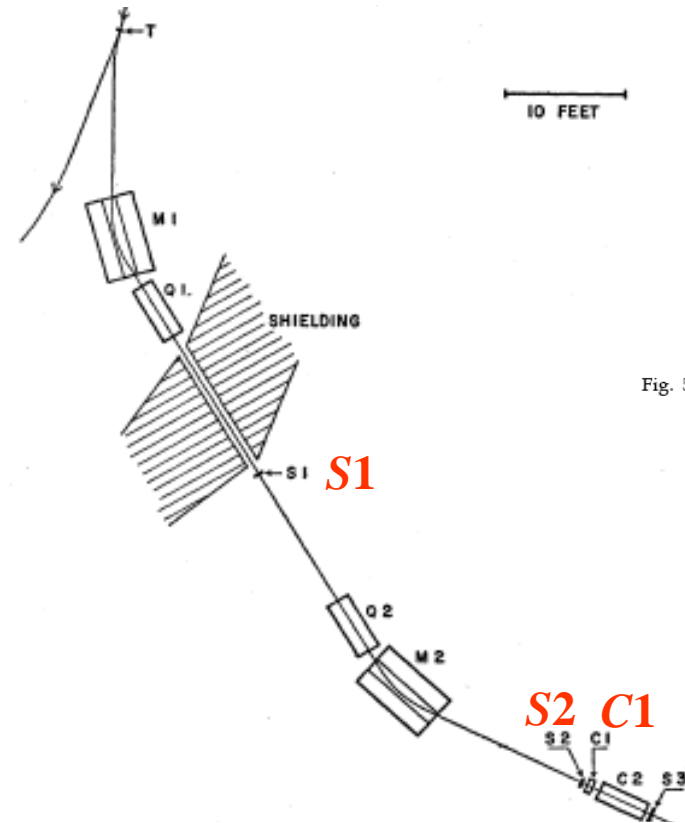


Fig. 5. Diagram of Čerenkov radiation. The angle of emission of Čerenkov depends on the speed of the charged particle.

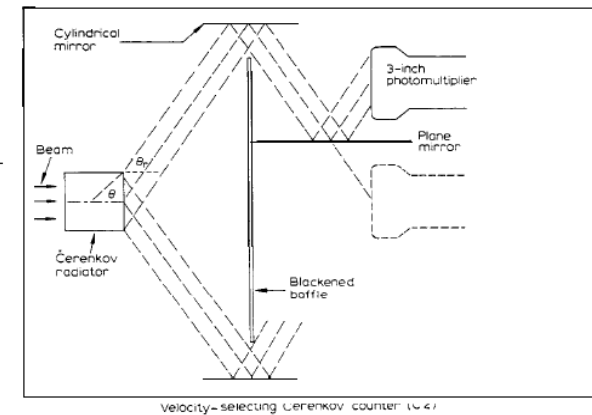


Fig. 7. View of the velocity-selecting Čerenkov counter.

TABLE I. Characteristics of components of the apparatus.

S1, S2	Plastic scintillator counters 2.25 in. diameter by 0.62 in. thick.
C1	Čerenkov counter of fluorochemical 0-75, ($C_8F_{16}O$); $\mu_D = 1.276$; $\rho = 1.76 \text{ g cm}^{-3}$. Diameter 3 in.; thickness 2 in.
C2	Čerenkov counter of fused quartz: $\mu_D = 1.458$; $\rho = 2.2 \text{ g cm}^{-3}$. Diameter 2.38 in.; length 2.5 in.
Q1, Q2	Quadrupole focusing magnets: Focal length 119 in.; aperture 4 in.
M1, M2	Deflecting magnets 60 in. long. Aperture 12 in. by 4 in. $B \approx 13 \text{ 700 gauss}$.

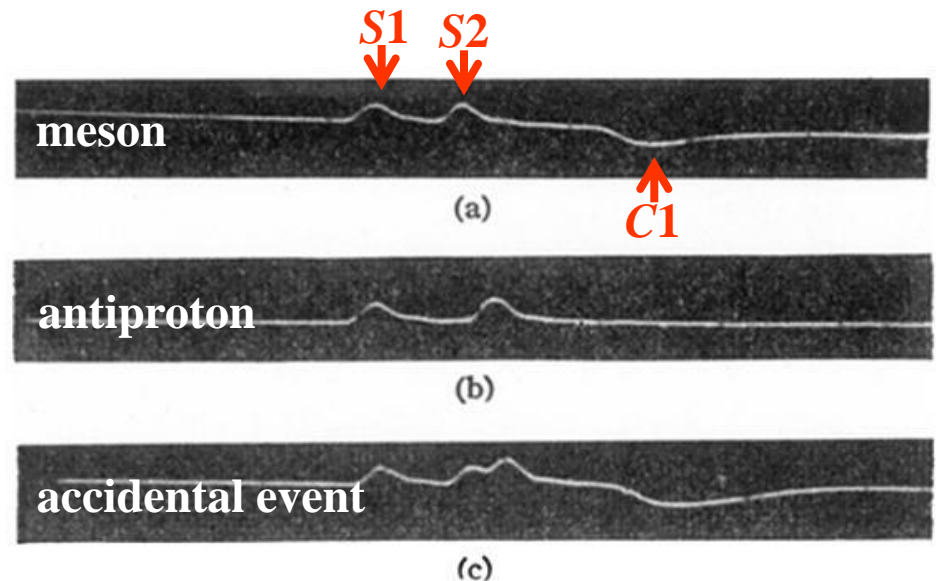


FIG. 2. Oscilloscope traces showing from left to right pulses from S1, S2, and C1. (a) meson, (b) antiproton, (c) accidental event.

The Cherenkov radiation condition:

ϵ real ✓

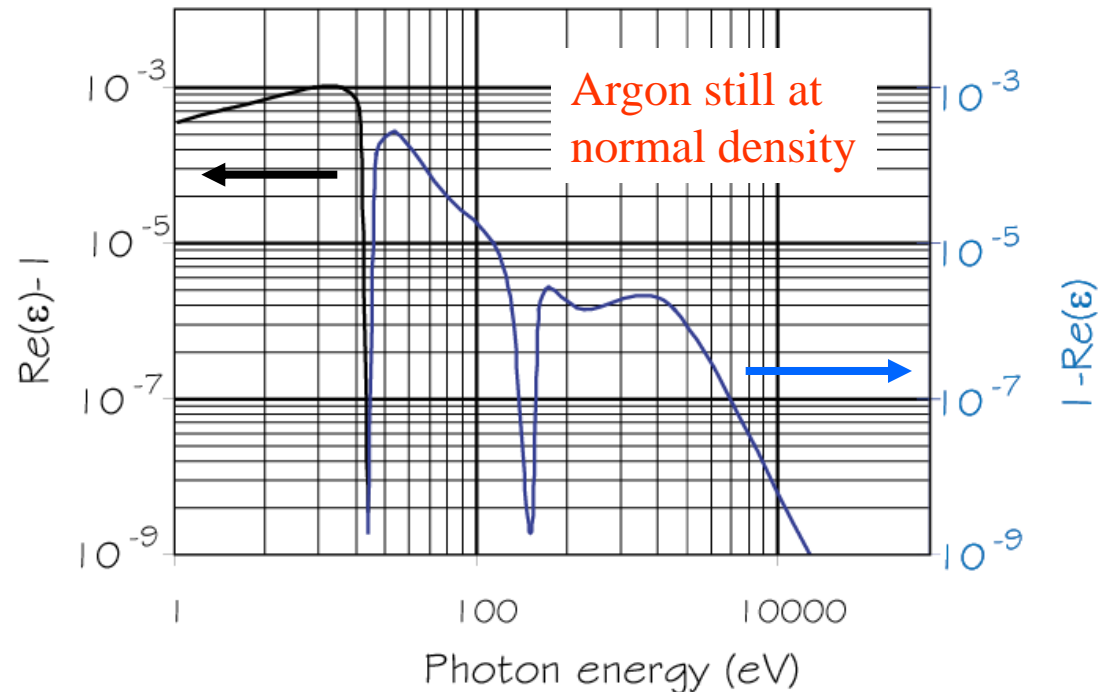
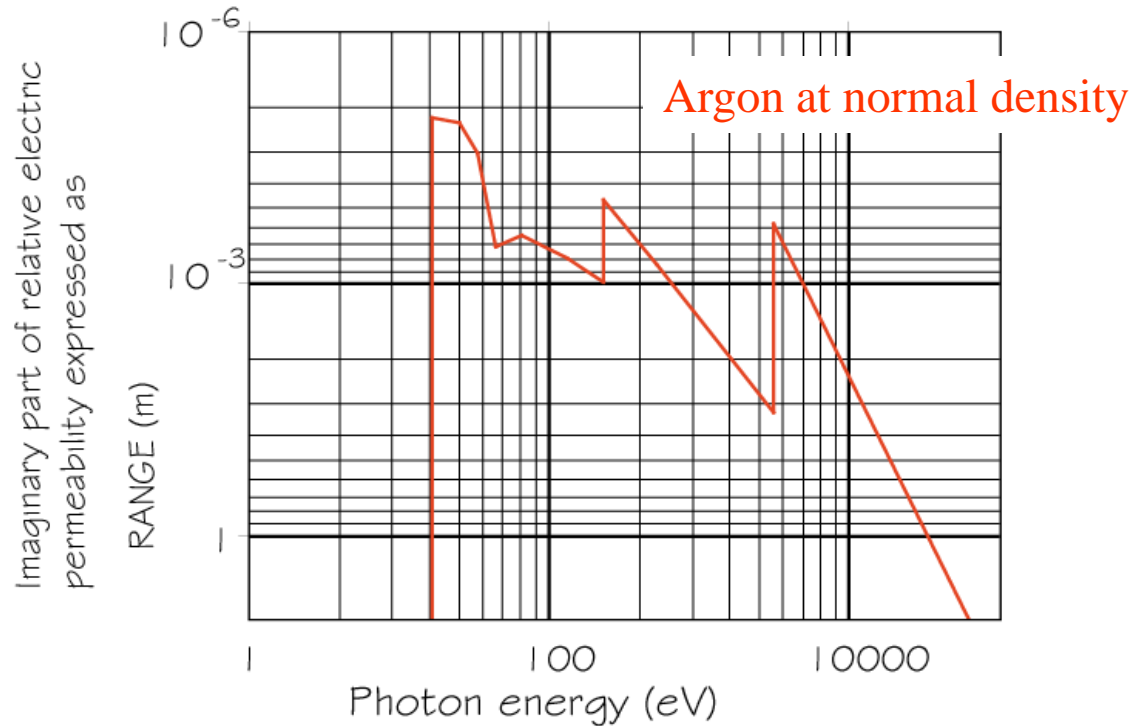
and

$0 \leq \cos(\Theta) \leq 1$ ✓

$$\cos \Theta_c = \frac{1}{\beta \cdot n}$$

where n is the refractive index

W.W.M. Allison and P.R.S. Wright, RD/606-2000-January 1984



Some words on refractive index

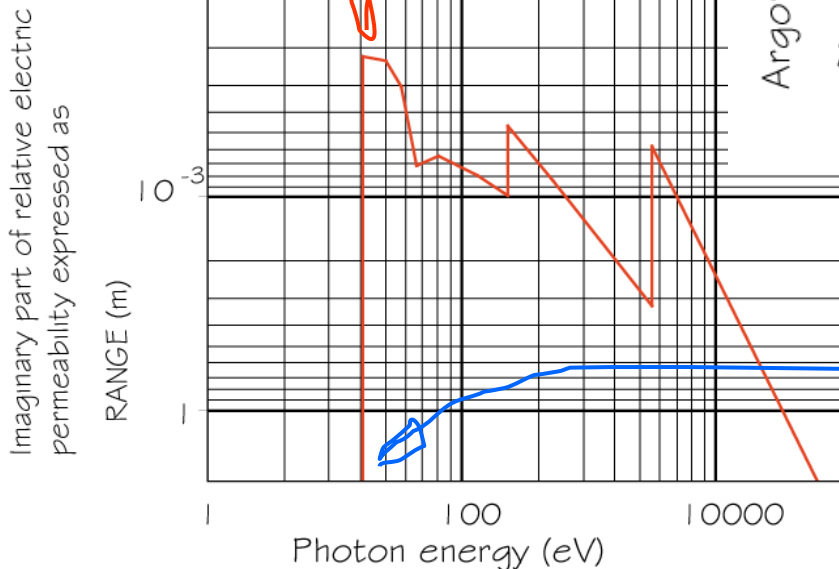
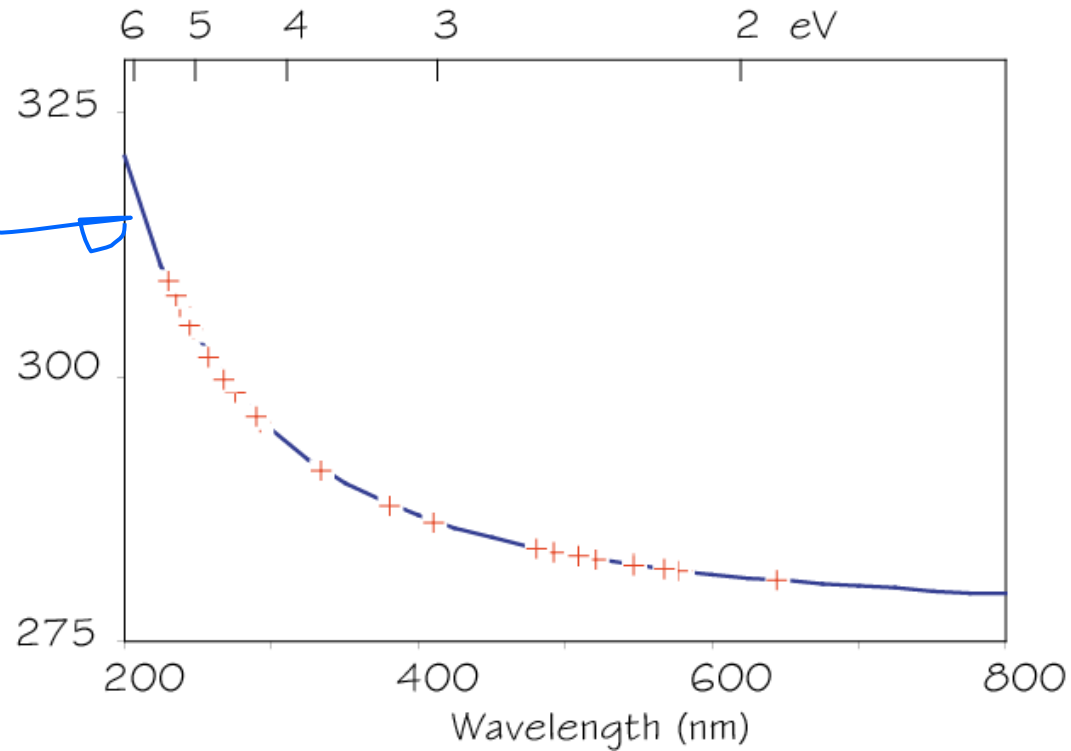
The normal way to express n is as a power series.
For a simple gas, a simple
one pole Sellmeier approximation:

$$(n-1) \cdot 10^6 = \frac{0.05085}{\left(\frac{1}{73.8}\right)^2 - \left(\frac{1}{\lambda(nm)}\right)^2}$$

Argon

=16.8 eV

Argon $(n-1) \cdot 10^6$ 760 torr 0 °C



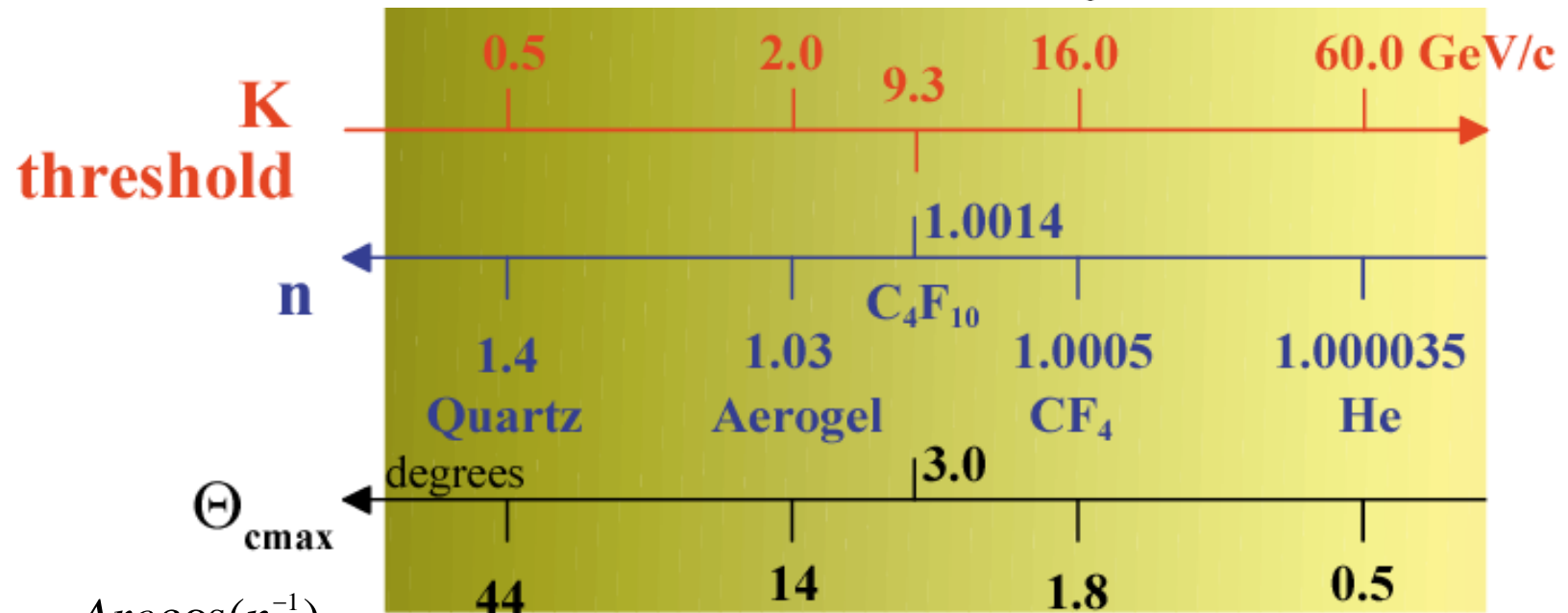
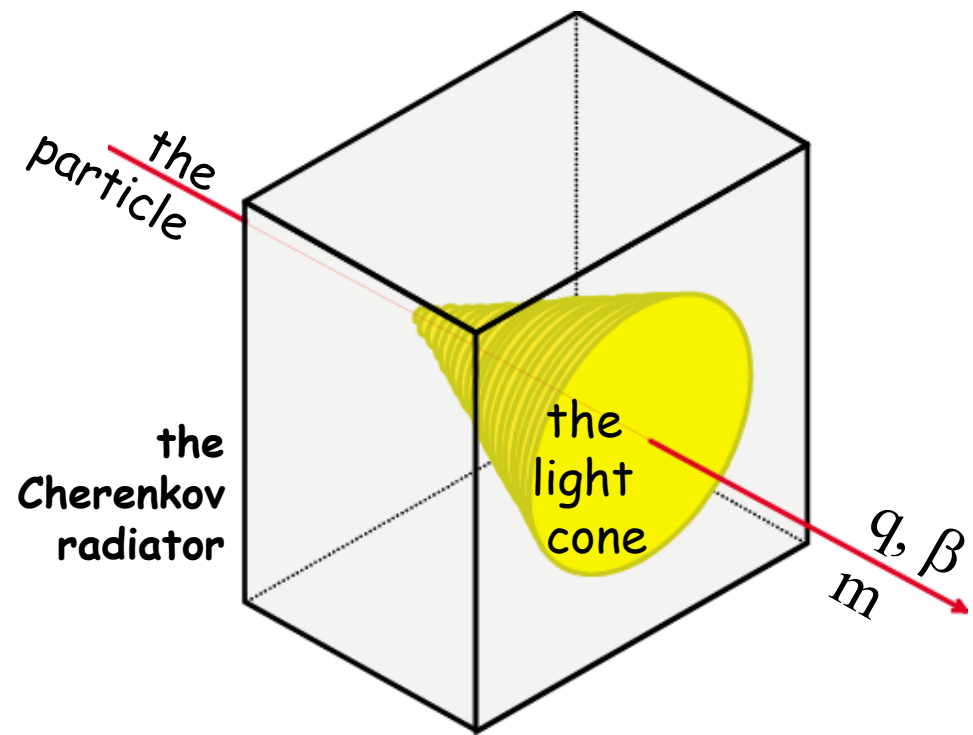
$$\omega_0^2 = (\text{plasma frequency})^2 \propto (\text{electron density})$$

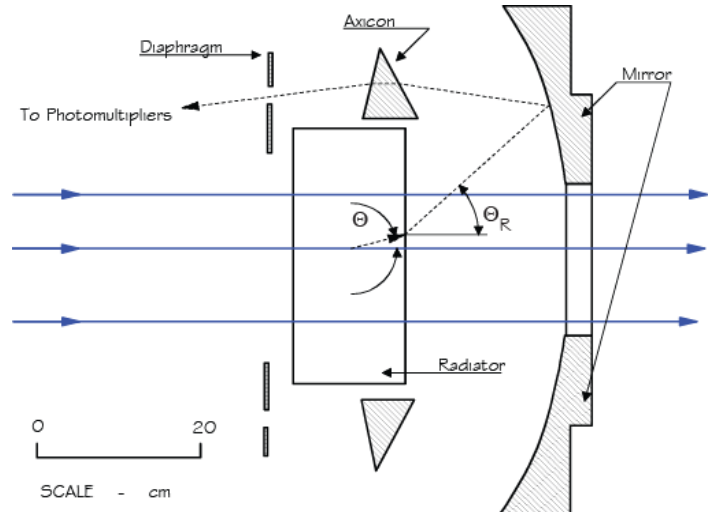
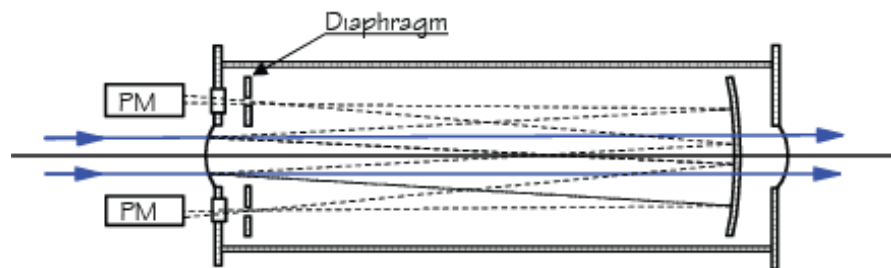
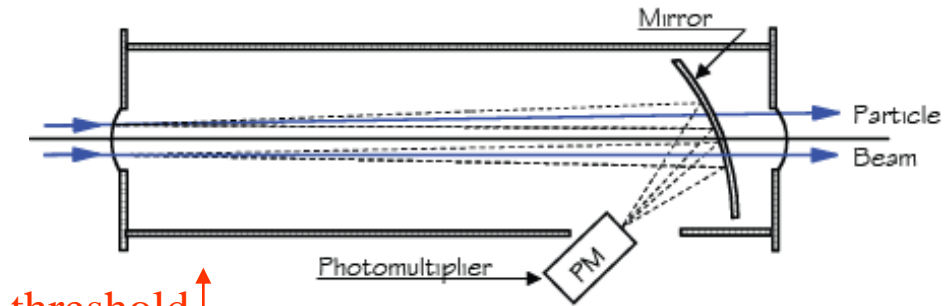
For more on the plasma frequency, try Jackson, Section 7 (or similar)
or go to sites like
<http://farside.ph.utexas.edu/teaching/plasma/lectures/node44.html>

$$n-1 = \frac{A}{\lambda_0^{-2} - \lambda^{-2}}$$

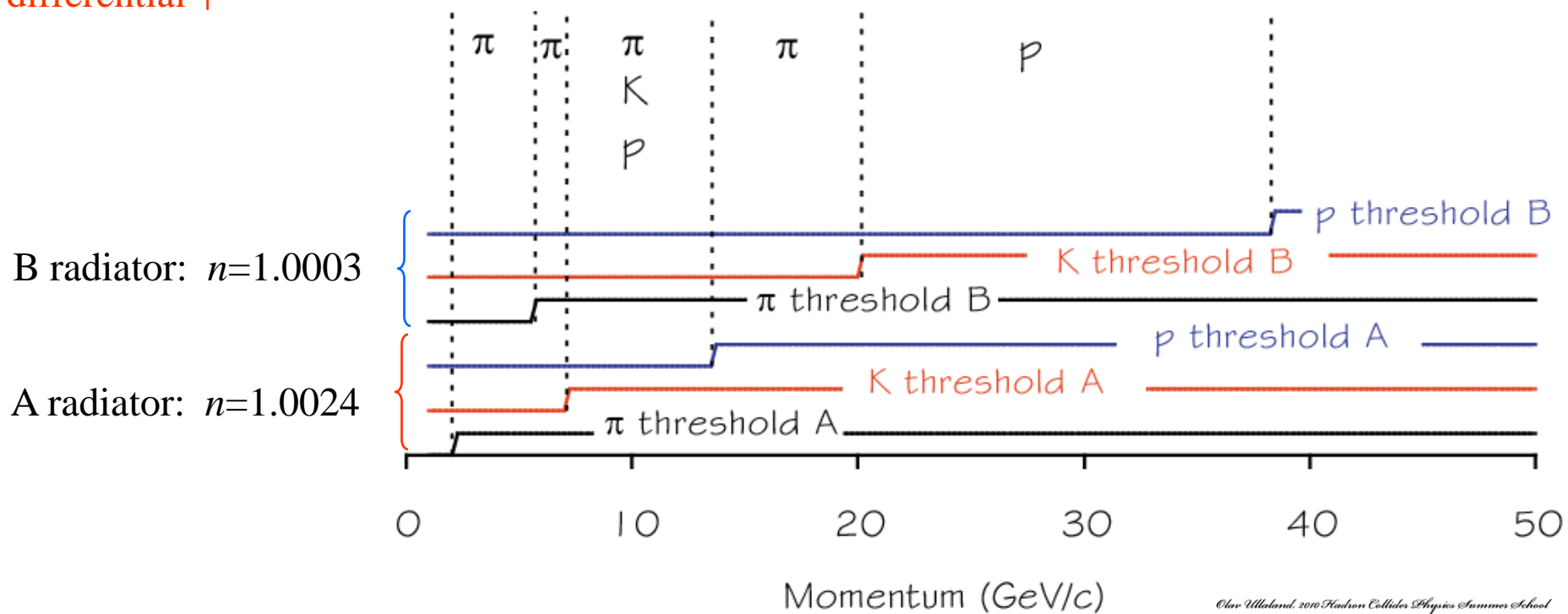
$$\frac{dN_{ph}}{dL d\lambda} = 2\pi\alpha Z^2 \frac{1}{\lambda^2} \sin^2 \Theta$$

$$\cos \Theta = \frac{1}{\beta n}$$





achromatic



Use all available information about the Cherenkov radiation:

- _____ The existence of a threshold
- _____ The dependence of the number of photons
- _____ The dependence of Cherenkov angle on the velocity $\beta = p/E$ of the particle
- _____ The dependence on the charge of the particle

+

Capability to do single photon detection

- _____ with high efficiency
- _____ with high space resolution

Ring
Imaging
Cherenkov
detector

the RICH



The Ring Image

θ, β

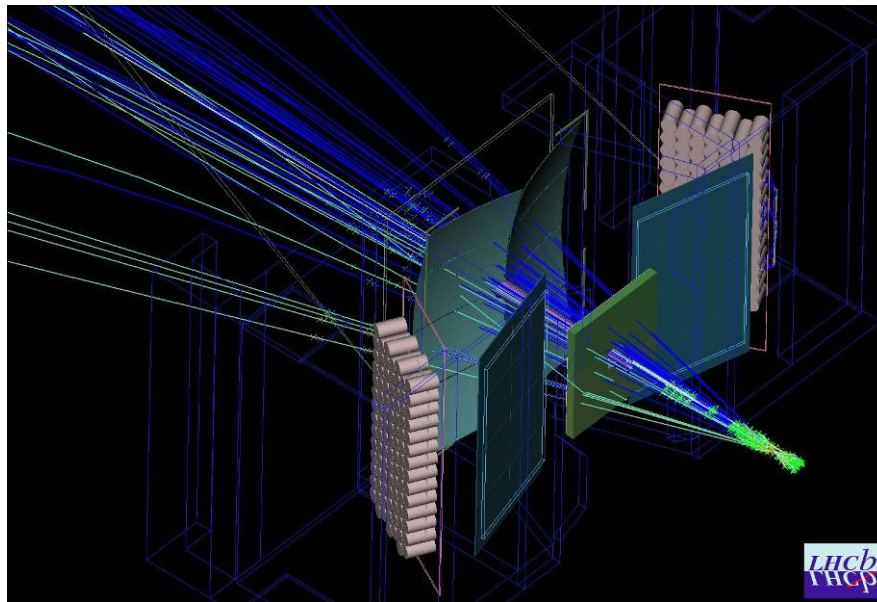
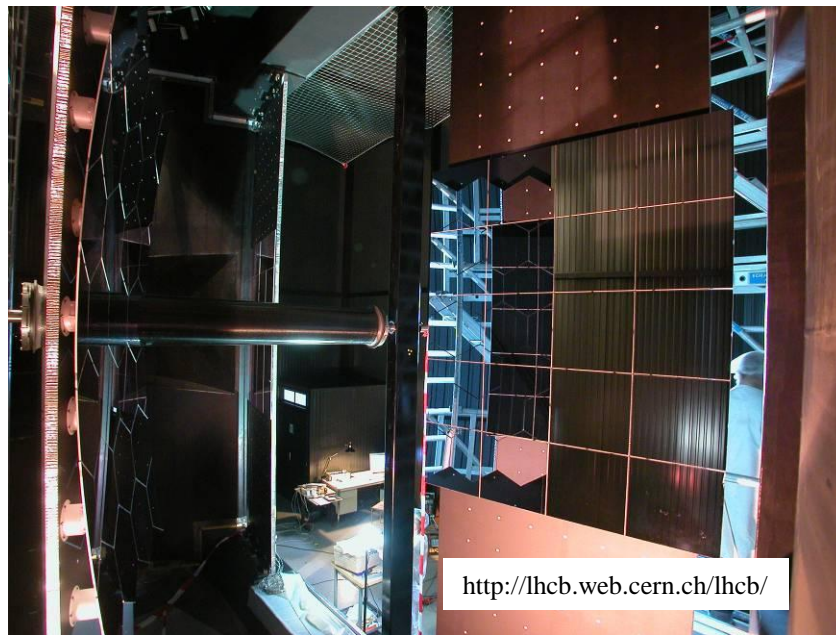
Interaction
point

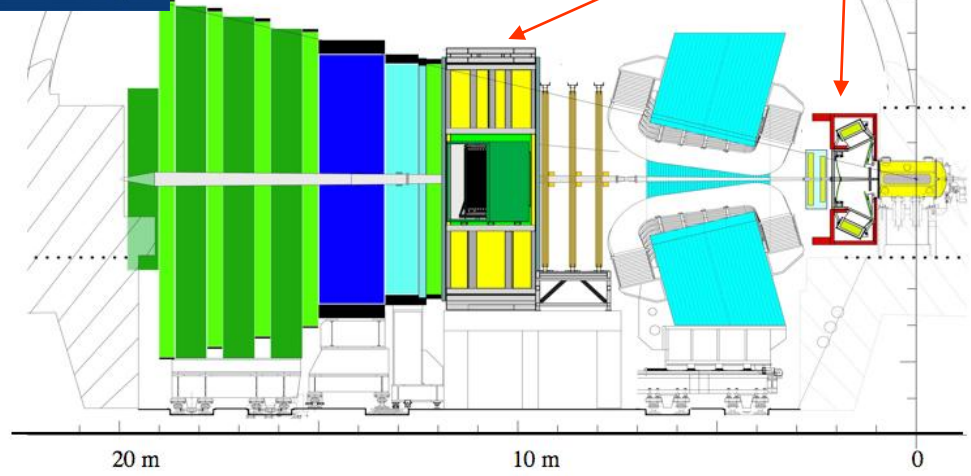
The
photon
detector

The photons

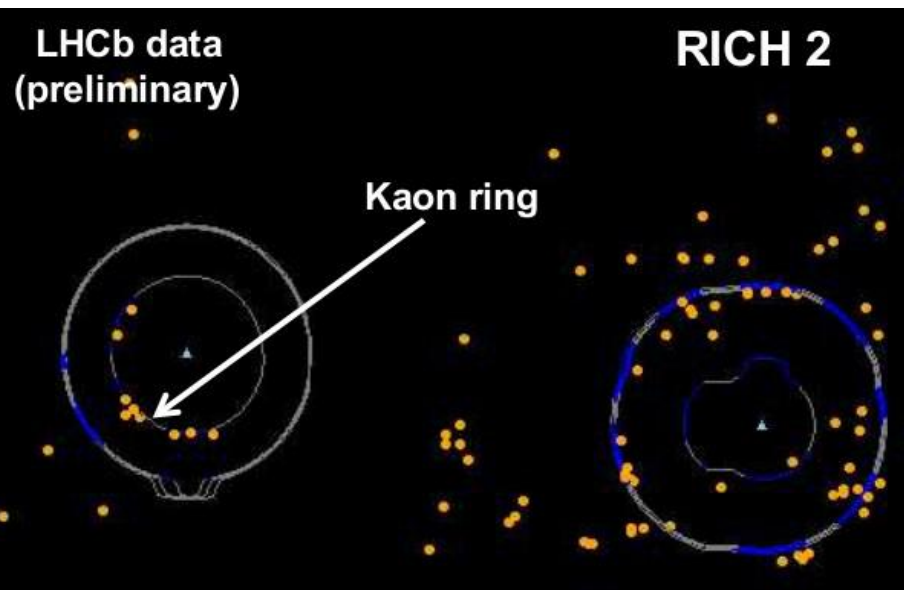
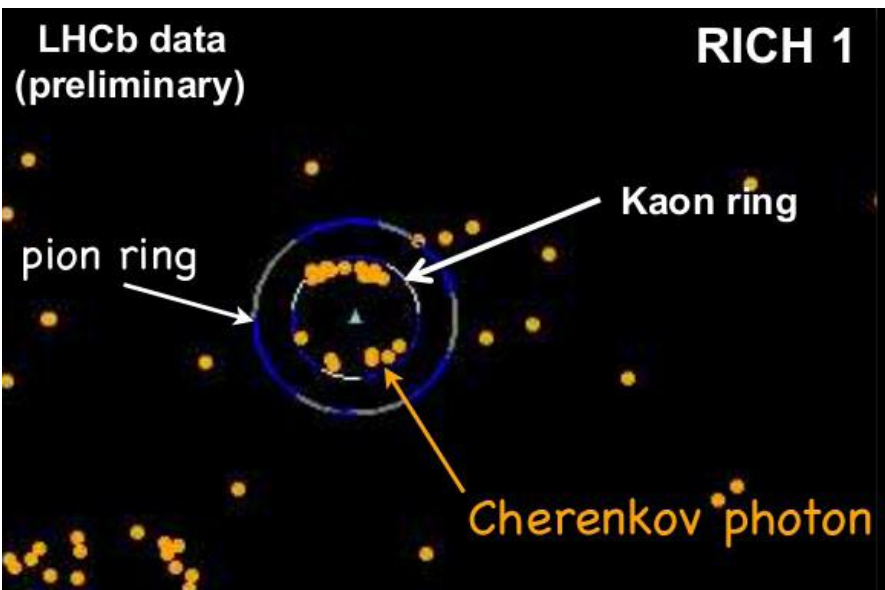
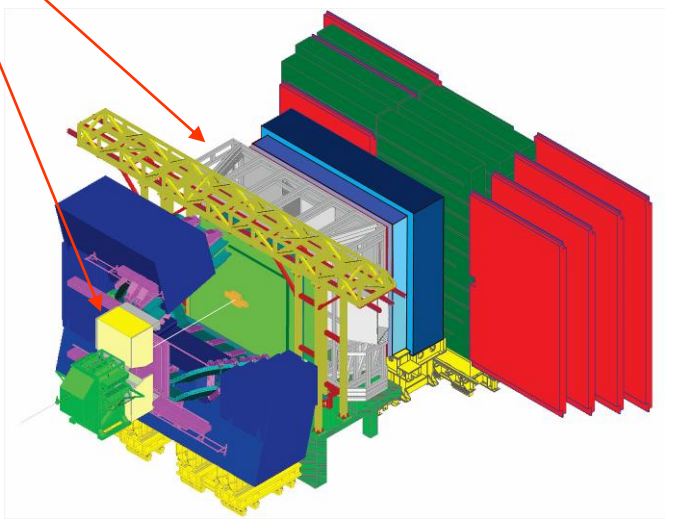
The
mirror

The beginning:
J. Seguinot and T. Ypsilantis,
Photo-ionisation and Cherenkov
ring imaging, Nucl. Instr. and
Meth. 142(1977)377

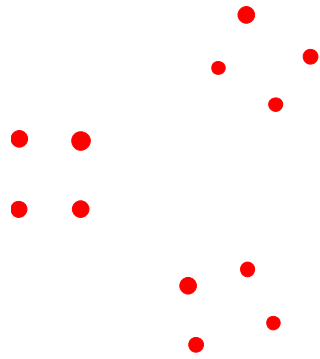




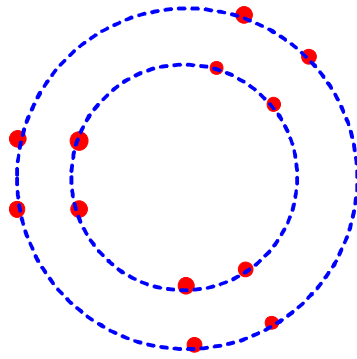
RICH 2
RICH 1



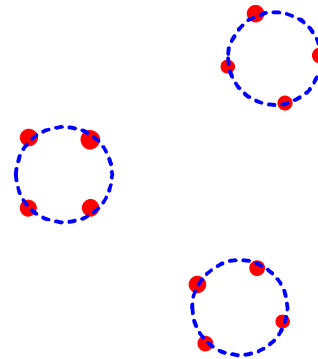
From **Photons** \Rightarrow **Hits** \Rightarrow **Rings**.



(a)



(b)



(c)

There is no way to recognise a pattern if one does not know what one is looking for!

What rings should we see in (a)?

Are there two large concentric rings as indicated in (b)?

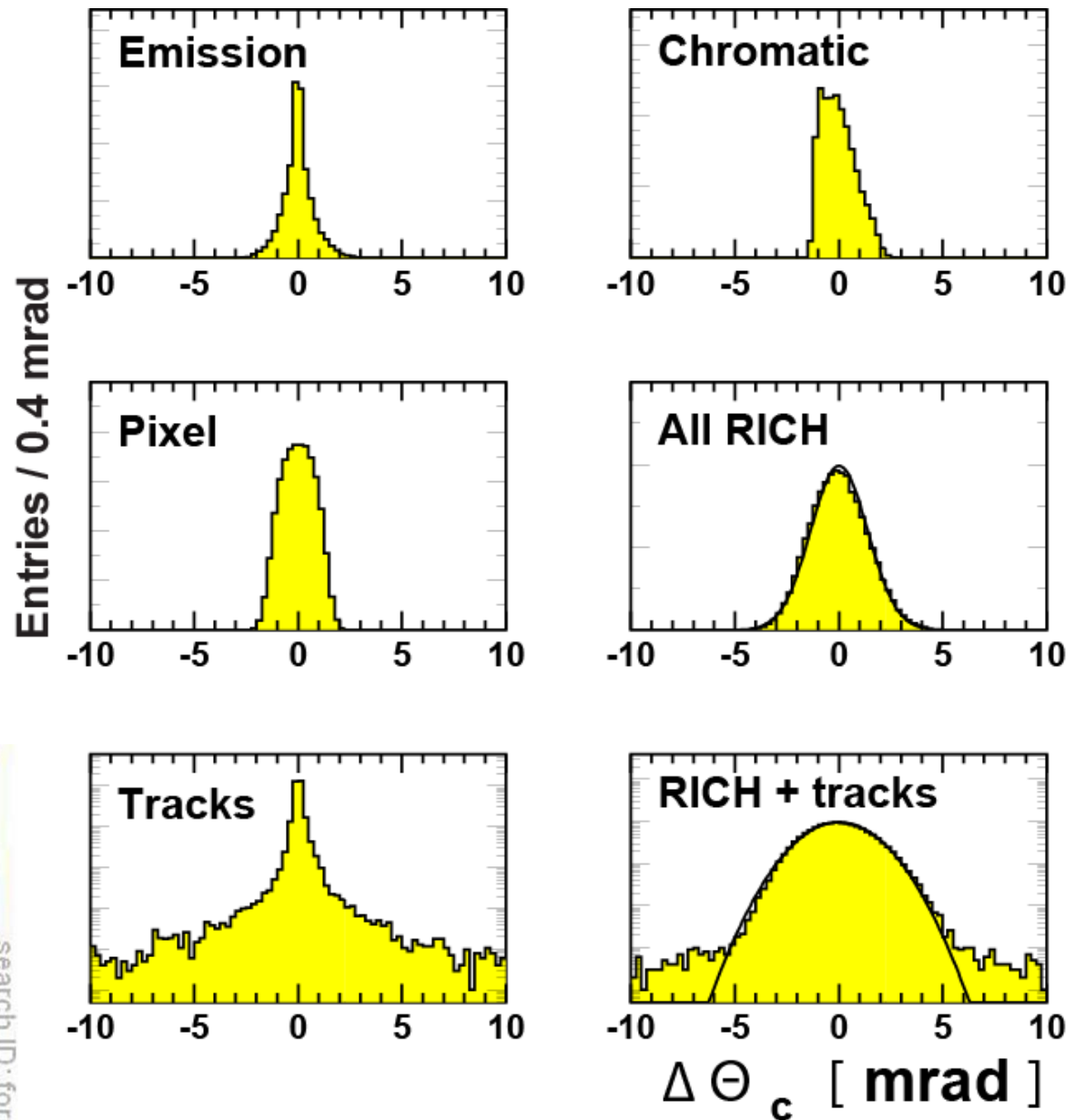
Perhaps there are three small rings of equal radii as indicated in (c).

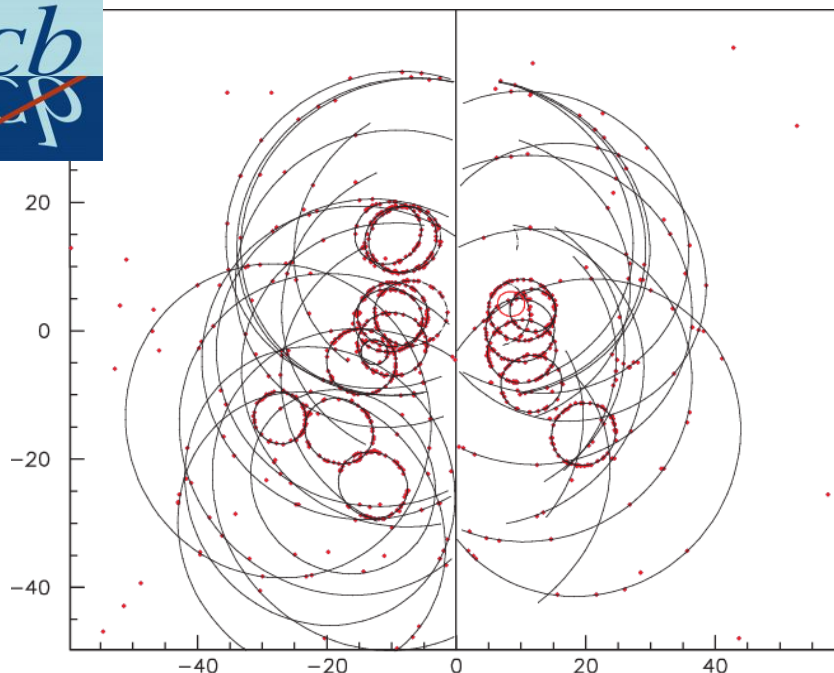
The answer *must* depend on what rings we expect to see!

Equivalently, the answer *must* depend on the process which is believed to have lead to the dots being generated in the first place. If we were to know *without doubt* that the process which generated the rings which generated the dots in (a) were only capable of generating large concentric rings, then only (b) is compatible with (a). If we were to know *without doubt* that the process were only capable of making small rings, then (c) is the only valid interpretation. If we know the process could do either, then both (b) and (c) might be valid, though one might be more likely than the other depending on the relative probability of each being generated. Finally, if we were to know that the process only generated *tiny* rings, then there is yet another way of interpreting (a), namely that it represents 12 *tiny* rings of radius too small to see. 43

Doom
Gloom
and
Despair

as in
inAccuracy
unCertainty
misCalculation
imPerfection
inPrecision
or plain
blunders
errors and
faults.





Local analysis: _____
Each track is taken in turn.

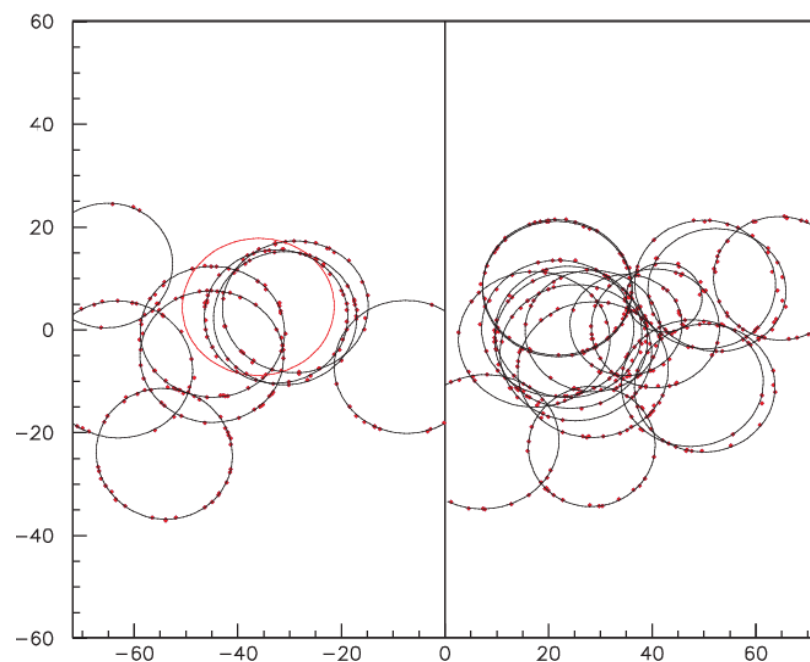
$$\ln \mathcal{L} = \sum_i \ln \left(1 + \frac{1}{\sqrt{2\pi\sigma_\Theta \kappa}} \exp \left[-\frac{(\Theta_i - \Theta_x)^2}{2\sigma_\Theta^2} \right] \right)$$

Θ_i : calculated emission angle for hit i

Θ_x : expected angle for hypothesis x

σ_Θ : angular resolution

κ : hit selection parameter



Global analysis: _____
The likelihood is constructed for the whole event:

$$\ln \mathcal{L} = - \sum_{\text{track } j} \mu_j + \sum_{\text{pixel } i} n_i \ln \left(\sum_{\text{track } j} a_{ij} + b_i \right)$$

a_{ij} : expected hits from track j in detector/pixel i

$\mu_j = \sum_i a_{ij}$

n_i : hits in detector i

b_i : expected background in detector i

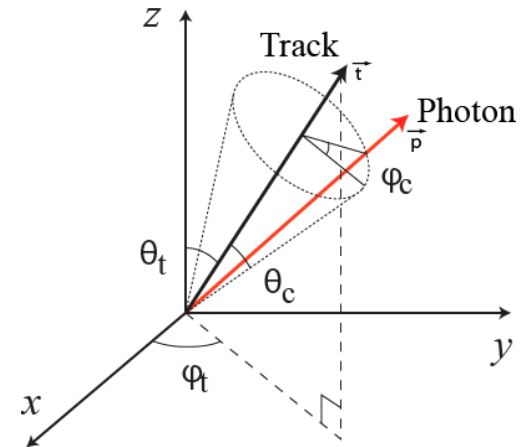
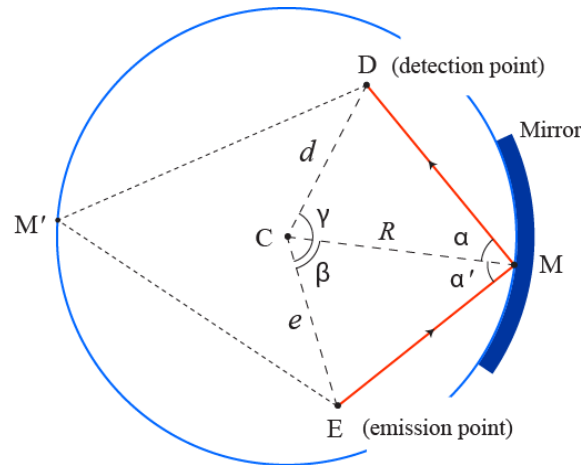
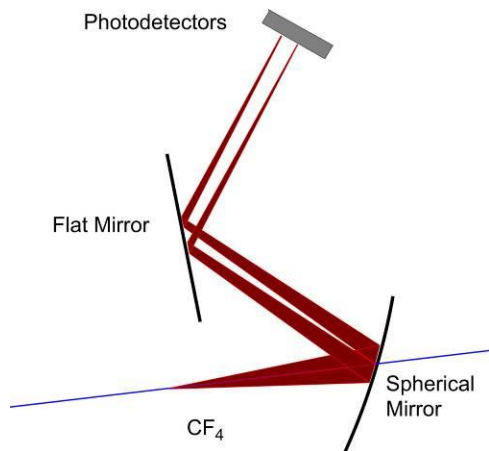
Putting some meat to these bare bones.

Will follow R. Forty and O. Schneider, RICH pattern recognition, LHCb/98-40

C.P. Buszello, LHCb RICH pattern recognition and particle identification performance, NIM A 595(2008) 245-247

Cherenkov angle reconstruction:

reconstructing the Cherenkov angle for each hit and for each track assuming all photons are originating from the mid point of the track in the radiator. (If the radiator is photon absorbing, move the emission point accordingly.)

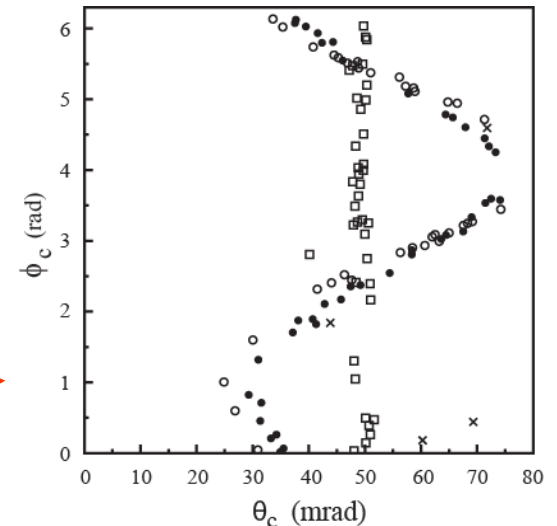


This gives a quartic polynomial in $\sin \beta$ which is solved via a resolvent cubic equation.

And then:

$$\cos \Theta_c = \vec{p} \cdot \vec{t}$$

$$\cos \phi_c = \frac{\cos \Theta_t \cos \Theta_c - \cos \Theta_p}{\sin \Theta_t \sin \Theta_c}$$



Building the Likelihood.

M^{tot} : Total number of pixels

n_i : number of hits in pixel i

N^{track} : number of tracks to consider

N^{back} : number of background sources to consider

$h=(h_1, h_2, ..., h_N)$ is the event hypothesis. $N=N^{track}+N^{back}$ and h_j : mass hypothesis for track j

$a_{ij}(h_j)$: expected number of hits in pixel i from source j under hypothesis h_j

then the expected signal in pixel i is given by:

$$\nu_i = \sum_{j=1}^N a_{ij} \Rightarrow \mathcal{L} = \prod_{i=1}^{M^{tot}} P_{\nu_i}(n_i)$$

for $P_{\nu_i}(n_i) = \frac{e^{-\nu_i} \nu_i^{n_i}}{n_i!}$ = probability for signal n_i when ν_i is expected

or

$$\ln \mathcal{L} = -\sum_{j=1}^N \mu_j + \sum_{i=1}^M n_i \ln \sum_{j=1}^N a_{ij} = C$$

for $\mu_j = \sum_{i=1}^{M^{tot}} a_{ij}$ total expectation from source j with h_j



"According to this theory, it's strongly improbable that anything should ever happen anytime, anywhere."

$a_{ij}(h_j)$: the expected number of hits in pixel i from source j under hypothesis h_j
 is a function of the detector efficiency ε_i and the expected number of Cherenkov photons
 arriving at pixel i and emitted by track j under the mass hypothesis h_j .

Let $\lambda_j(h_j)$ be the expected number of Cherenkov photons emitted by track j under the mass
 hypothesis h_j .

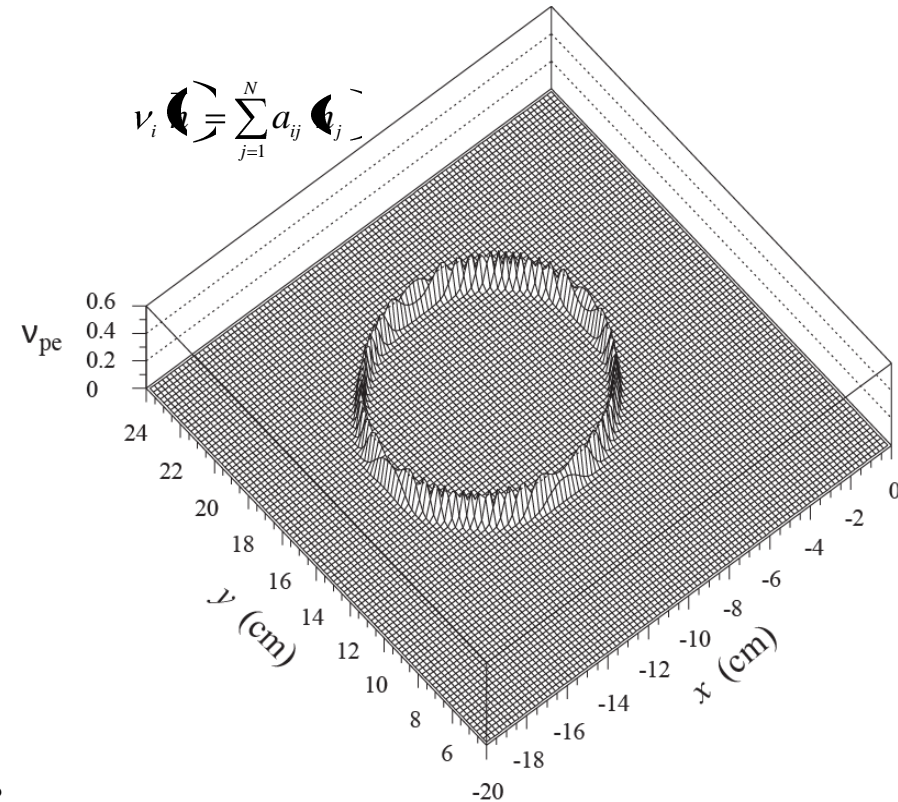
Then

$$\begin{aligned} a_{ij} &= \varepsilon_i b_{ij} = \varepsilon_i \lambda_j \iint_{\text{pixel } i} f_{h_j}(\theta, \phi) d\theta d\phi \\ &\cong \varepsilon_i \lambda_j \iint_{\text{pixel } i} f_{h_j}(\theta_{ij}, \phi_{ij}) d\theta d\phi \\ &\approx \varepsilon_i \lambda_j \frac{4A}{R^2 \theta_{ij}} \end{aligned}$$

Where θ_{ij} and ϕ_{ij} are the reconstructed angles.

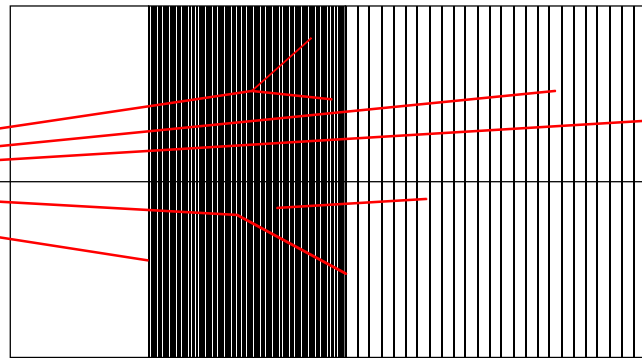
Then add:

- ☐ Photon scattering like Rayleigh and Mie
- ☐ Mirror inaccuracy
- ☐ Chromatic aberration
- ☐



Expected number of
photoelectrons in each pixel

Calorimeter Cherenkov Muon detector



This absolute likelihood value itself is not the useful quantity since the scale will be different for each event.

$$\mathcal{L}^{RICH} \begin{bmatrix} e \\ \mu \\ \pi K p \end{bmatrix} \quad \mathcal{L}^{CALO} \begin{bmatrix} e \\ \text{non } e \end{bmatrix} \quad \mathcal{L}^{MUON} \begin{bmatrix} \mu \\ \text{non } \mu \end{bmatrix}$$

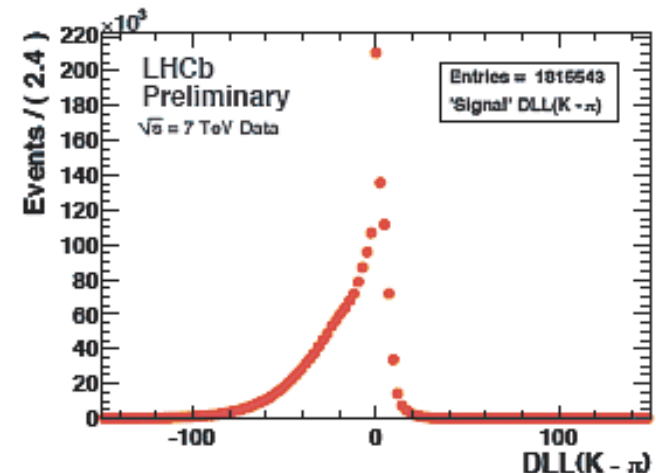
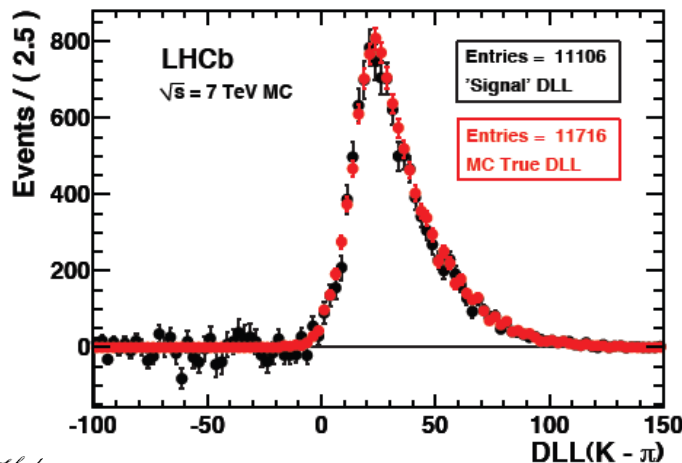


$$\mathcal{L}(e) = \mathcal{L}^{RICH}(e) \cdot \mathcal{L}^{CALO}(e) \cdot \mathcal{L}^{MUON}(\text{non } \mu) \dots$$

Rather use the differences in the log-likelihoods:

$$\Delta \ln \mathcal{L}_{K\pi} = \ln \mathcal{L}(K) - \ln \mathcal{L}(\pi)$$

$$\Delta \log \mathcal{L}(K - \pi)$$

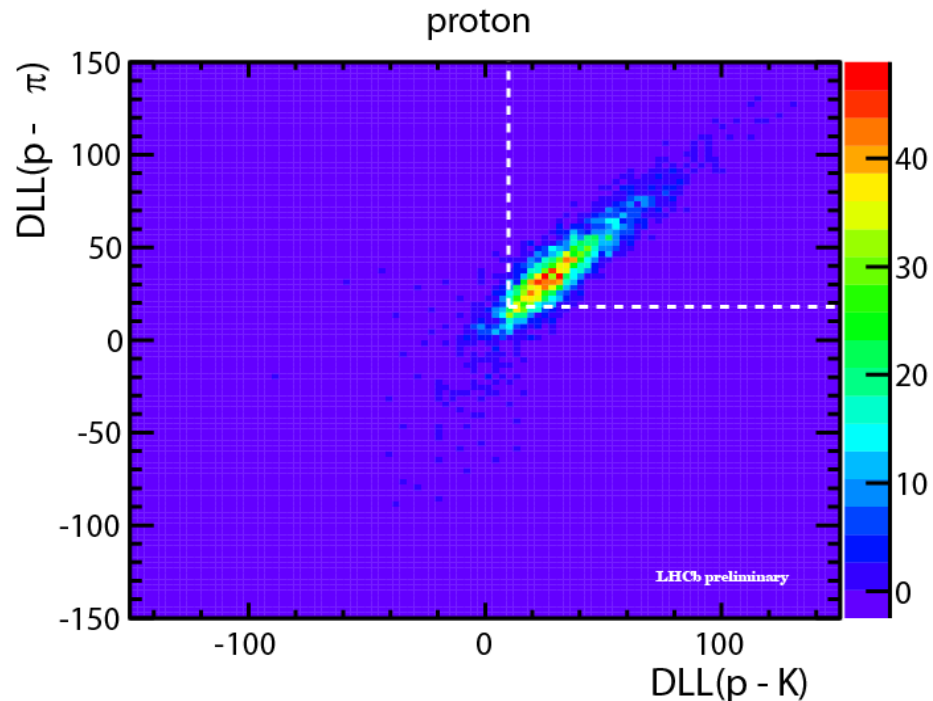
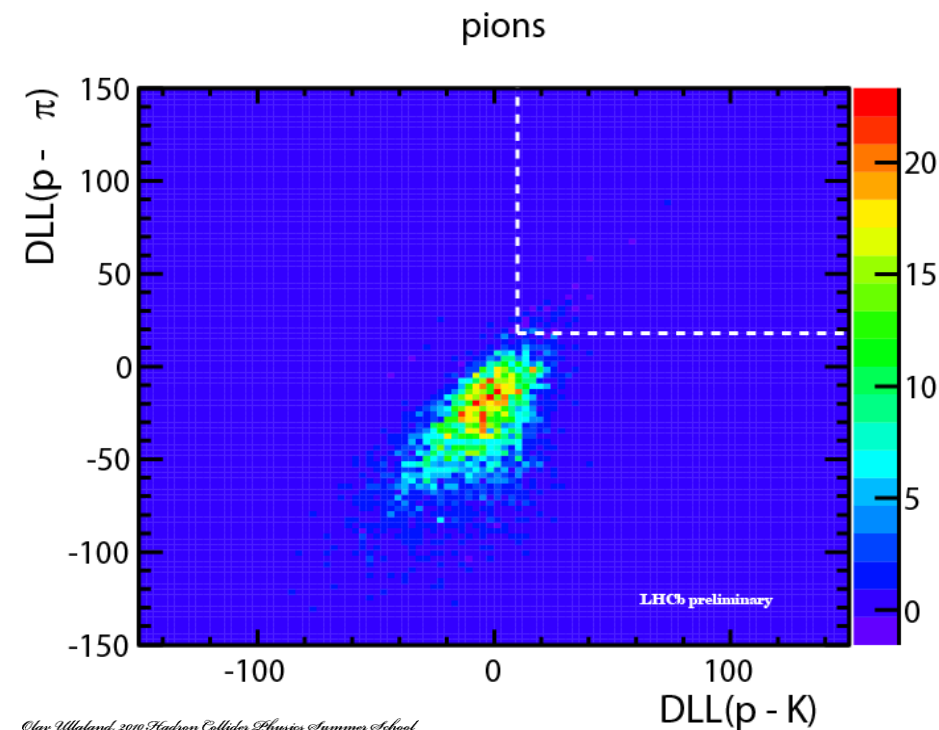
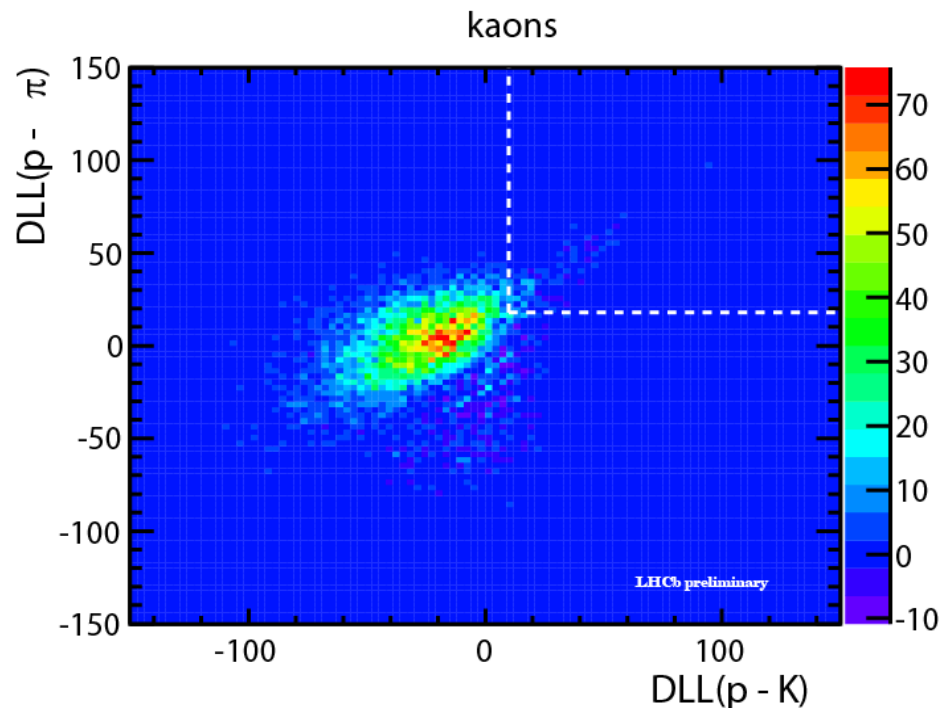


LHCb preliminary

pbar/p analysis

DLL in p-K, p- π space for pions, kaons and protons (obtained from data calibration samples) in one bin in p_t, η space.

Top right box is region selected by cuts.



It is not sufficient to confirm the efficiency. Misidentification must also be assessed.

Plots demonstrating the LHCb RICH performance from assessment of a Monte Carlo D^* selection sample.

The efficiency to correctly identify

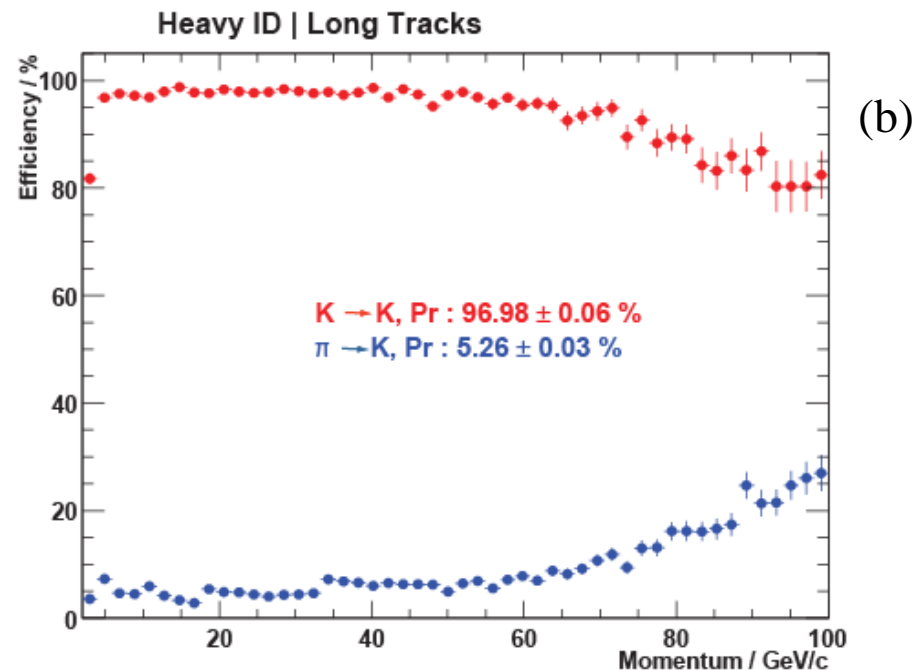
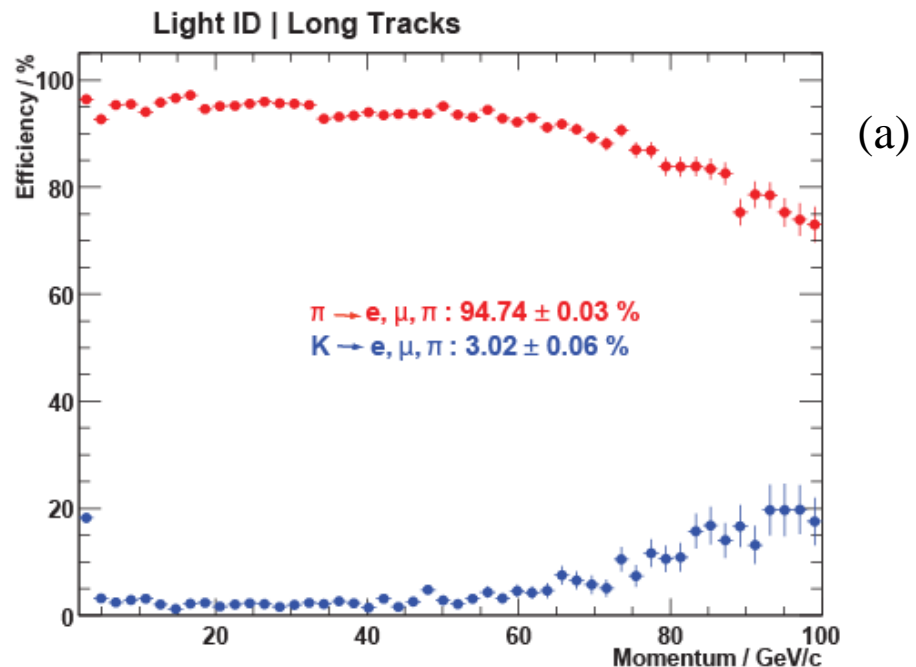
(a) pions

and

(b) kaons

as a function of momentum is shown by the **red data points**.

The corresponding misidentification probability is shown by the **blue data points**. The events selected to generate both plots possessed high quality long tracks

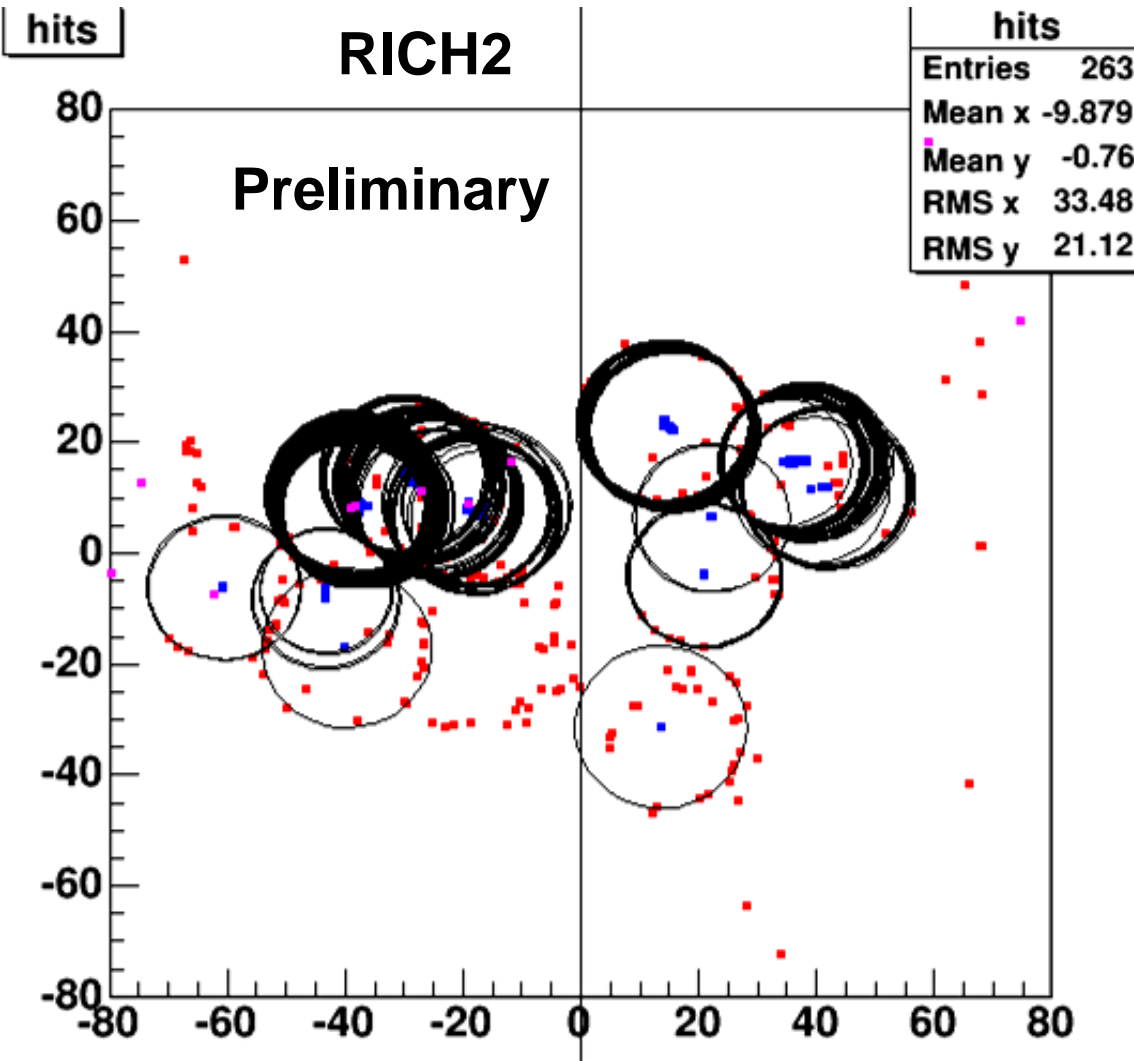


Trackless ring finding



*Paraguay v Spain:
World Cup quarter-
final match
(The ring from Spain
was diffuse when the
image was recorded)*

Trackless Ring Reconstruction_____1



**hits, Hough centres,
track impact points**

cm

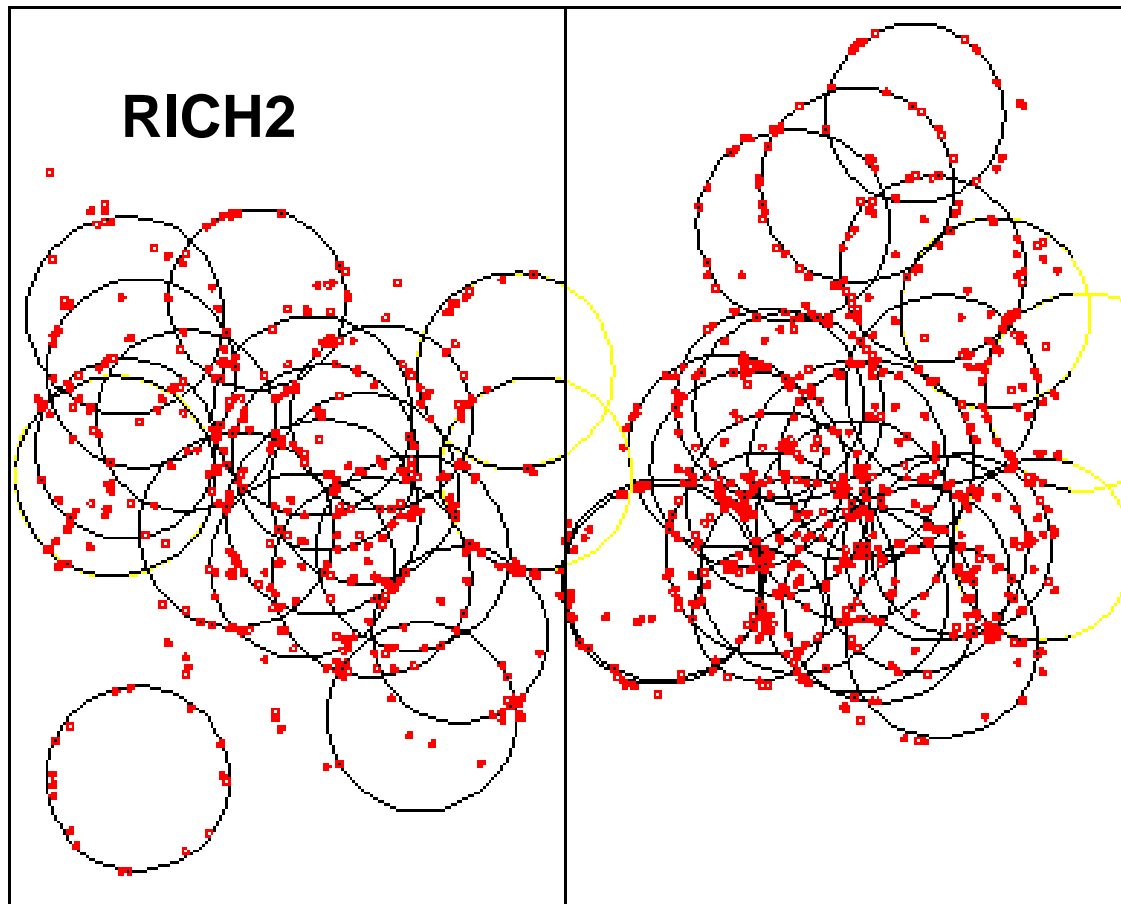
Hough transform:

Reconstruct a given family of shapes from discrete data points, assuming all the members of the family can be described by the same kind of equation. To find the best fitting members of the family of shapes the image space (data points) is mapped back to parameter space.

from Cristina Lazzeroni, Raluca Muresan, CHEP06

53

Trackless Ring Reconstruction_____2



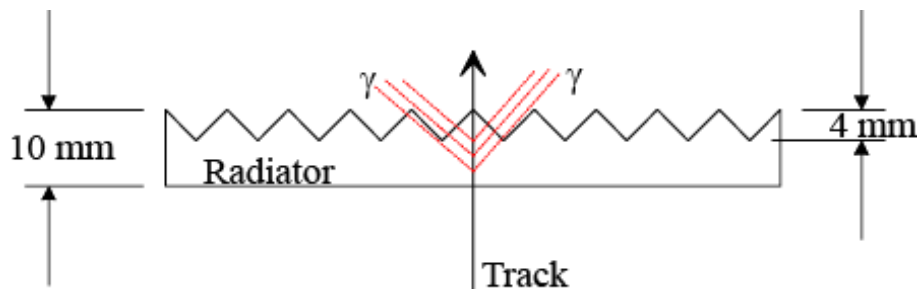
Markov rings

Metropolis- Hastings Markov chains:

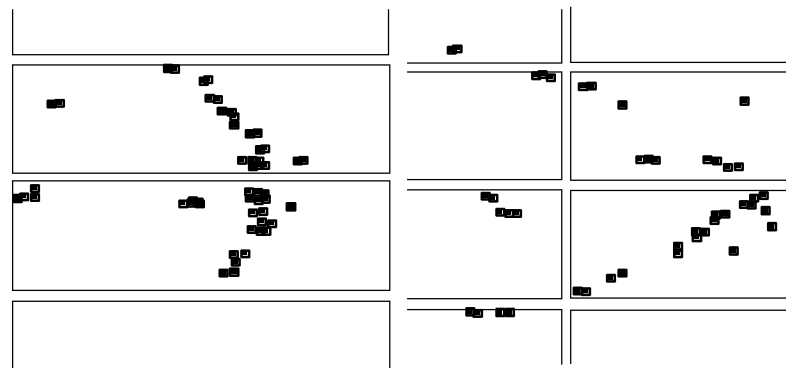
Sample possible ring distributions according to how likely they would appear to have been given the observed data points. The best proposed distribution is kept.

(Preliminary results are encouraging, work on going to assess the performance of the method)

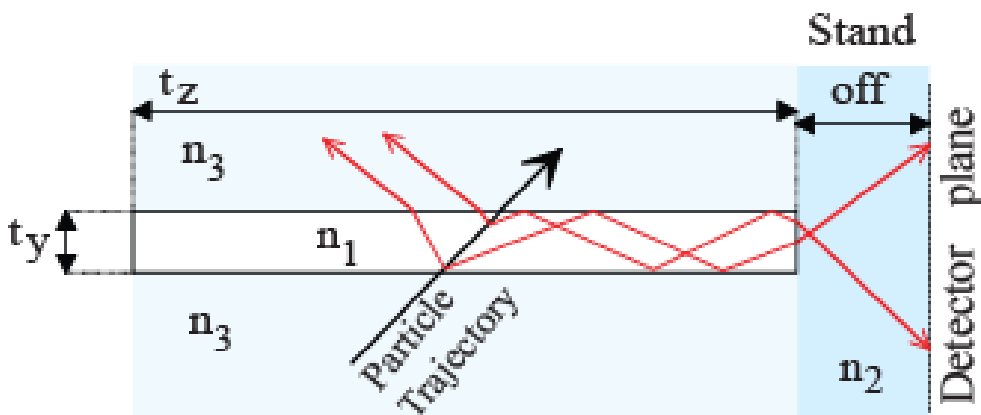
Some ways to work with quartz.



<http://www.lepp.cornell.edu/Research/EPP/CLEO/>
Nucl. Instr. and Meth. in Phys. Res. A 371(1996)79-81
CLEO at Cornell electron storage rings.



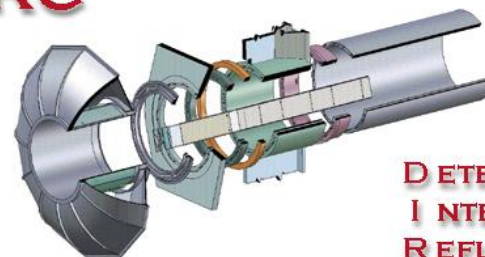
Hit patterns produced by the particle passing the plane (left) and saw tooth (right) radiators



The standoff region is designed to maximize the transfer efficiency between the radiator and the detector.

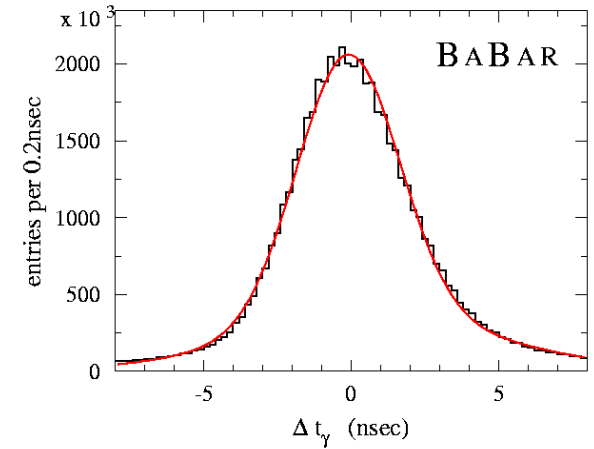
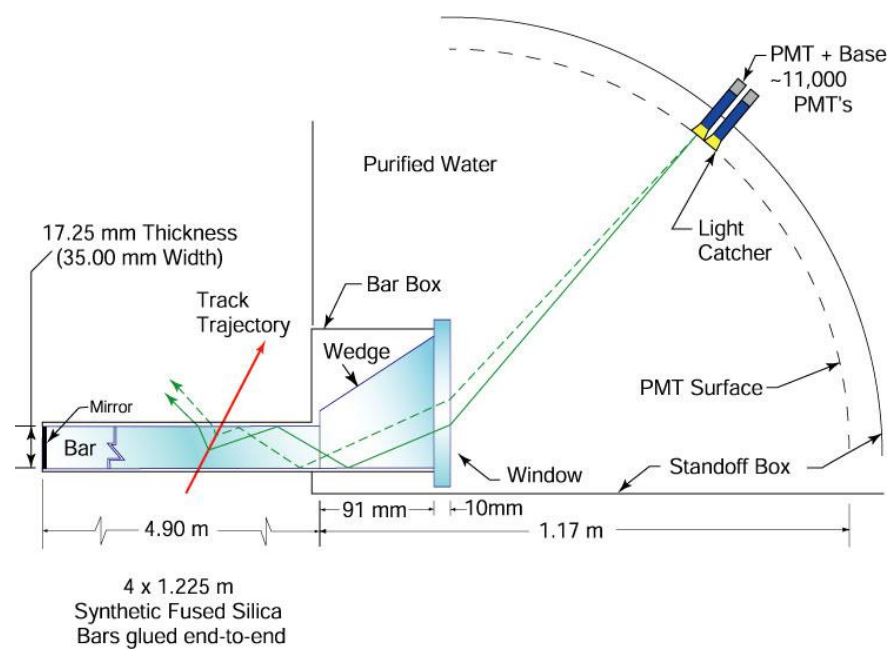
If this region has the same index of refraction as the radiator, $n_1 \cong n_2$, the transfer efficiency is maximized and the image will emerge without reflection or refraction at the end surface.

DIRC



DETECTION OF
INTERNALLY
REFLECTED
CHERENKOV LIGHT

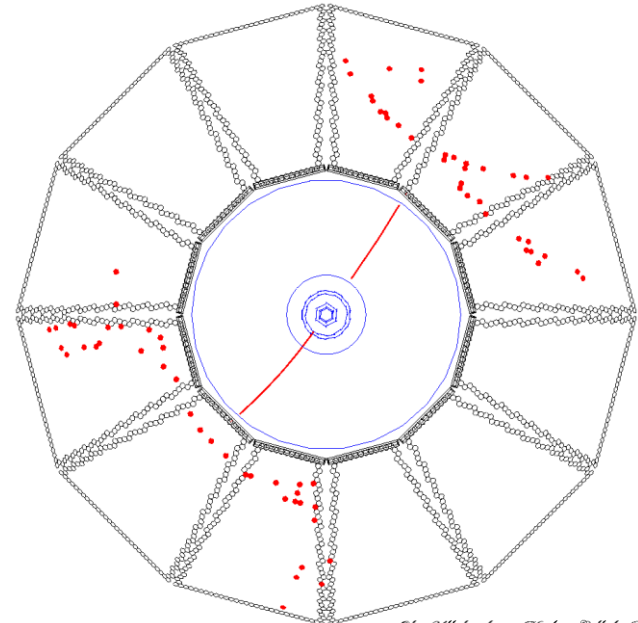
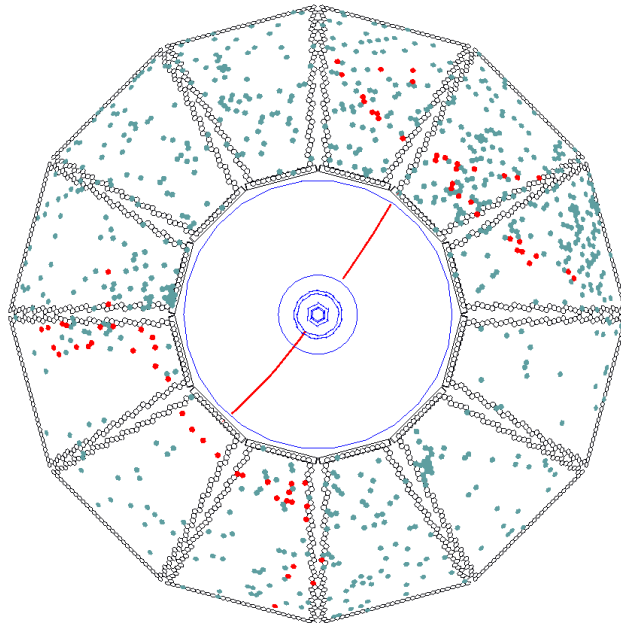
Schematic of the radiator bar for a DIRC detector.
Nucl. Instr. and Meth. in Phys. Res. A 343(1994)292-299
<http://www.slac.stanford.edu/BFROOT/www/Detector/DIRC/PID.htm>

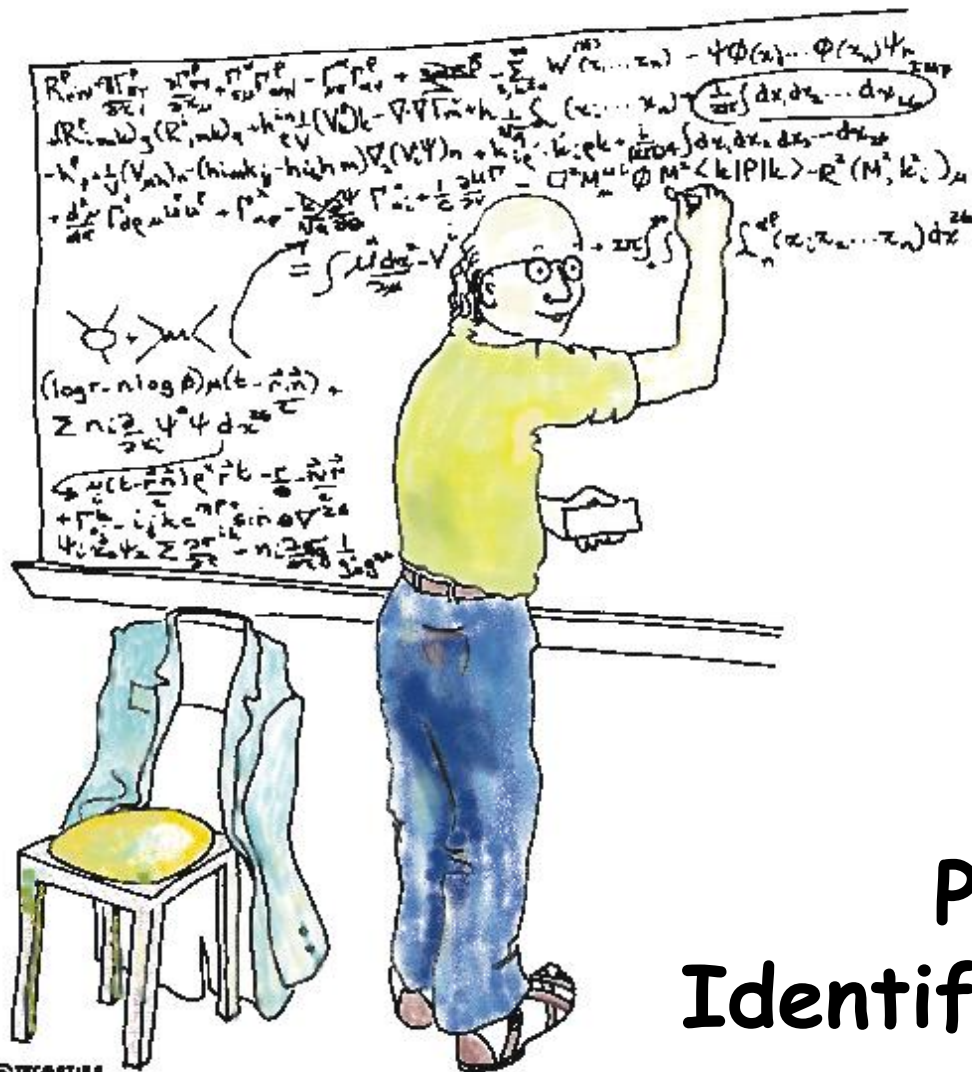


± 300 nsec trigger window
(~500-1300 background hits/event)



± 8 nsec Δt window
(1-2 background hits/sector/event)





At this point we notice that this equation is beautifully simplified if we assume that particle identification has 92 dimensions and transition radiation can be added as a subset.

Particle Identification with Transition Radiation

Transition Radiation. A primer.

A quote from

M.L.Ter-Mikaelian, High-Energy Electromagnetic Processes in Condensed Media, John Wiley & Sons, Inc, 1972, ISBN 0-471-85190-6 :

We believe that the reader will find it more convenient, however, to derive the proper formulas by himself, instead of perpetuating the particularities of all the original publications. This is due to the fact that the derivation of the corresponding formulas (for oblique incidence and in the case of two interfaces in particular), usually based on well-known methods, requires simple although time-consuming algebraic calculations.

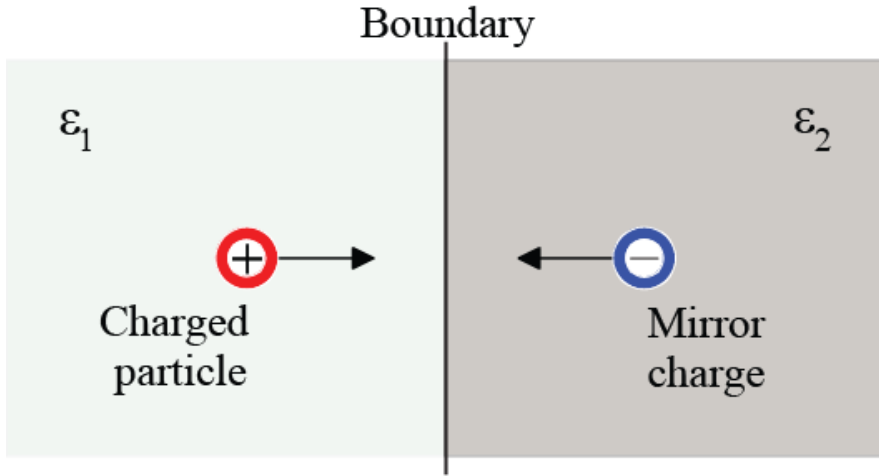


We will not do that.

V.L. Ginzburg and I.M. Frank predicted in 1944 the existence of transition radiation. Although recognized as a milestone in the understanding of quantum mechanics, transition radiation was more of theoretical interest before it became an integral part of particle detection and particle identification.

Start a little slow with Transition Radiation.

Schematic representation of the production of transition radiation at a boundary.



For a perfectly reflecting metallic surface:

$$J(\Theta) = \omega \frac{dN}{d\omega d\Omega} = \frac{\alpha}{\pi^2} \left(\frac{\Theta}{\gamma^{-2} + \Theta^2} \right)^2$$

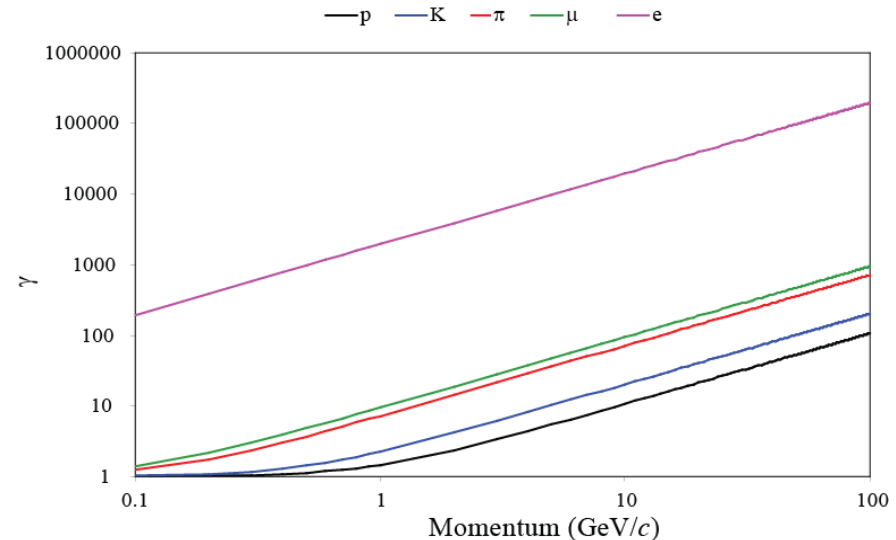
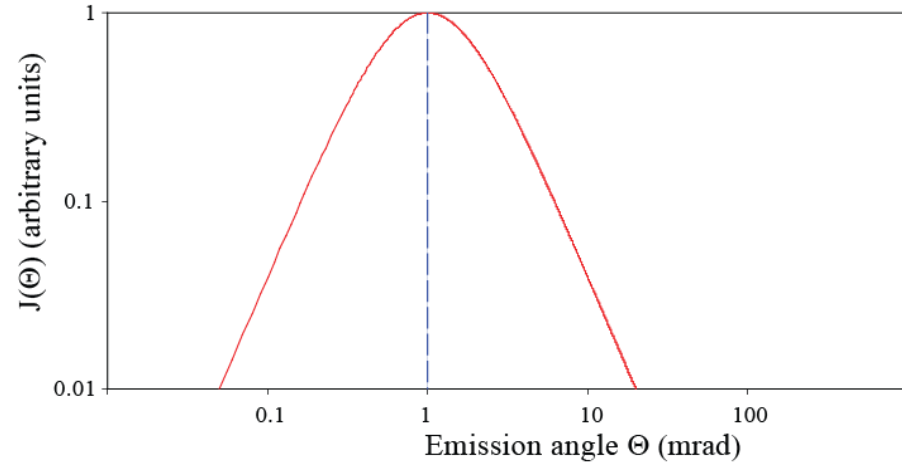
Energy radiated from a single surface:

$$\varepsilon_0 \rightarrow \varepsilon$$

$$W = \frac{1}{3} \alpha Z^2 \omega_p \gamma$$

ω_p : plasma frequency

Transition radiation as function of the emission angle for $\gamma = 10^3$



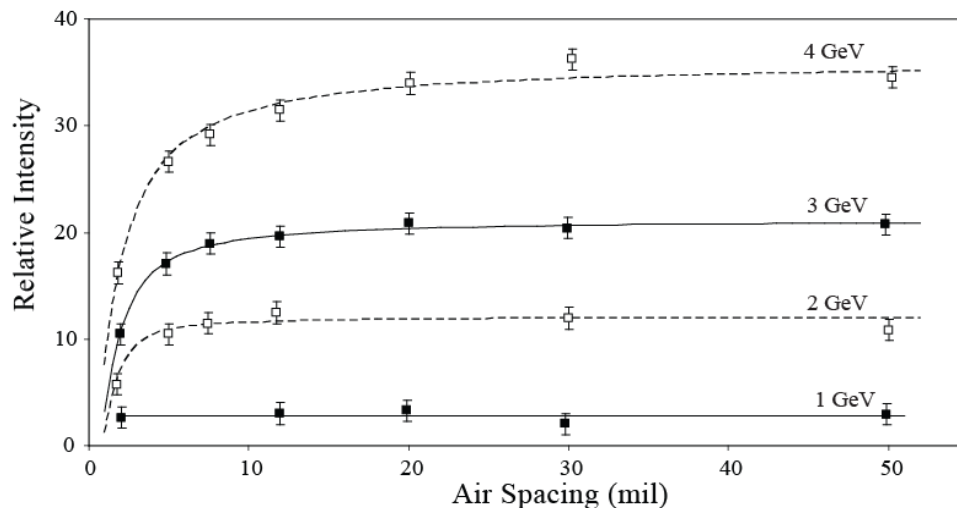
Formation zone. _____

The transient field has a certain extension:

$$\text{Formation zone : } d = \frac{2c}{\omega} \left[\gamma^{-2} + \Theta^2 + \left(\frac{\omega_p}{\omega} \right)^2 \right]$$

$$\text{for } \Theta = \gamma^{-1} \text{ or } \omega = \frac{1}{\sqrt{2}} \gamma \omega_p$$

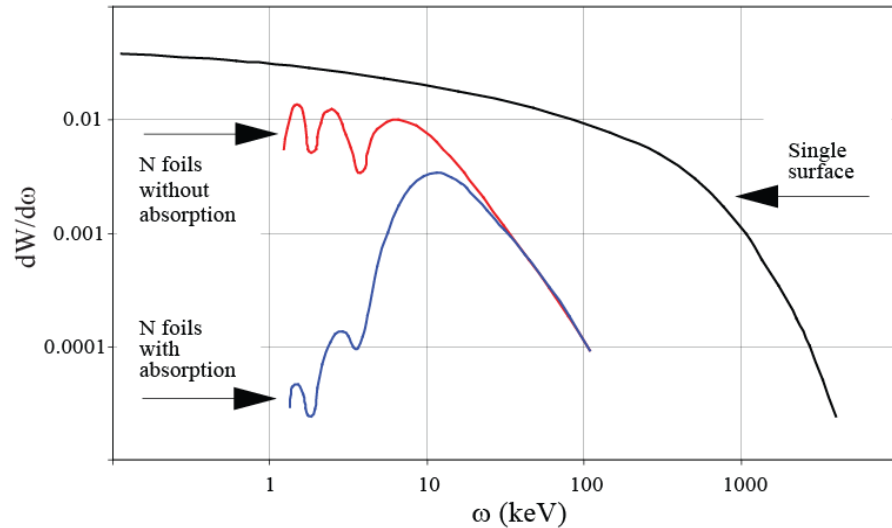
$$d(\mu\text{m}) \approx 140 \cdot 10^{-3} \frac{\gamma}{\omega_p(\text{eV})}$$



Relative intensity of transition radiation for different air spacing. Each radiator is made of 231 aluminium foils 1 mil thick. (1 mil = 25.4 μm). Particles used are positrons of 1 to 4GeV energy ($\gamma = 2000$ to 8000). Phys. Rev. Lett. 25 (1970) 1513-1515

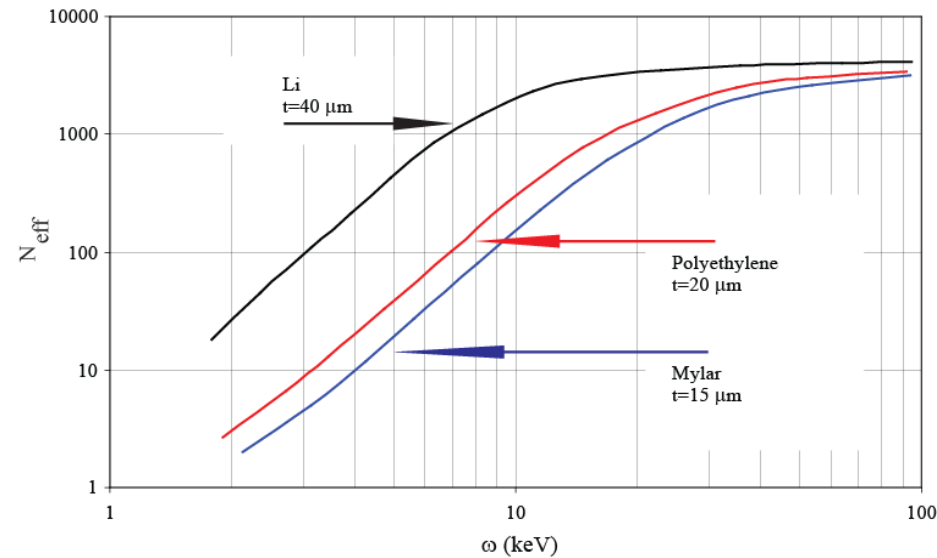
1. Transition radiation is **a prompt signal**.
2. Transition radiation is **not a threshold phenomenon**.
3. The **total radiated power** from a single interface is **proportional to γ** .
4. The **mean emission angle** is **inversely proportional to γ** .

I will only cover detectors working in the X-ray range.



Intensity of the forward radiation divided by the number of interfaces for $20\ \mu\text{m}$ polypropylene ($\omega_p = 21\ \text{eV}$) and $180\ \mu\text{m}$ helium ($\omega_p = 0.27\ \text{eV}$).

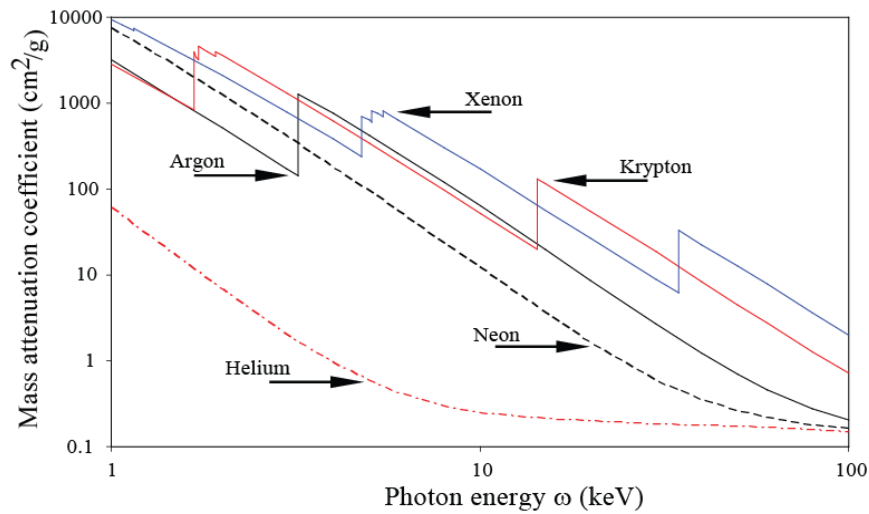
L. Fayard, Transition radiation, les editions de physiques, 1988, 327-340



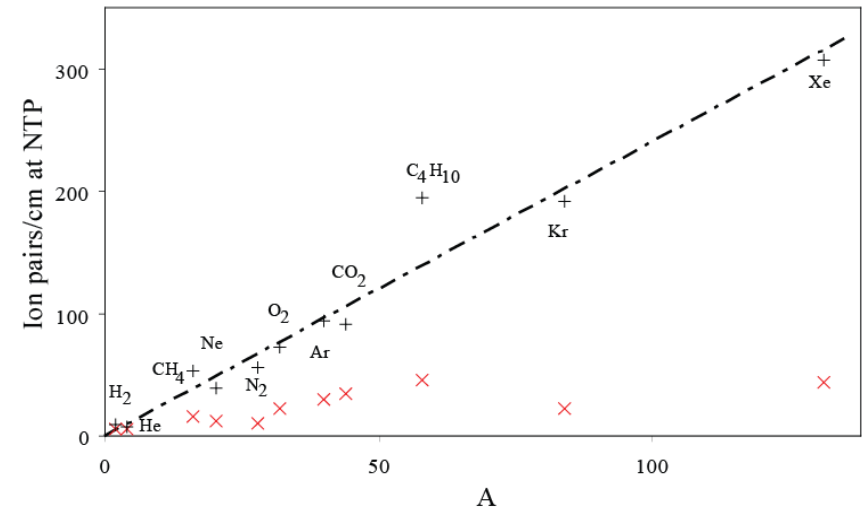
The effective number of foils in a radiator as function of photon energy.

Nucl. Instrum. Methods Phys. Res., A: 326(1993) 434-469

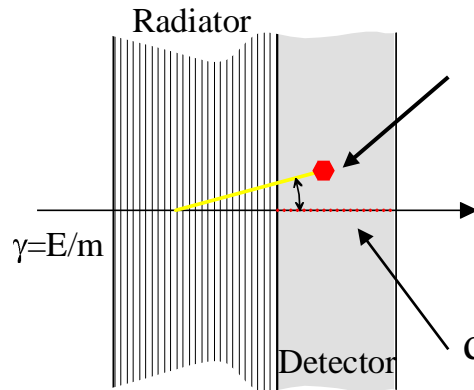
An efficient transition radiation detector is therefore a large assembly of radiators interspaced with many detector elements optimised to detect X-rays in the 10 keV range.



X-ray mass attenuation coefficient, μ/ρ , as function of the photon energy. $\mu/\rho = \sigma_{\text{tot}}/uA$, where $u = 1.660 \cdot 10^{-24}$ g is the atomic mass unit, A is the relative atomic mass of the target element and σ_{tot} is the total cross section for an interaction by the photon.



The () primary and (+) total number of ion pairs created for a minimum ionizing particle per cm gas at normal temperature and pressure as function of A .



~ 22 eV/ion pair. 10 keV X-ray \rightarrow ~ 450 ion pairs

$dE/dX_{\text{MIP}} \sim 310$ ion pairs/cm * relativistic rise ~ 550 ion pairs/cm

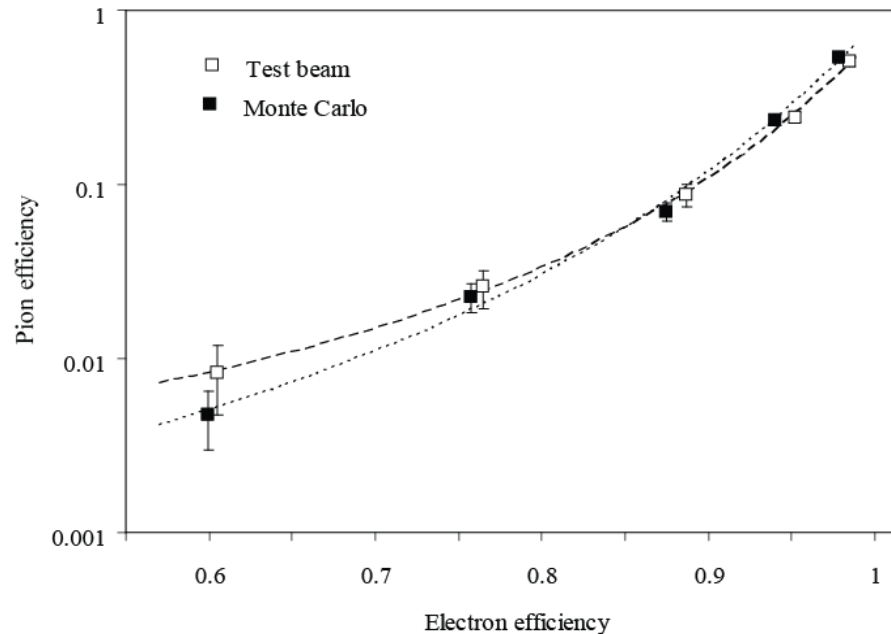
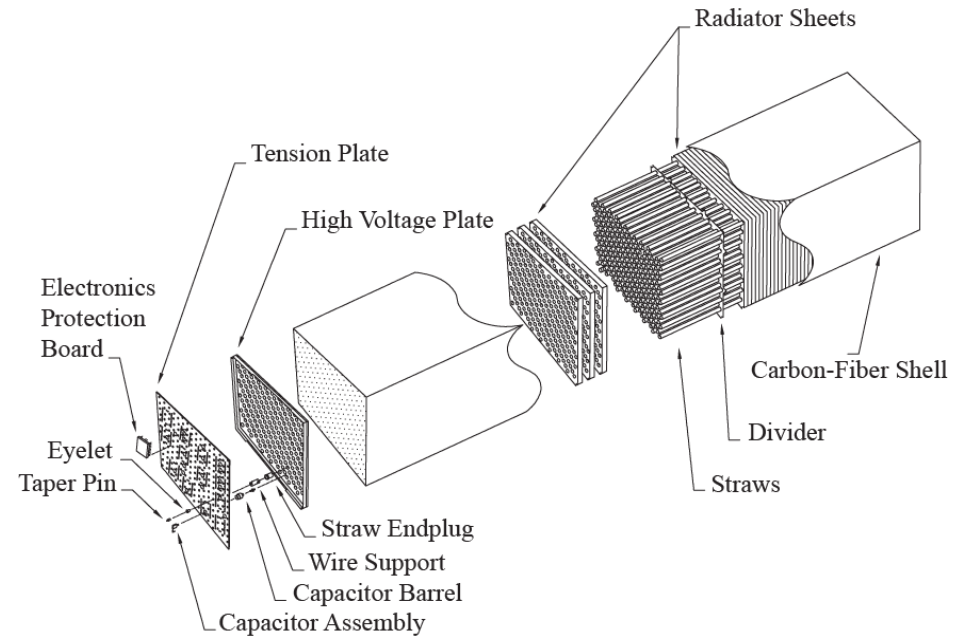
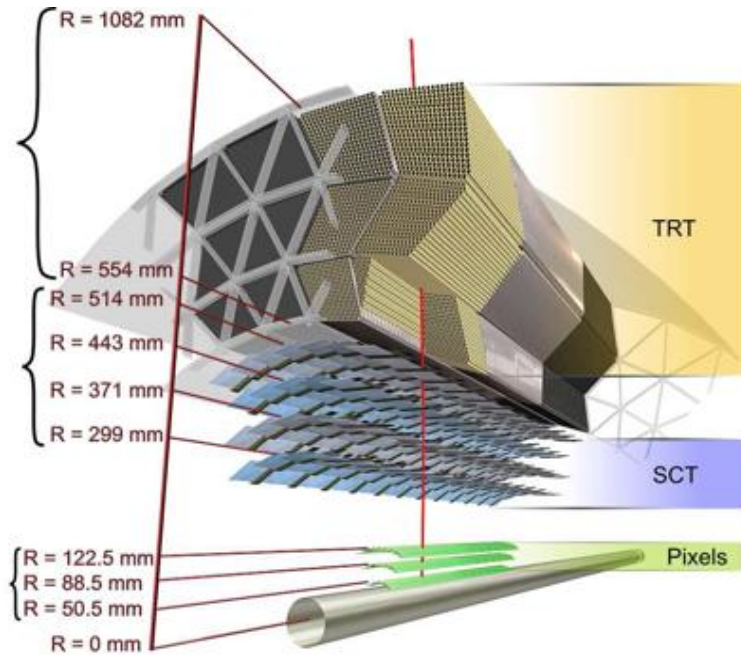
Not to scale

10-15 mm
Xe

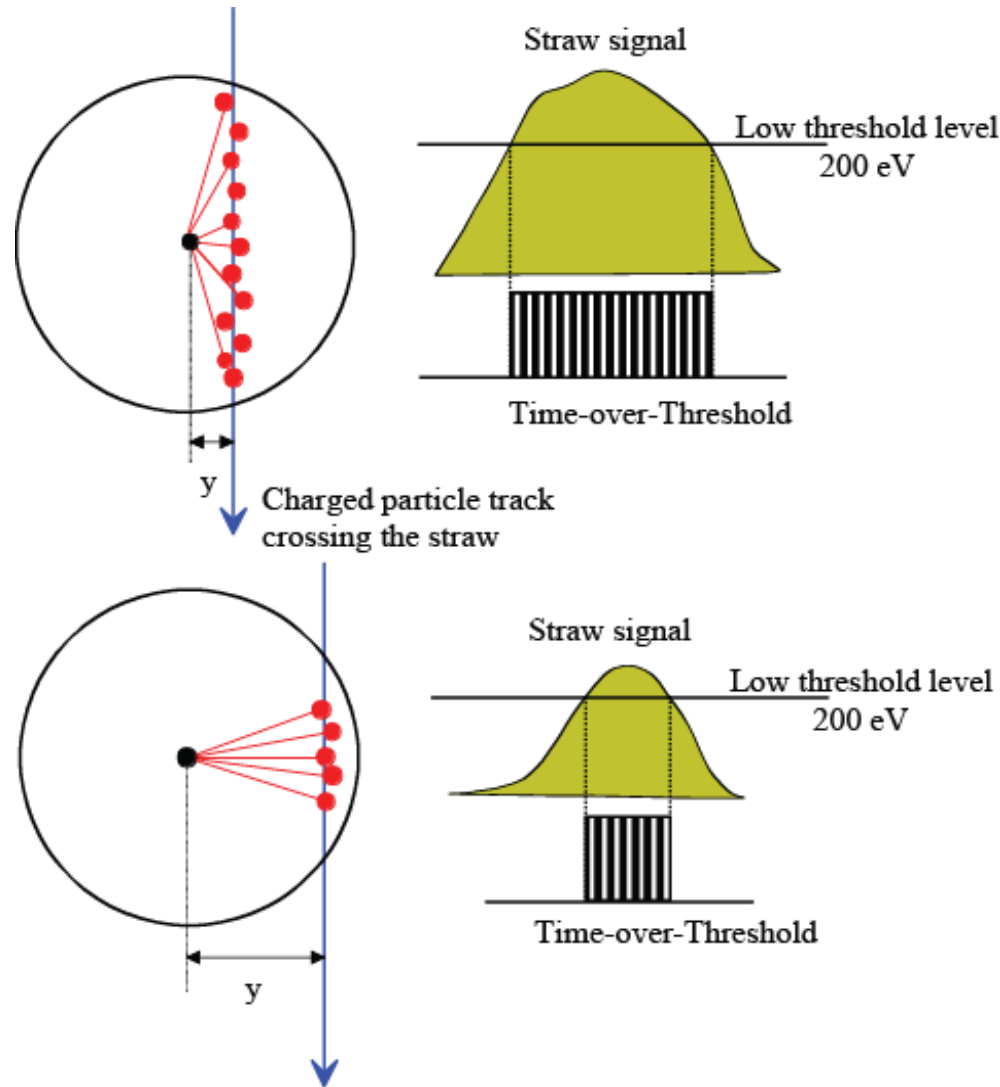
Additional background might arise from curling in a magnetic field, Bremsstrahlung and particle conversions.

Use ATLAS as an example.

<http://atlas.web.cern.ch/Atlas/Collaboration/>



Normalized Time-over-Threshold in TRT



Time-over threshold depends on

- Energy deposited through ionization loss
- Depends on particle type
- Length of particle trajectory in the drift tube

- Study uses only low-threshold hits to avoid correlation with PID from high-threshold hit probability

Electron PID from the TRT

Transition radiation (depending on Lorentz γ) in scintillating foil and fibres generate high threshold hits in TRT

Turn-on for e^\pm around $p > 2$ GeV

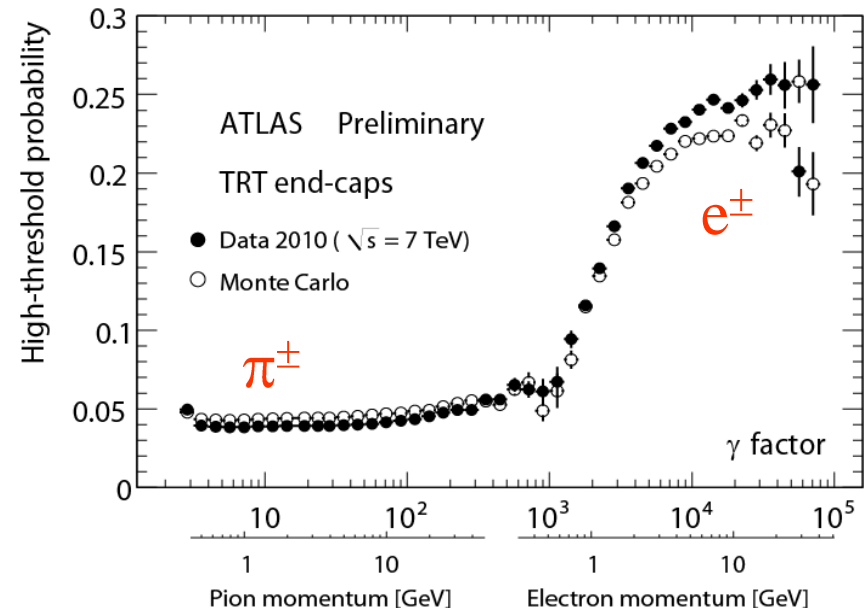
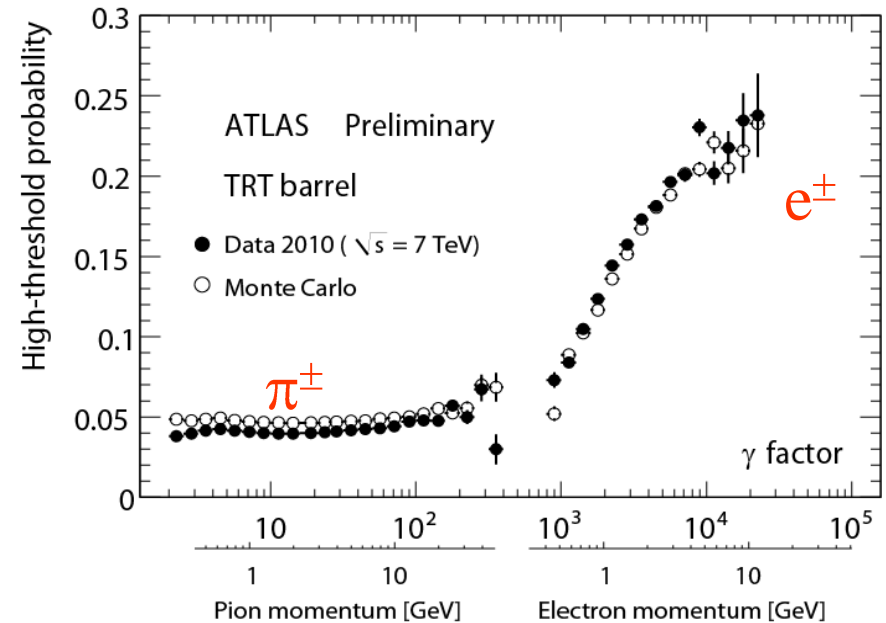
Photon conversions supply a clean sample of e^\pm for measuring HT probability at large γ

Tag-and-probe: Select good photon conversions, but require large HT fraction only on one leg

π^\pm sample for calibration at small γ

Require B-layer hit

Veto tracks overlapping with conversion candidates



That was all
planned for this lecture



FIFTH CERN-FERMILAB HADRON COLLIDER PHYSICS SUMMER SCHOOL

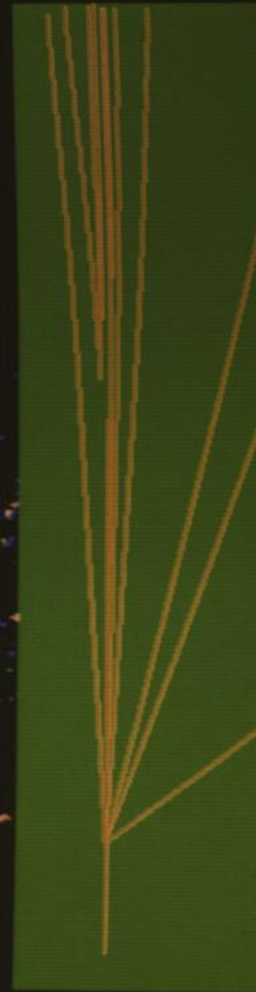
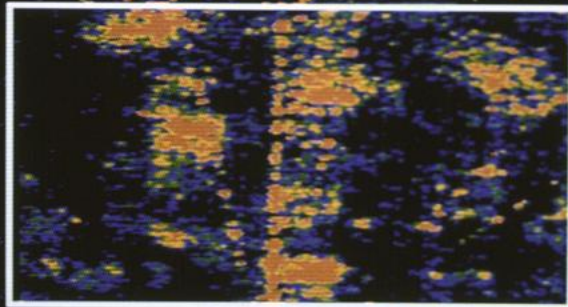
August 16-27, 2010

PARTICLE IDENTIFICATION OLAV ULLALAND (CERN)

Mainly nuts and bolts
and how they could fit
together.



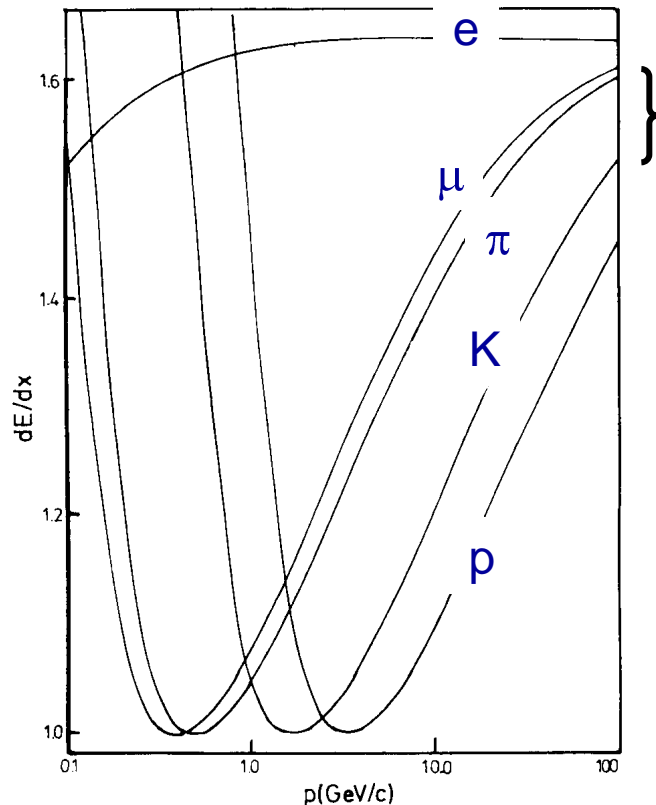
Particle
Identification
with
energy
loss
measurement
 dE/dX



CERN-PHOTO-8305795

Particle identification through ionization losses.

Energy loss detection with MWPC started more or less at the same time as the first MWPC was operational.



Average energy loss in
80/20 Ar/CH₄ (NTP)
(J.N. Marx, Physics today, Oct.78)

π/K separation at a 2σ level
requires a dE/dx resolution
in the range of 2 to 3% -
depending on the momentum
range.

but:

GE LUCTUATIONS

Show me another
of them tails!



!WARNING! !WARNING! !WARNING!

*Yeah, just
gloat about
your tail. It
still looks like a
Vavilov to me!*



**Before attempting to assess a
Charged Particle Identification
Estimate from energy loss of a
charged particle in a thin¹ detector,
read and (if possible) understand:**

W.W.M. Allison and J.H. Cobb, *Relativistic
Charged Particle Identification By Energy
Loss*, Ann. Rev. Nucl. Part. Sci. 1980. 30:253-
98

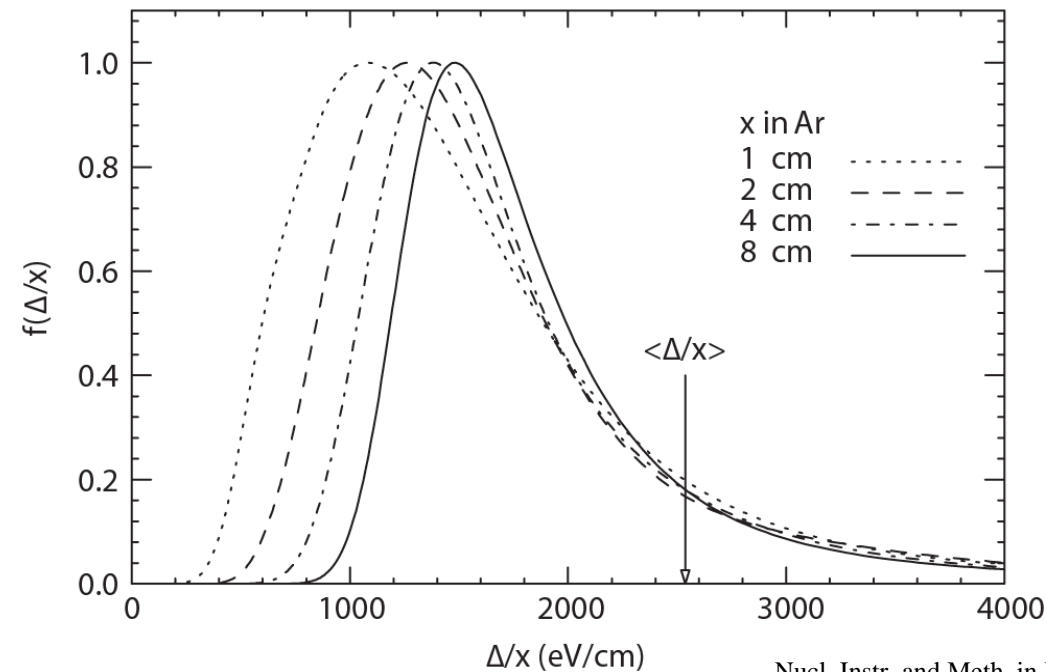
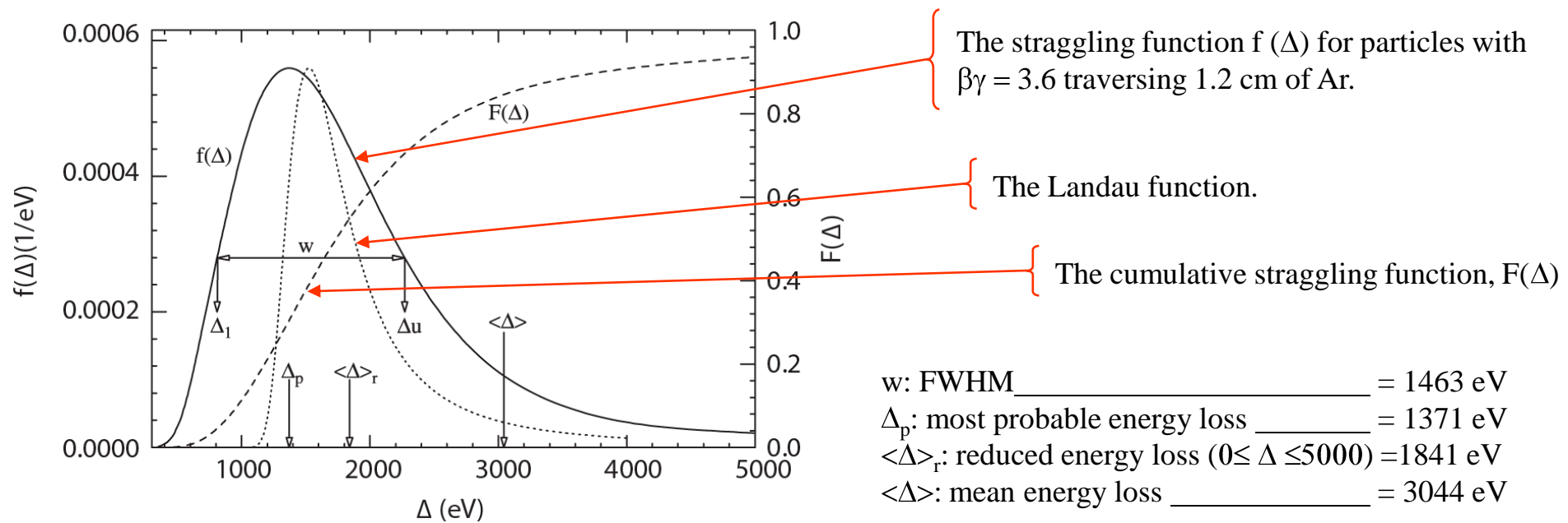
and

H. Bichsel, *A method to improve tracking and
particle identification in TPC and silicon
detectors*, Nucl. Instr. and Meth. in Phys. Res.
A 562(2006)154-197

and references therein.

!WARNING! !WARNING! !WARNING!

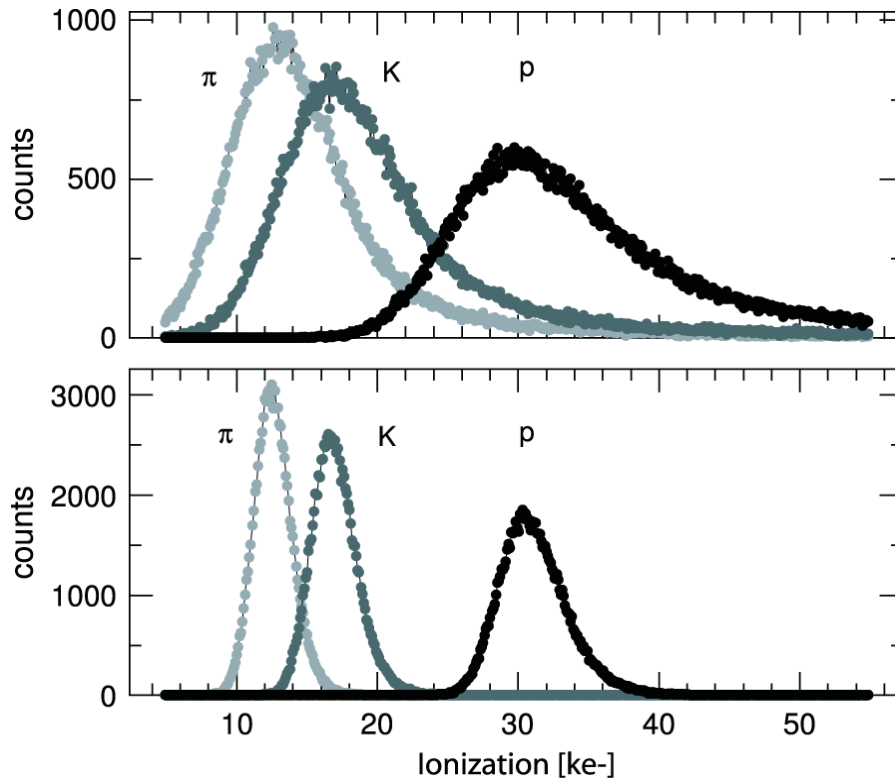
¹ Thin as in NOT a Totally Absorbing Calorimeter 70



In addition, there is:

- ☐ drift of electrons
- ☐ diffusion
- ☐ magnetic field
- ☐ gas amplification
- ☐ electronics
- ☐

Truncated mean.



Example of the truncated mean method.

The ionization distributions of 0.8 GeV/c particles in a single 150 μm silicon sensor.

The truncated mean of three out of four samples of 150 μm silicon.

NIM A 568(2006)359-363

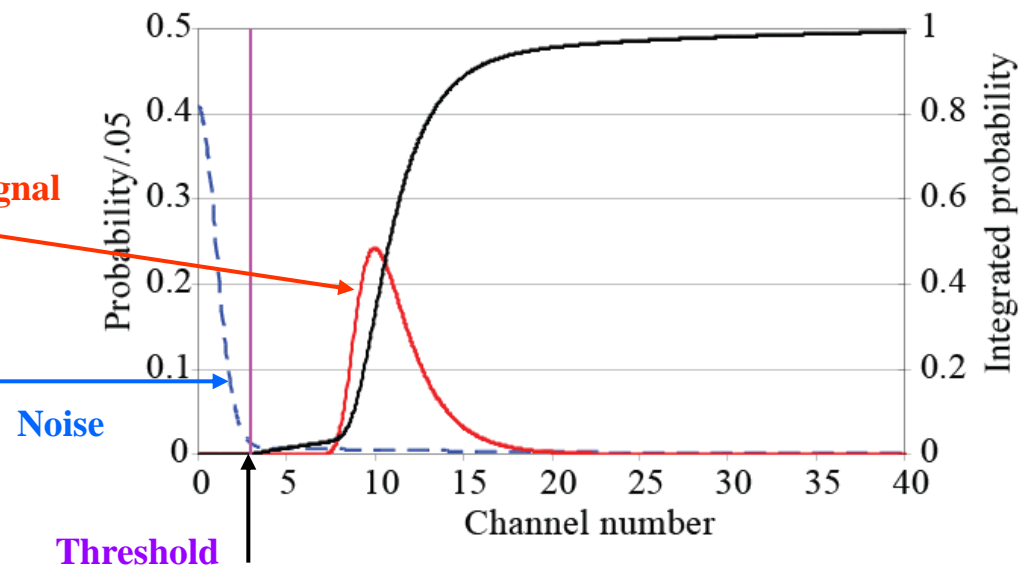
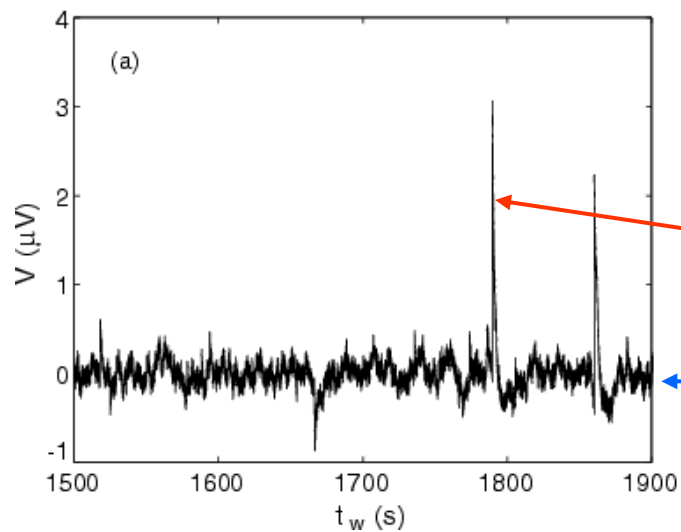
Tests like

Maximum Likelihood Method

or

Kolmogorov-Smirnov tests

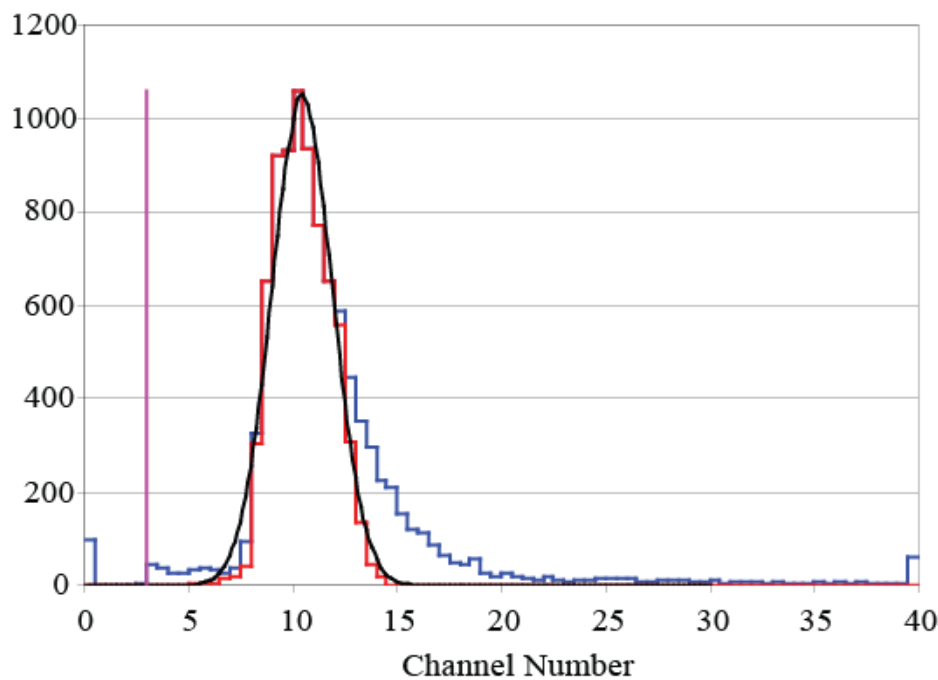
might give a better result.



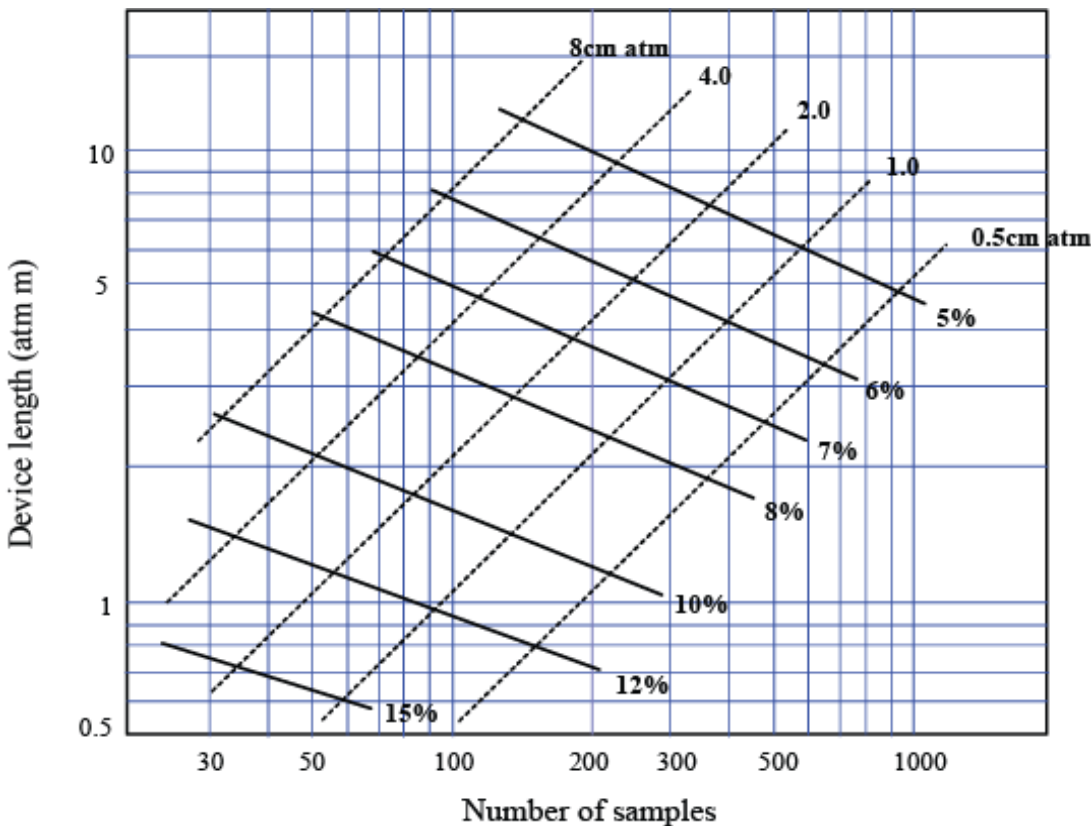
Truncated mean of
100 measurements:

20% highest
5% lowest

σ : 1.5



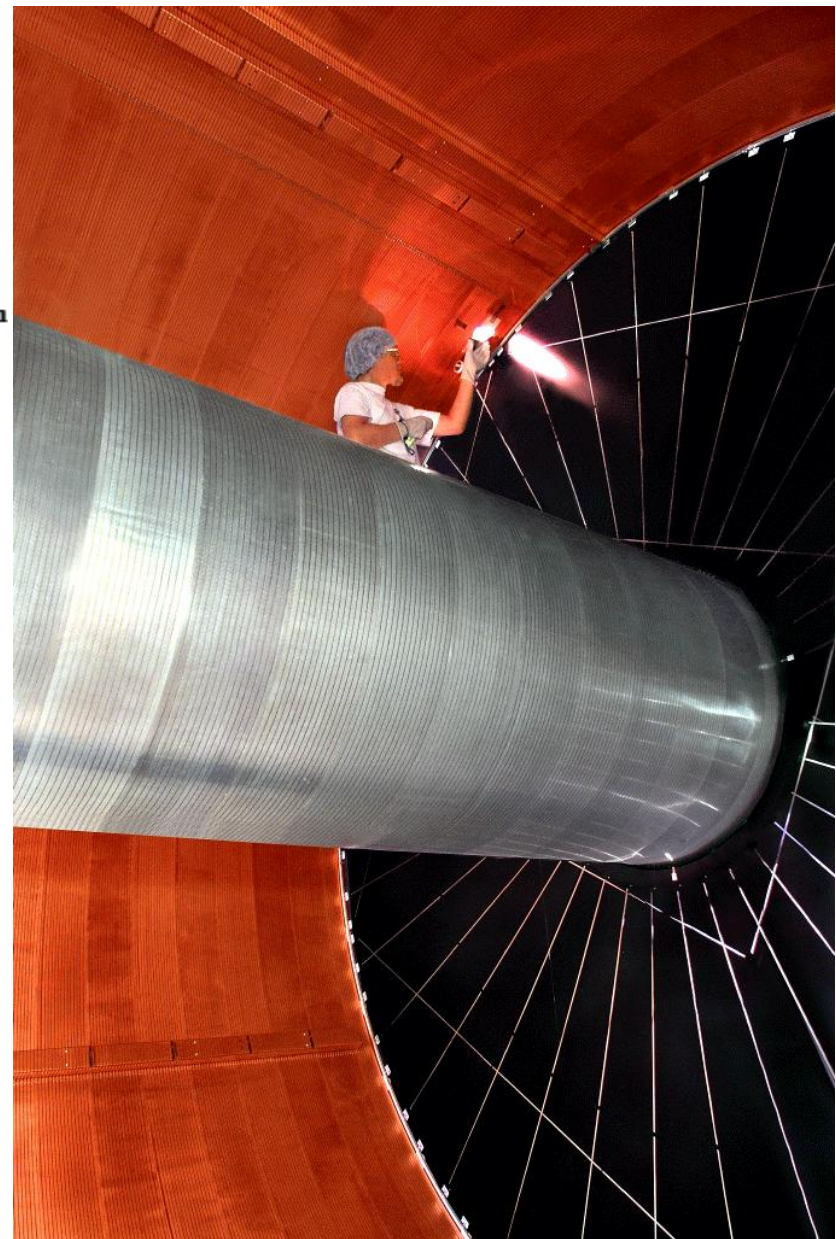
How large must/should a detector be?

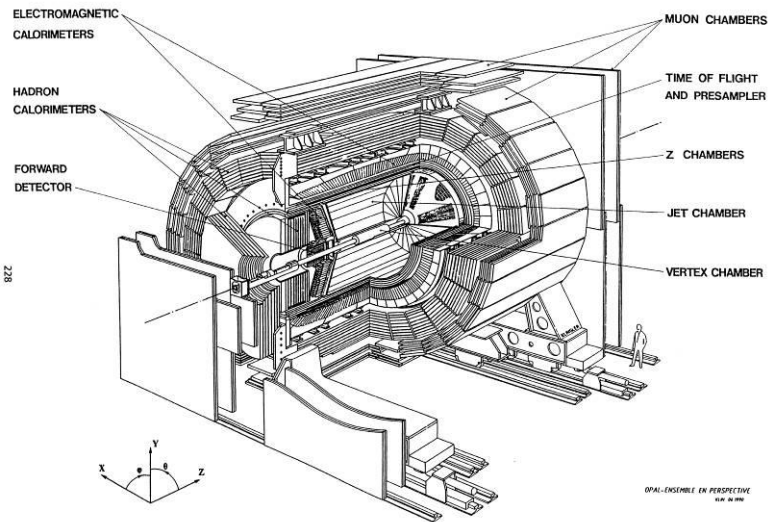


The ionization resolution (% FWHM) of a multisampling detector filled with pure argon calculated with the PAI model for $\beta\gamma = 100$. Likelihood method is used.

(PAI: Photon Absorption Ionization)

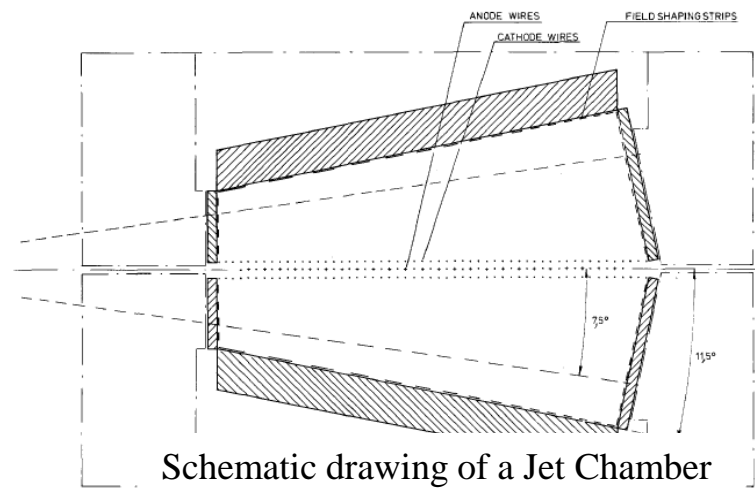
from W.W.M.Allison and J.H. Cobb





OPAL: The OPAL Detector (an Omni Purpose Apparatus for Lep)

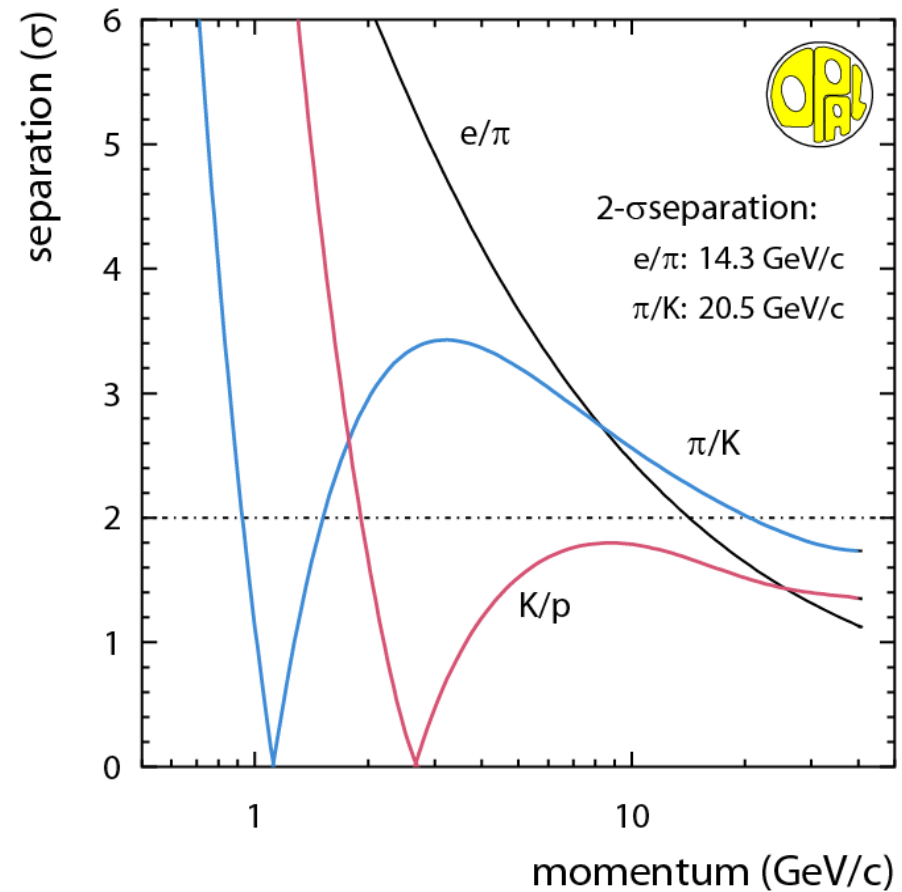
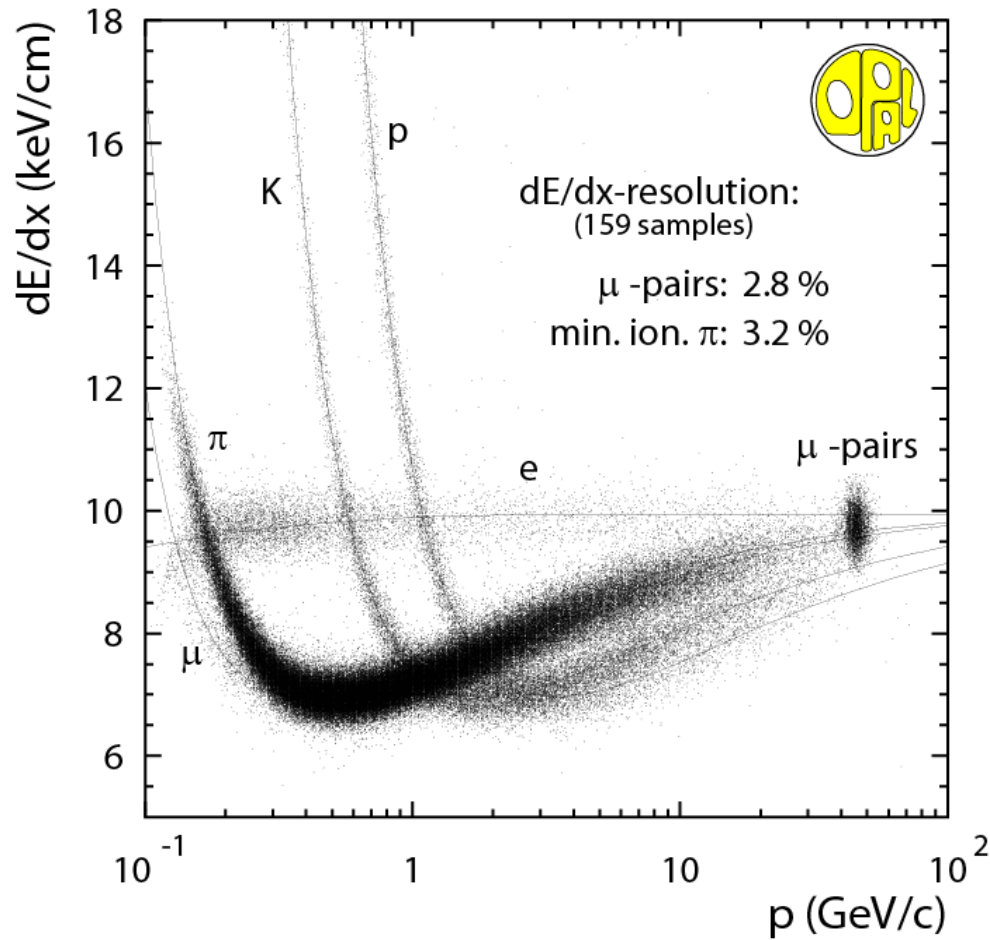
OPAL at LEP



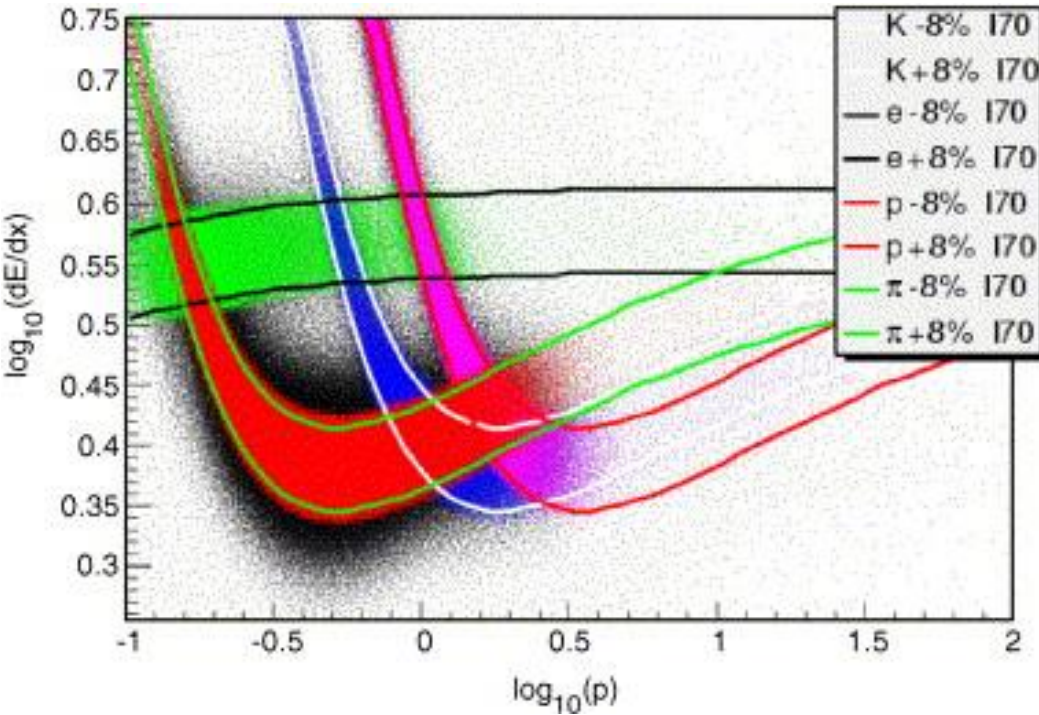
Schematic drawing of a Jet Chamber



OPAL at LEP results for dE/dX with 159 samples.

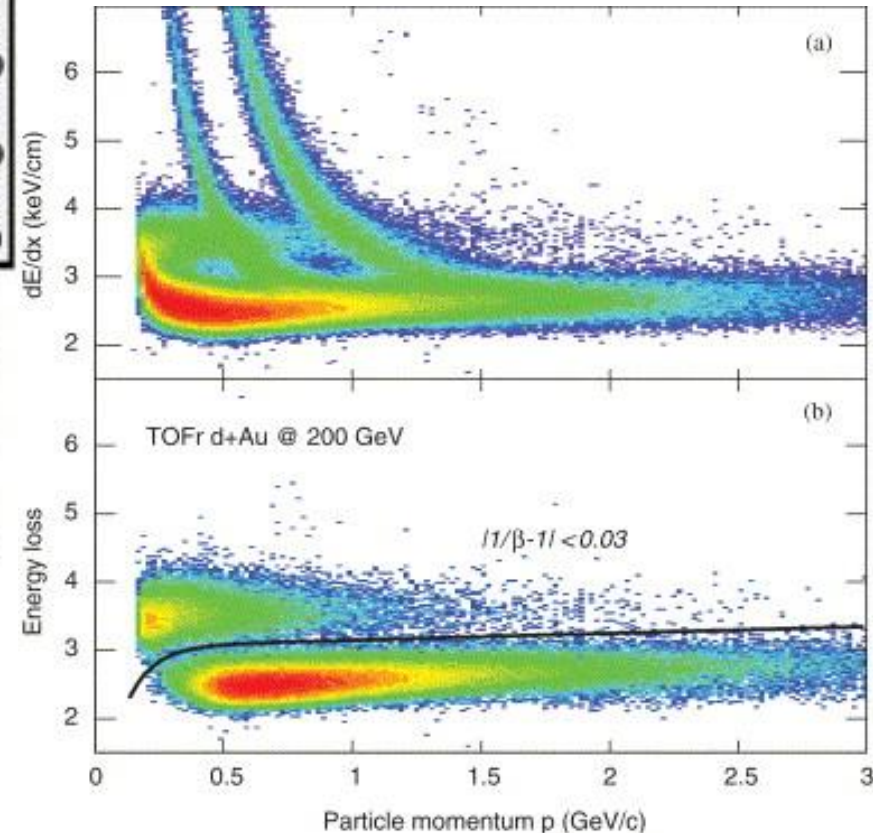


the STAR experiment



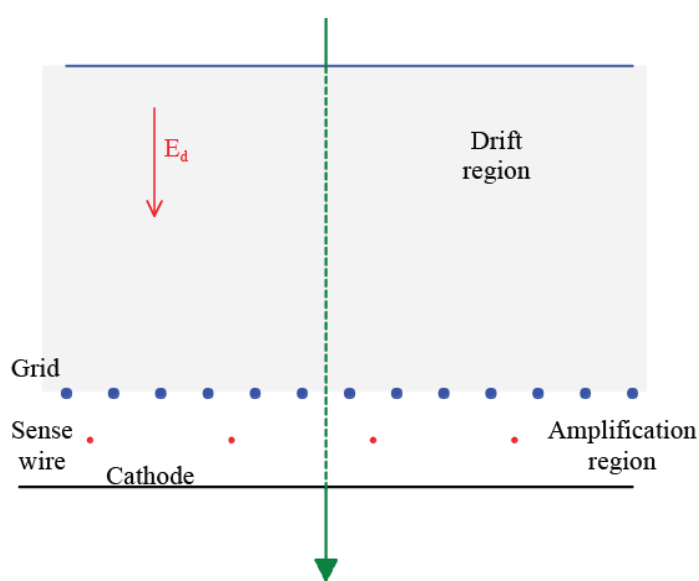
Distribution of $\log_{10}(dE/dx)$ as a function of $\log_{10}(p)$ for electrons, pions, kaons and (anti-)protons. The units of dE/dx and momentum (p) are keV/cm and GeV/ c , respectively. The colour bands denote within $\pm 1\sigma$ the dE/dx resolution.

I70 means Bichsel's prediction for 30% truncated dE/dx mean.

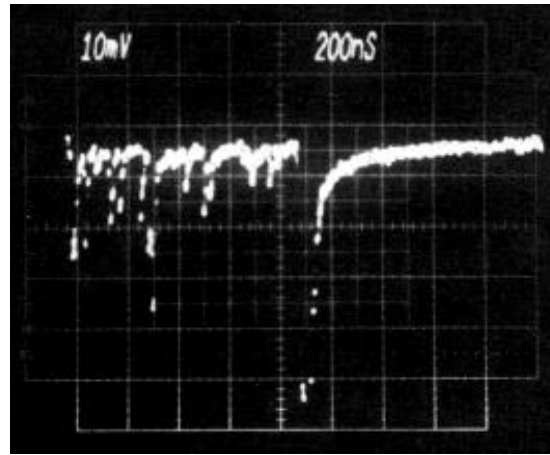


dE/dx in the TPC vs. particle momentum (p) without (upper panel) and with (lower panel) TOFr velocity cut of $|1/\beta - 1| < 0.03$.

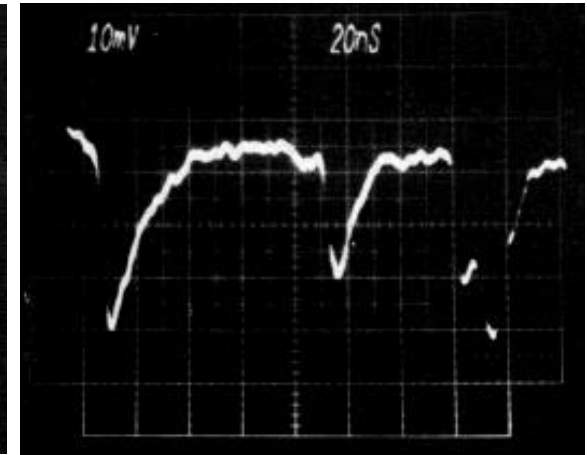
How to limit the Landau fluctuations.



Principle sketch of the
Time Expansion Chamber (TEC)
A.H. Walenta, IEEE Trans. Nucl. Sci. 26-1(1979)73



Full scale



Expanded view

Signal for a single β^- (^{90}Sr) crossing the chamber.

The main idea:

The primary ionisation is governed by Poisson statistics.

The drift region is made such that the electron drift velocity is slower than the saturated drift velocity. Thereby the separation between the primary clusters is made longer in time.

At the sense wire, each well separated cluster is amplified, detected and counted.

The spoiler:

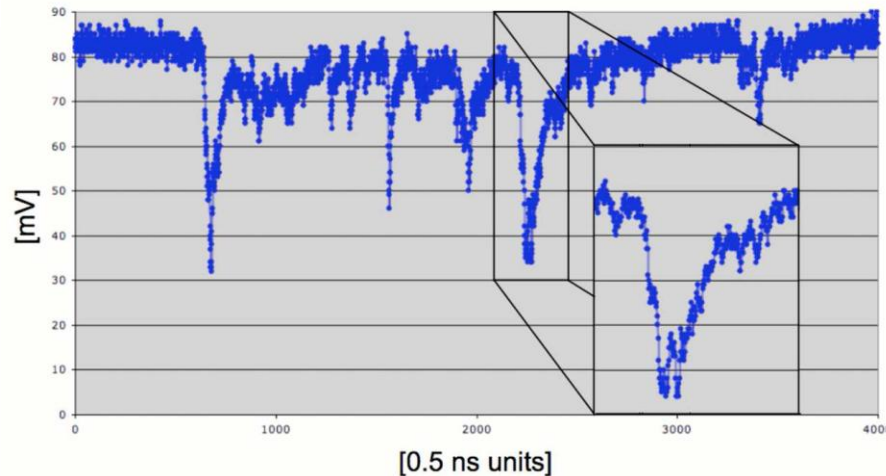
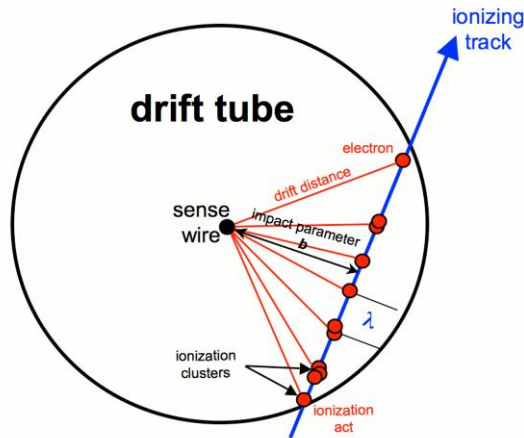
Longitudinal diffusion, detector resolution, detector dynamics, reduced relativistic rise, earlier Fermi saturation, two-track resolution,

A possible way out.

31 March 2009

Version 1.2

(4 April 09)



Digitized pulse shape showing individual clusters.

Drift tube

$r \sim 2 \text{ cm}$

Gas:

He/Isobutane : 90/10

Sampling rate:

$> 1 \text{ GSa/s}$

$$n_{clusters} = \frac{2\sqrt{r^2 - b^2}}{\lambda \beta \gamma \sin \theta} \text{ for } b = \int_{t_0}^{t_1} v_{drift} dt$$

λ : mean free path

The total number of ionization clusters along the trajectory of a charged track, for all the hit cells, one can reach a relative resolution of $1/\sqrt{N}$.

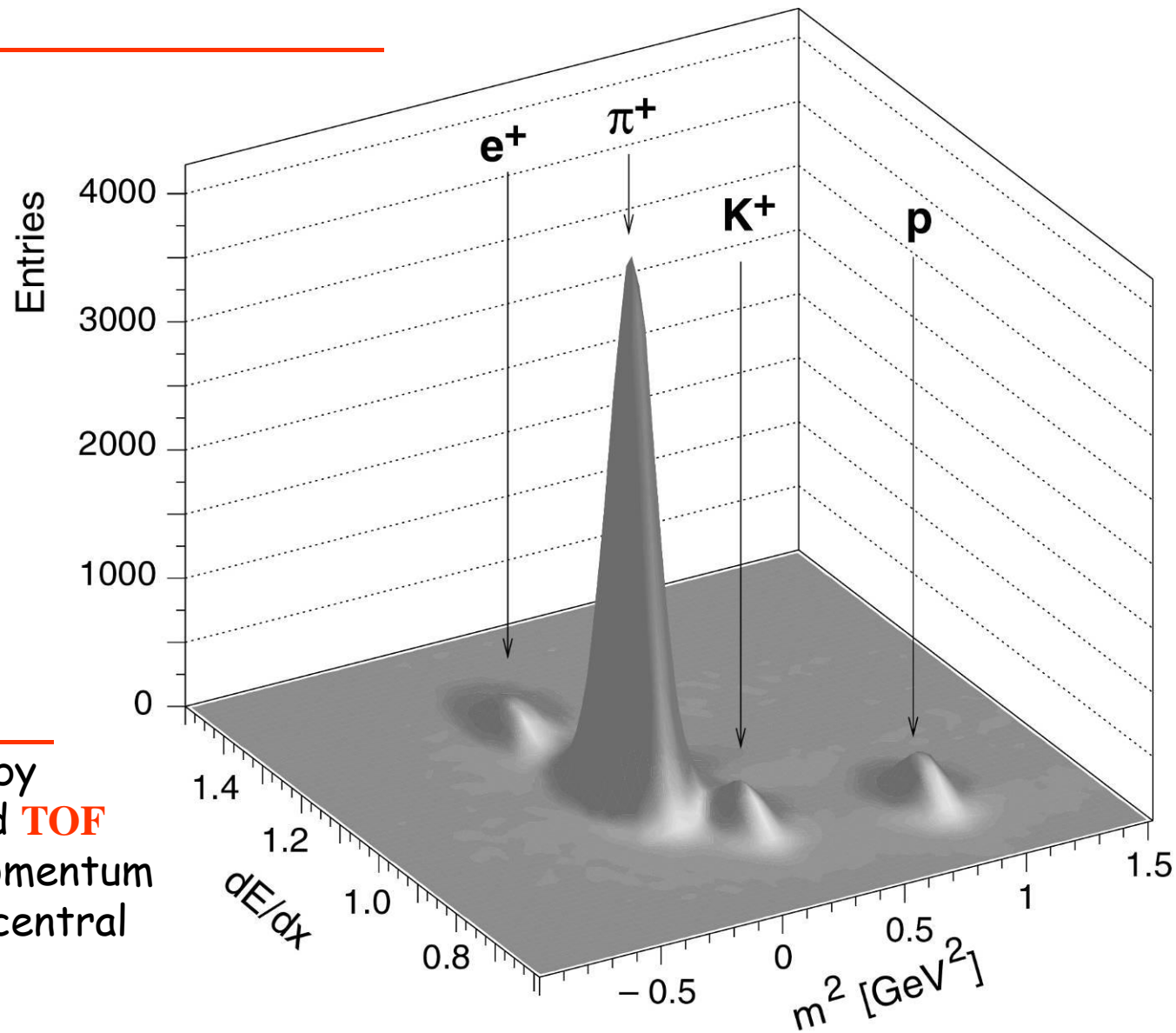
For the proposed helium gas mixture, $N = 12.5/\text{cm}$ and a track length of 1.3 m, one could, in principle, obtain a relative resolution of 2.5%.

see also:

G. Malamud et al., A study of relativistic charged particle identification by primary cluster counting, NIM A 372(1996)19-30

and - if we combine?

NA49
Particle identification by
simultaneous dE/dx and **TOF**
measurement in the momentum
range 5 to 6 GeV/c for central
Pb+Pb collision

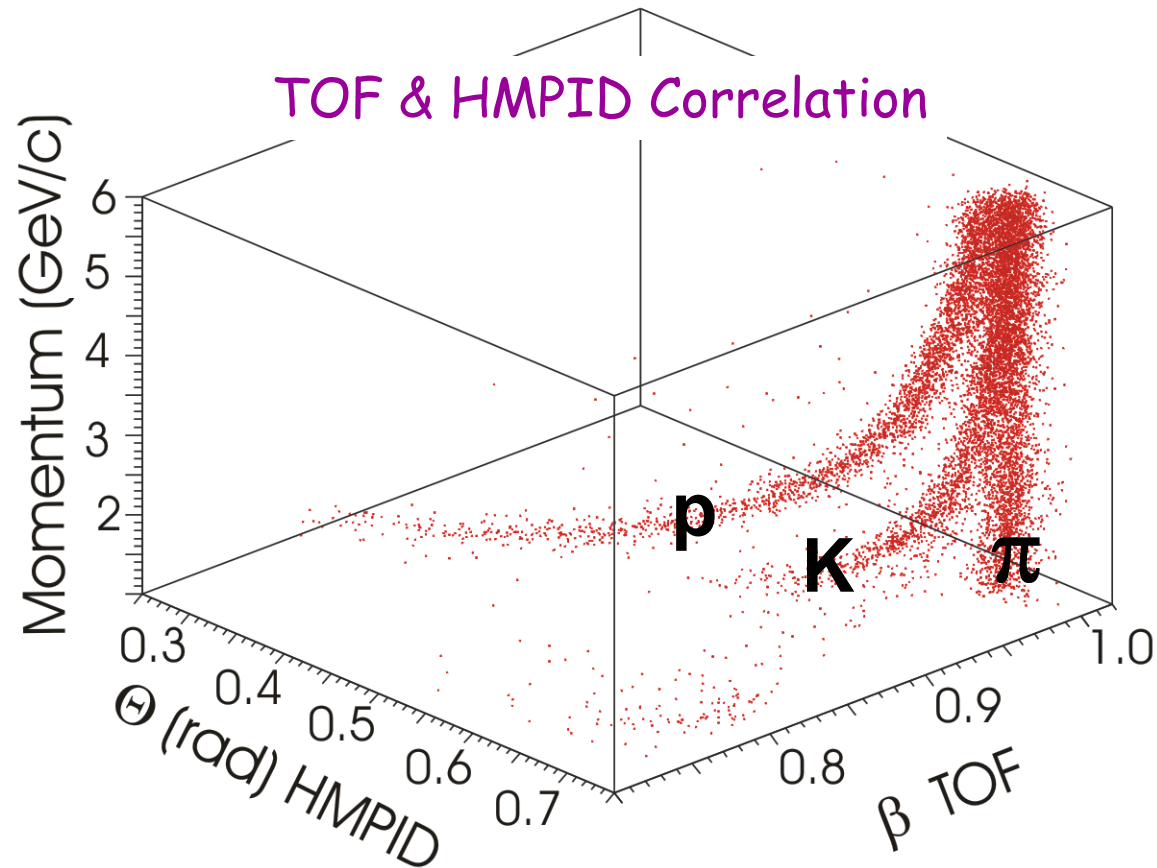


NA49, CERN-EP/99-001

what is expected at ALICE combining RICH and TOF

PID Performance

For $p > 2.5 \text{ GeV}/c$
K-ID also improved with
HMPID info
(on $\sim 8\%$ of the central
acceptance)



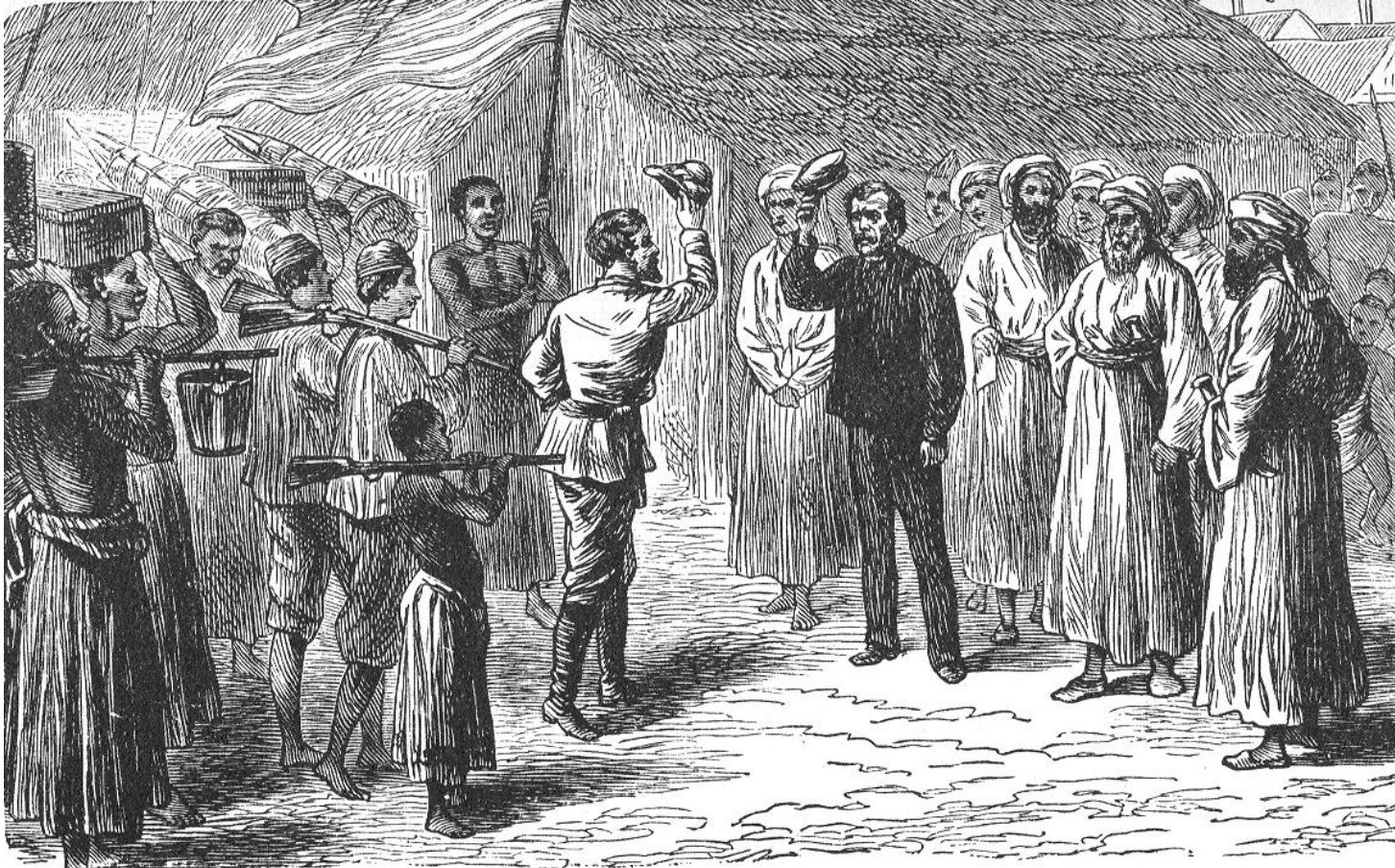
π and protons ID "easier" task, up to $5 \text{ GeV}/c$ with:

PID Efficiency $> 90\%$ and $< 10\%$ Contamination for π

PID Efficiency $90\%-70\%$ and $< 10\%$ Contamination for protons

For the first time, in full,
the accurate salutation:

*Doctor Livingstone,
you finally
identified
a muon,
I presume?*



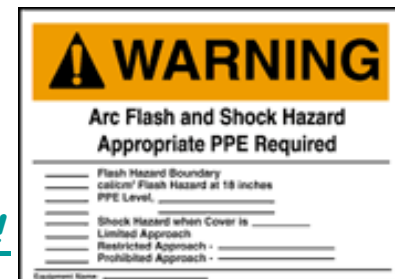
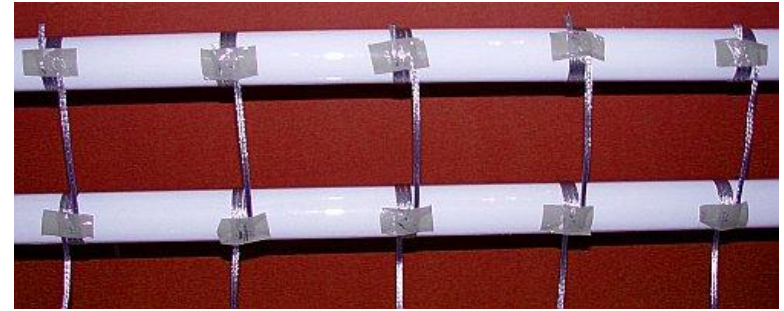
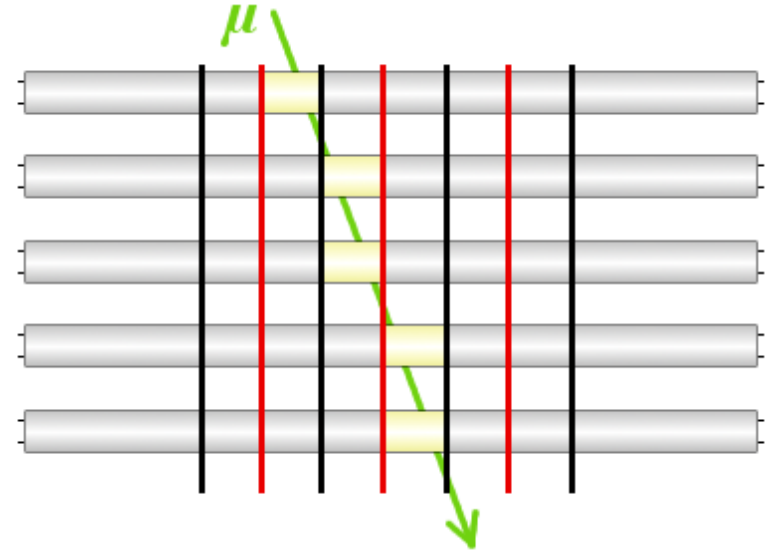
Henry Morton Stanley, How I found Livingstone.
Kessinger Publishing, LLC (May 23, 2010) ISBN-13: 978-1161435436.
First entered according to act of Congress, in the year, 1874.
(Gift-wrap available.)

Some fun with muons (before we have to be serious again and do what we were **P**resumed **I**n **D**oing).

Simple Do-It-Personally (**DIP**) "Spark Chamber"

Place at least 2 tubes above each other, wrap wire meshwork around each tube and pass the wire on to the next tube, wrap the wire around the tube again etc. as outlined in the schematic and connect the wires to the high voltage supply (**black** = GND; **red** = **high voltage**=100V to about 1000V DC).

- Use thick tubes (38mm diameter) - the 26mm type don't seem to work
- Also the length of the tube is critical: try to get at least 1200mm long tubes
- If you get old tubes from a recycling centre, check if they are for visible light.



This experiment was brought to you by

CosmicRays.org

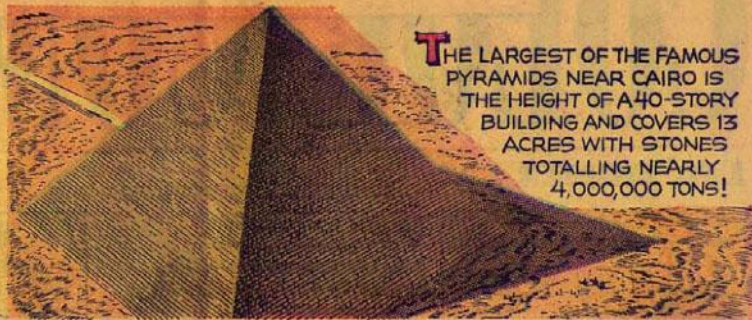
[Join the Particle Detector - Maillist now!](#)

Based on an experiment performed by Sascha Schmeling et al. in 2000 at CERN

(Be careful with HV! Be very careful with HV! Be extremely careful with HV!)

OUR NEW AGE

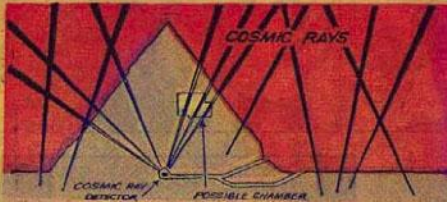
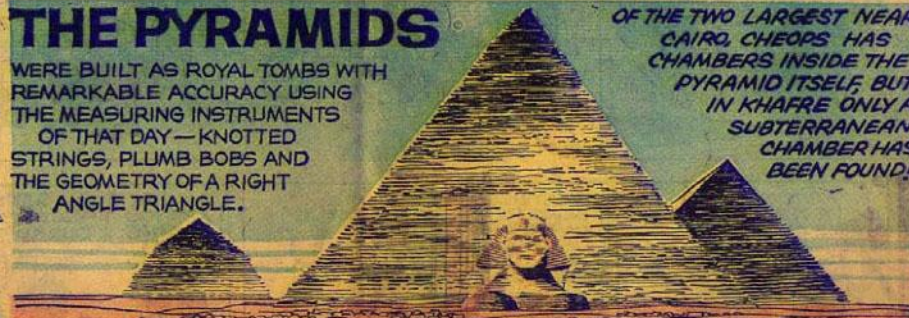
—by—
ATHELSTAN SPILHAUS
DEAN, UNIVERSITY OF MINNESOTA
INSTITUTE OF TECHNOLOGY



THE PYRAMIDS

WERE BUILT AS ROYAL TOMBS WITH REMARKABLE ACCURACY USING THE MEASURING INSTRUMENTS OF THAT DAY — KNOTTED STRINGS, PLUMB BOBS AND THE GEOMETRY OF A RIGHT ANGLE TRIANGLE.

OF THE TWO LARGEST NEAR CAIRO, CHEOPS HAS CHAMBERS INSIDE THE PYRAMID ITSELF, BUT IN KHAFRE ONLY A SUBTERRANEAN CHAMBER HAS BEEN FOUND!



PROFESSOR ALVAREZ OF BERKELEY SUSPECTS THERE ARE OTHER HOLLOW VAULTS AND WILL USE A SPARK CHAMBER IN THE SUBTERRANEAN PASSAGE TO X-RAY THE PYRAMID WITH INCOMING COSMIC RAYS.

THE SPARK CHAMBER HAS TWO PLATES, ONE ABOVE THE OTHER, TO RECORD DIRECTION AS WELL AS INTENSITY. RAYS COMING THROUGH A HOLLOW WILL BE MORE INTENSE THAN THOSE ABSORBED BY SOLID ROCK.



Pyramid Internal Discovery with Muons.



Lawrence Berkeley Laboratory

University of California
Berkeley, California 94720
Telephone 415/843-2740

August 2, 1978

Senorita Linda Manzanilla
Cerro Del Agua No. 106
Mexico 21, D. F.
Mexico

Dear Senorita Manzanilla:

I have not been working in Egypt for the last several years, so it won't be possible for you to be with me in Giza, in the near future.

I am enclosing some printed material on the work that my colleagues and I did at Giza, and I can say that since those things were published, we completed a survey of the Second Pyramid, pointing our cosmic ray telescope in six or seven different compass directions, tilted each time at 45 degrees above the horizon. We also repeated the vertical scan that is described in the material I am sending you. The results of all this is that we found the pyramid to be quite solid, with no chambers comparable in size to those found above the plateau level, in the Great Pyramid.

Very sincerely,

Luis W. Alvarez

Luis W. Alvarez

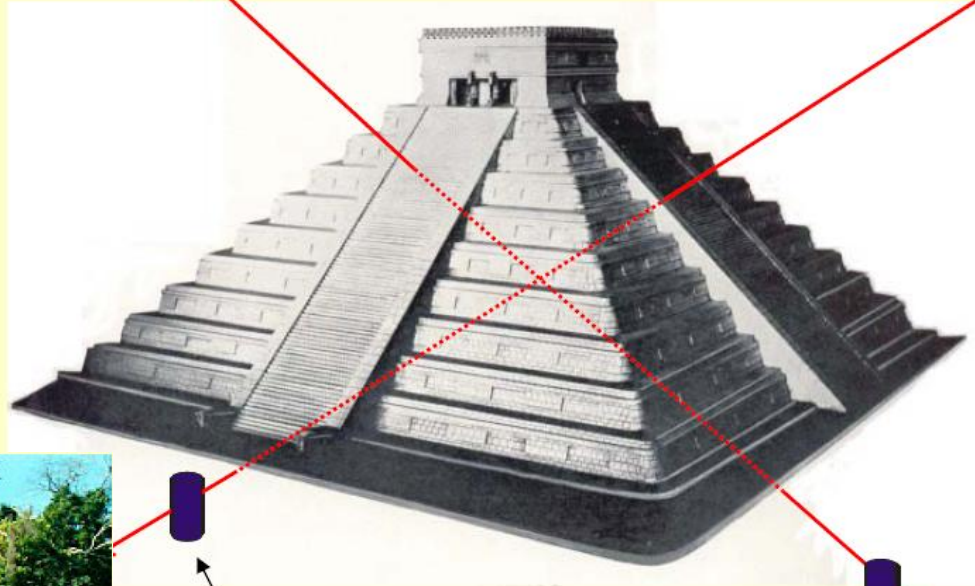
LWA/lb
Encls.

Roy Schwitters
et al.,

Mayan Muons
and
Unmapped Rooms

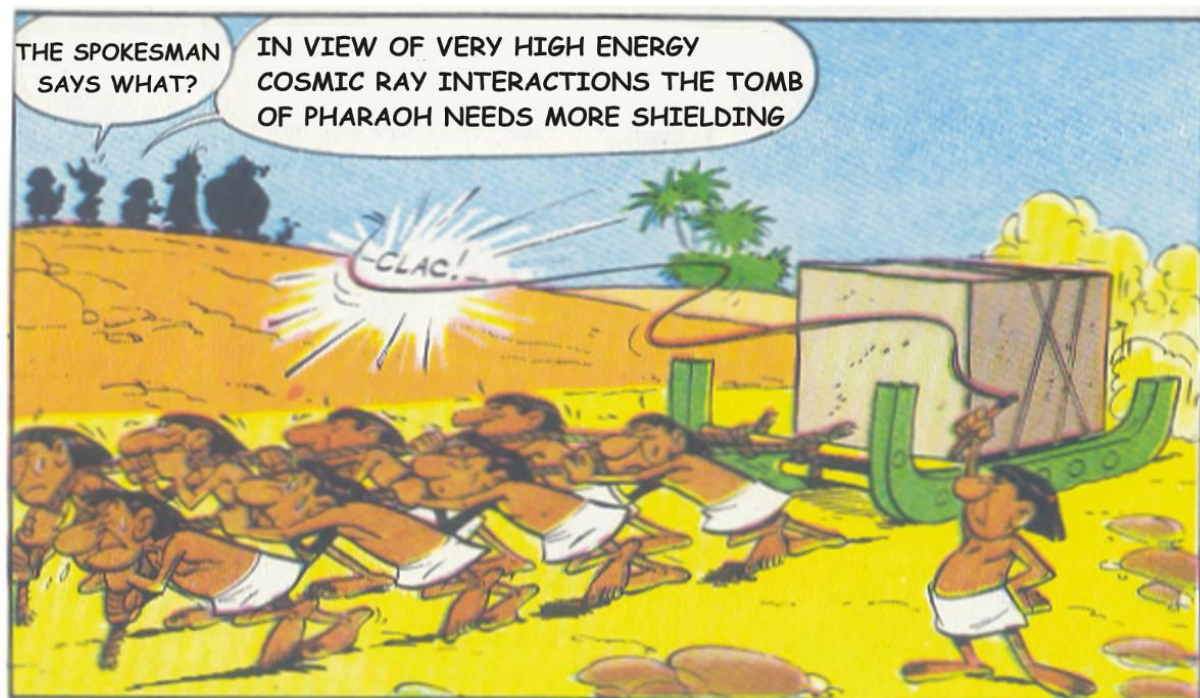
What is the internal structure?

Measure Spatial Distribution of Material *Inside*
by Muon Tomography



Underground Muon Detectors





Definitely not for the faint of heart:

Muon Radiography of Active Volcanoes with Pointlike Ionisation Detectors



H. K. M. Tanaka et al., Development of an emulsion imaging system for cosmic-ray muon radiography to explore the internal structure of a volcano, Mt. Asama, *Nucl. Instr. Meth. A*, 575, 489–497, 2007a

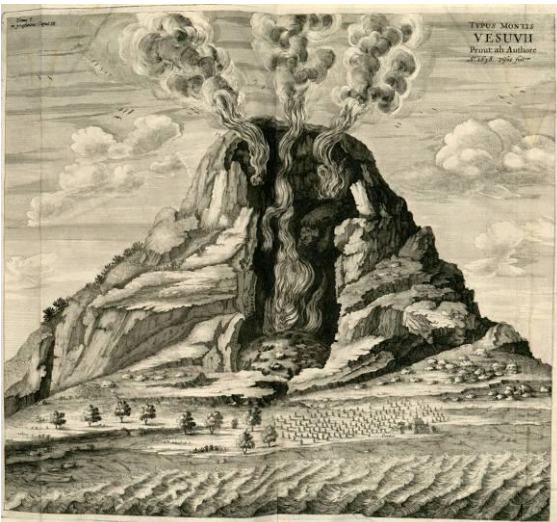
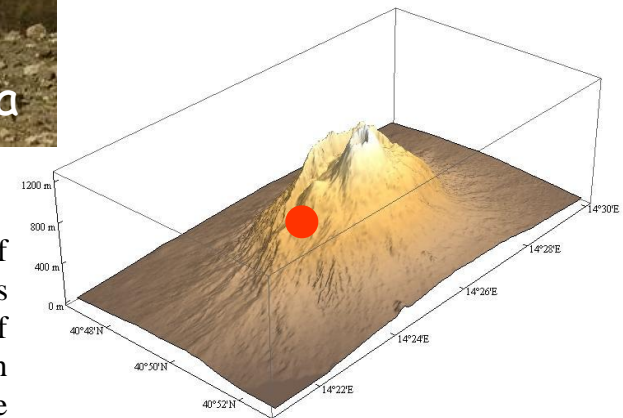


Illustration of mount Vesuvius as seen by the author in 1638 (the 1631 eruption). From Athanasius' Kircher *Mundus Subterraneus*, 1664

Mt. Vesuvius:

The full detector will be formed by a sequence of detector planes, to form what in Particle Physics is called a “telescope”. A telescope is capable of measuring position and angle of particles, of which for muon radiography only the angle matters as the detector is essentially pointlike with respect to the mountain. We aim at an angular resolution of the order of 15 mrad, which at e.g. 1 km distance projects to a 15 m spatial resolution in the determination of internal structures. The deterioration of the spatial resolution due to the multiple scattering in the rock will have to be estimated.

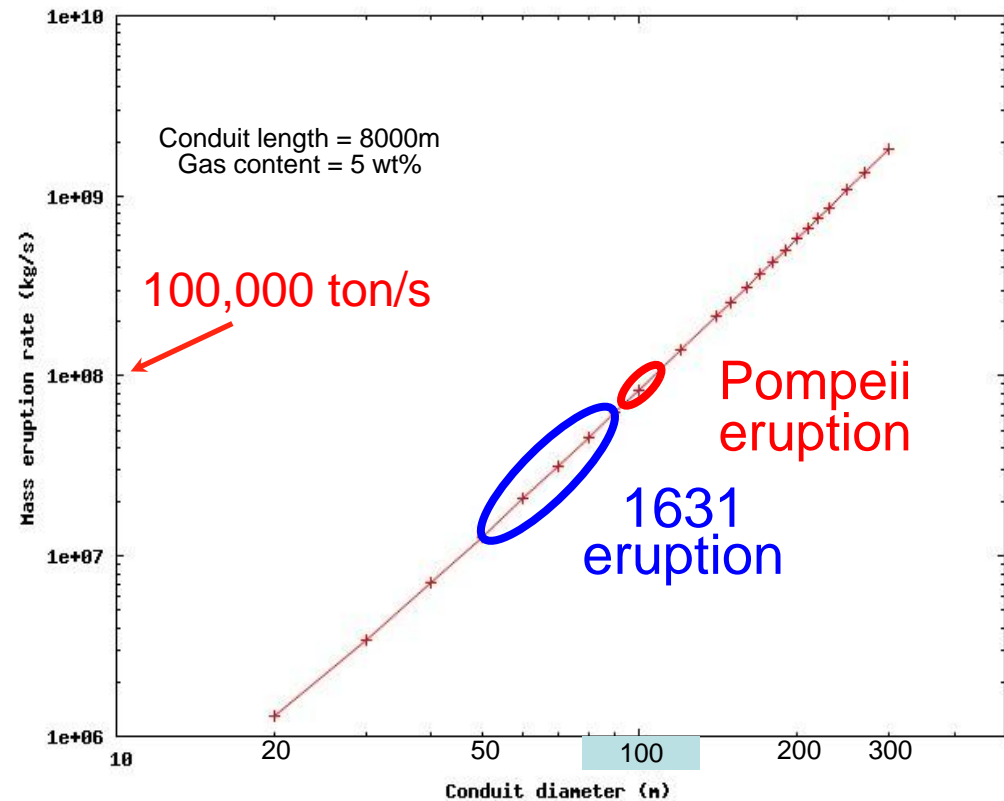
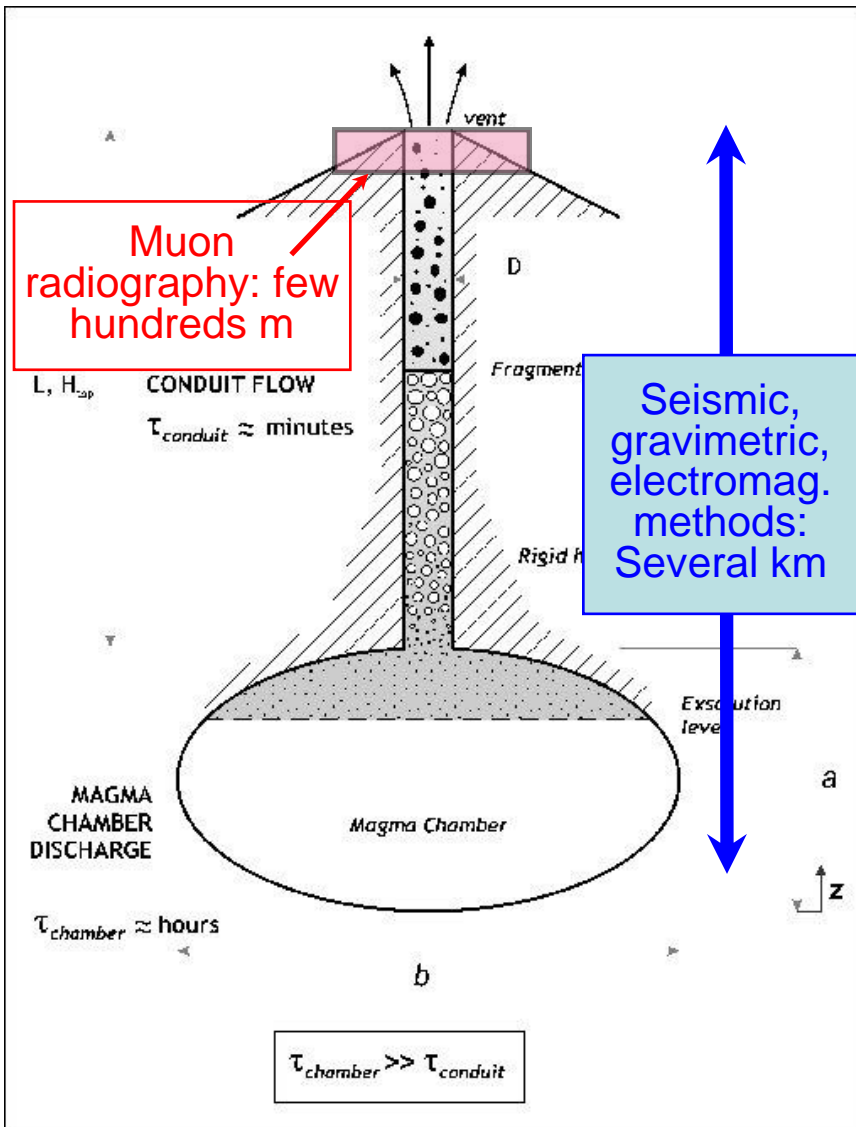


The 3D Digital Elevation Map of the complex Mt. Vesuvius - Mt. Somma and the location (•) of the Vesuvian Observatory.

<http://people.na.infn.it/~strolin/MU-RAY.pdf>

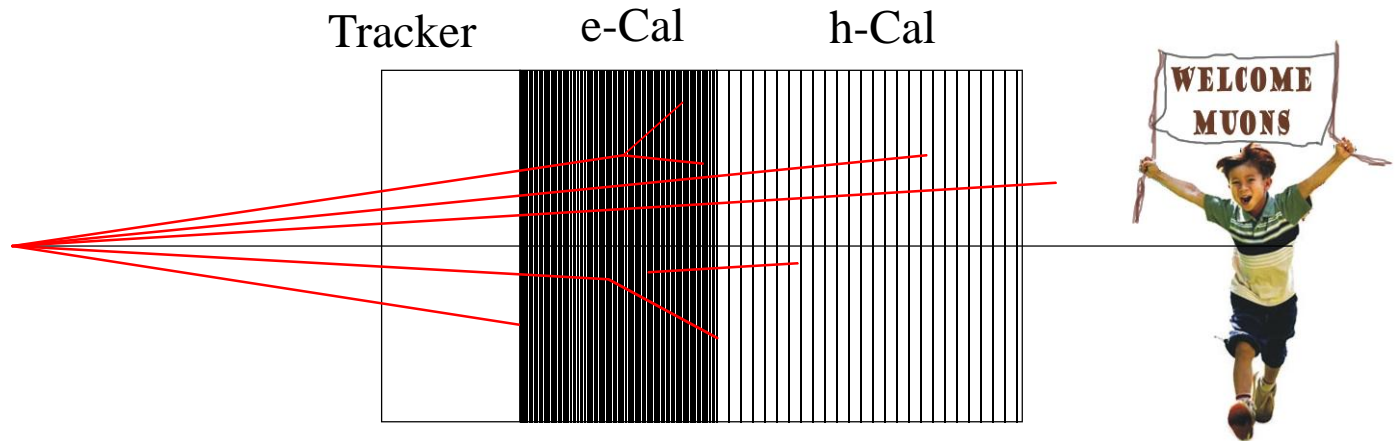
The eruption dynamics mostly depends on:

- Gas content
- Chemical composition of magma
- Conduit dimensions and shape



Very important to measure the conduit diameter to foresee how the next eruption will be. (the when can not be treated here)

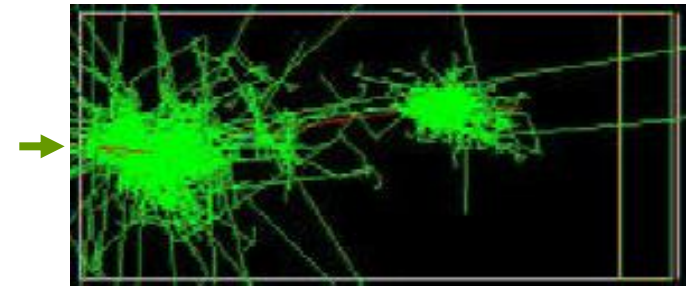
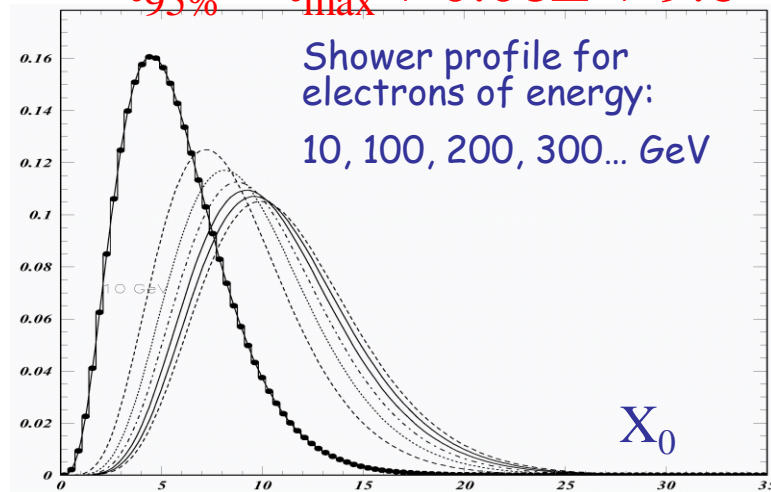
Whatever is left
after the
calorimeters.
(Just a reminder.)



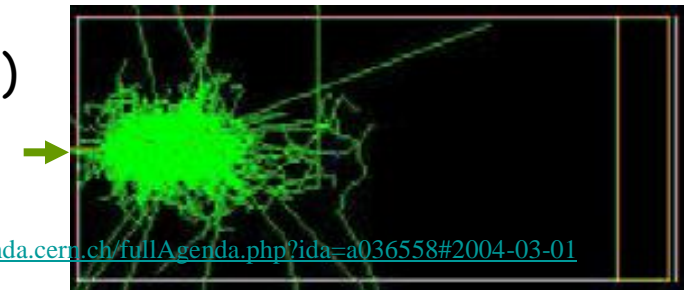
Hadronic Showers (π , n, p, ...)
Propagation :
inelastic hadron interactions
→ multi particle production
Nuclear disintegration

Longitudinal containment:

$$t_{95\%} = t_{\max} + 0.08Z + 9.6$$



20 GeV π
in copper
(simulation)

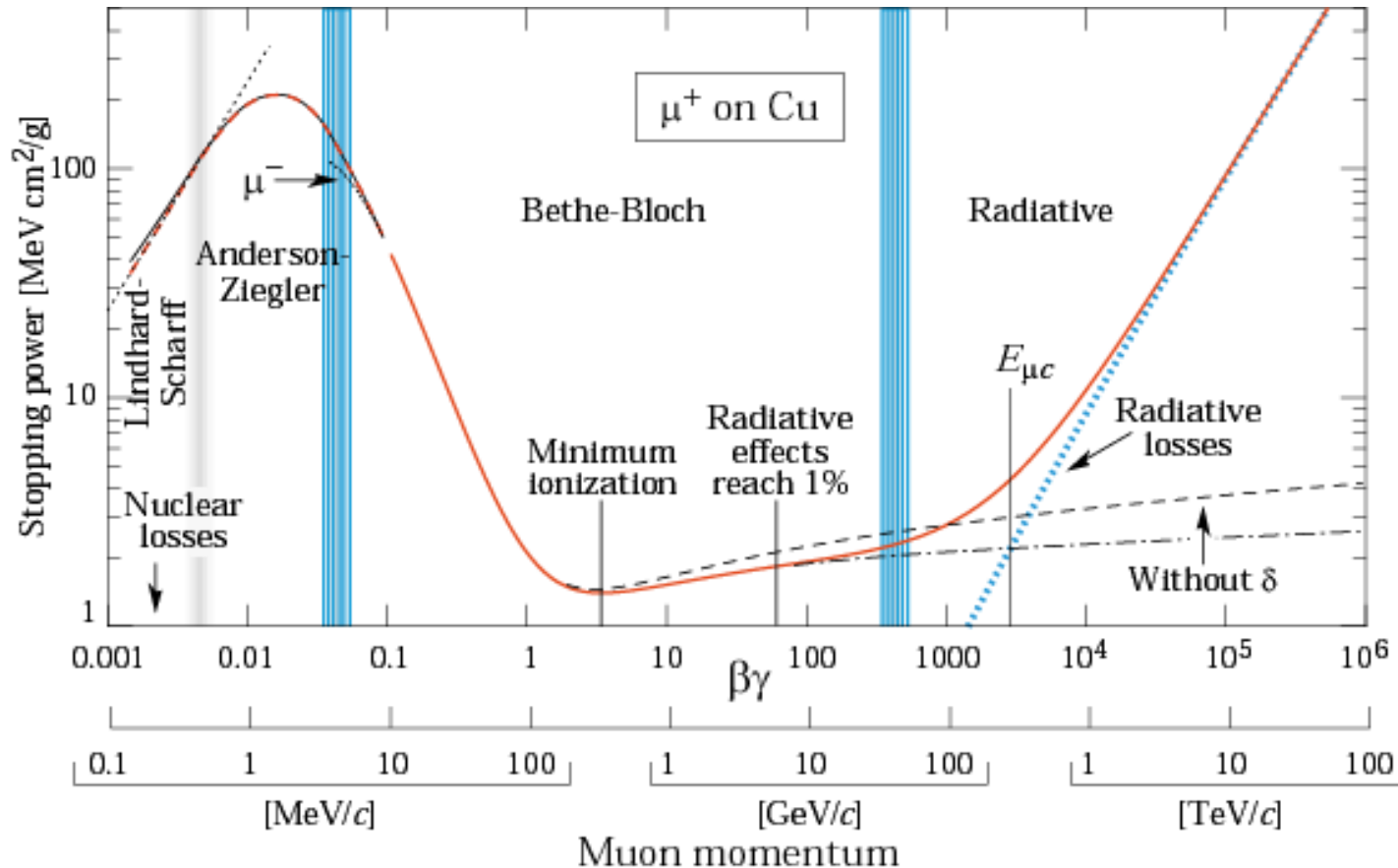


A μ has the following properties:

Charge _____ $+/-1$
 Mass _____ 105.658367 MeV
 Lifetime _____ $2.197019 \mu\text{s}$
 Decay (H100%) _____ $e^- \bar{\nu}_e \nu_\mu$
 No strong interaction

For our purpose:

If the charged particle penetrates large amount of absorber with minor energy losses and small angular displacement such a particle is considered a muon.



If $p_\mu < 100 \text{ GeV}/c$
 energy loss mainly
 ionisation

If $p_\mu > 200 \text{ GeV}/c$
 the μ behaves like
 an electron.
 Electromagnetic
 showers along the
 track.

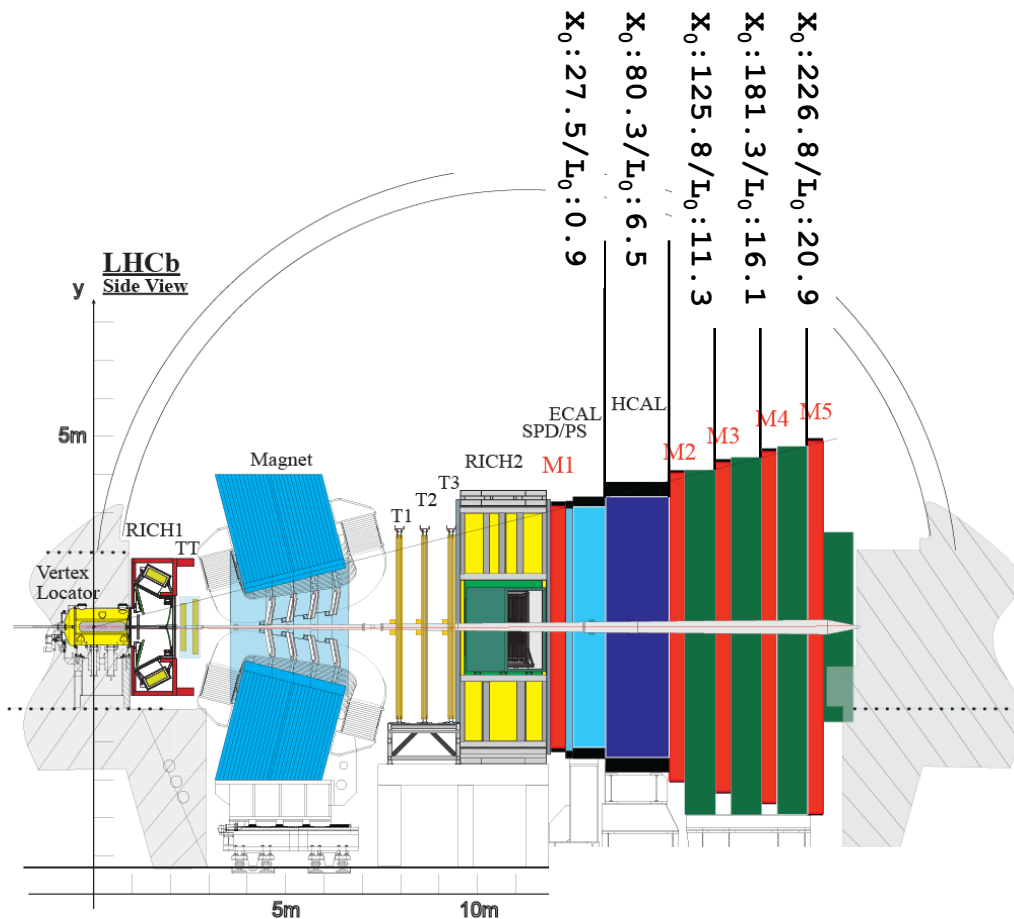
Stopping power ($\equiv \langle dE/dx \rangle$) for positive muons in copper as a function of $\beta\gamma = p/Mc$

Material in the muon arm of the LHCb experiment.

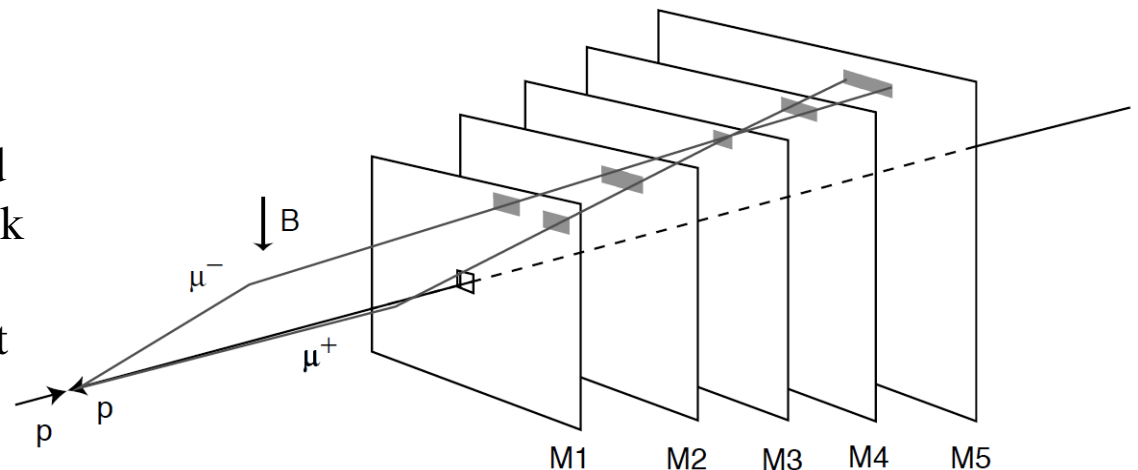
Will follow:

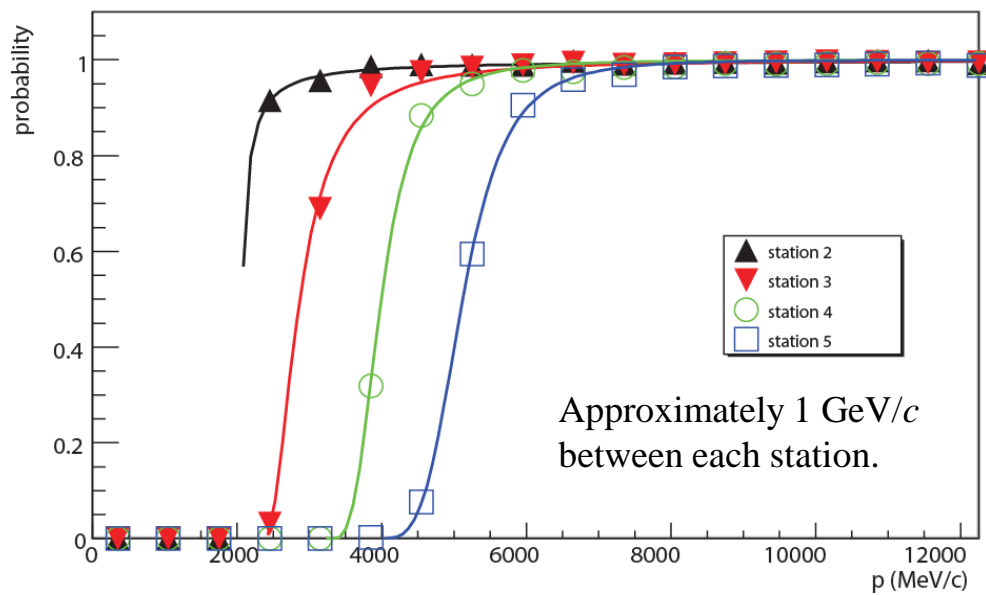
G. Lanfranchi et al., LHCb-PUB-2009-013

X.C. Vidal, Muon Identification in the LHCb experiment, Rencontres de Moriond EW 2010



The μ ID hypothesis is calculated starting from a reconstructed track and looking for hits in the muon stations, within a Field of Interest (FOI), around the track extrapolation direction.





The efficiency of a muon algorithm can be strongly dependent on small variations of the performance of the detector

and the fine-tuning can be very much dependent on the specific sample used to calibrate it.

One can then make a practical loose decision function:

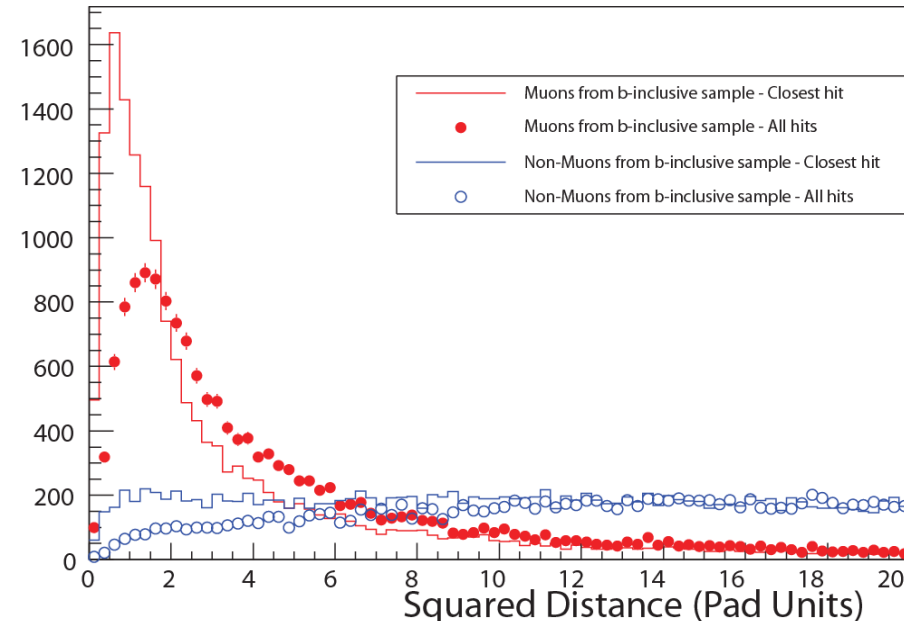
If $3 < p(\text{GeV}/c) < 6$ then at least 1 hit in at least 2 stations of M2, M3, M4

$p > 6$ then at least 1 hit in at least 3 stations of M2, M3, M4, M5

and define a proximity variable, D , as:

$$D = \frac{1}{N} \sum_{i=0}^N \left\{ \left(\frac{x_{\text{closest},i} - x_{\text{track}}}{\text{pad}_x} \right)^2 + \left(\frac{y_{\text{closest},i} - y_{\text{track}}}{\text{pad}_y} \right)^2 \right\}$$

where i runs over the fired stations



If we measure the quantity $D=D_0$ in the region R for a track of momentum p , and the probability density function, $pdf=P$, is correctly normalised, then

$$P_{\mu,h}(D_0) = \int_0^{D_0} P_{\mu,h}(p,R,D) dD$$

gives directly the probability that a track with a given (p,R,D_0) is a muon or a non-muon.

We then build from the probabilities

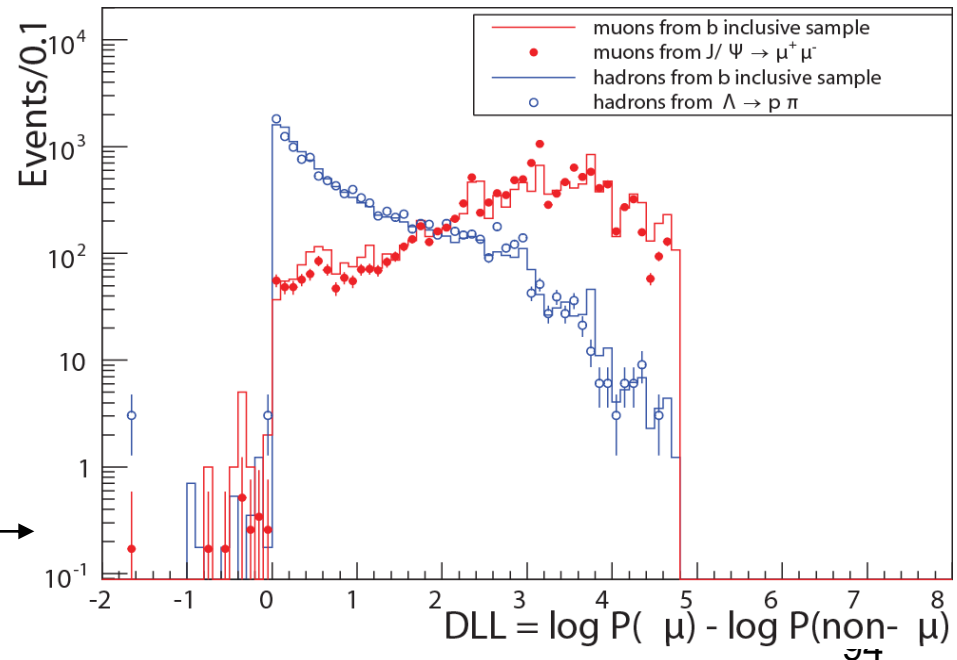
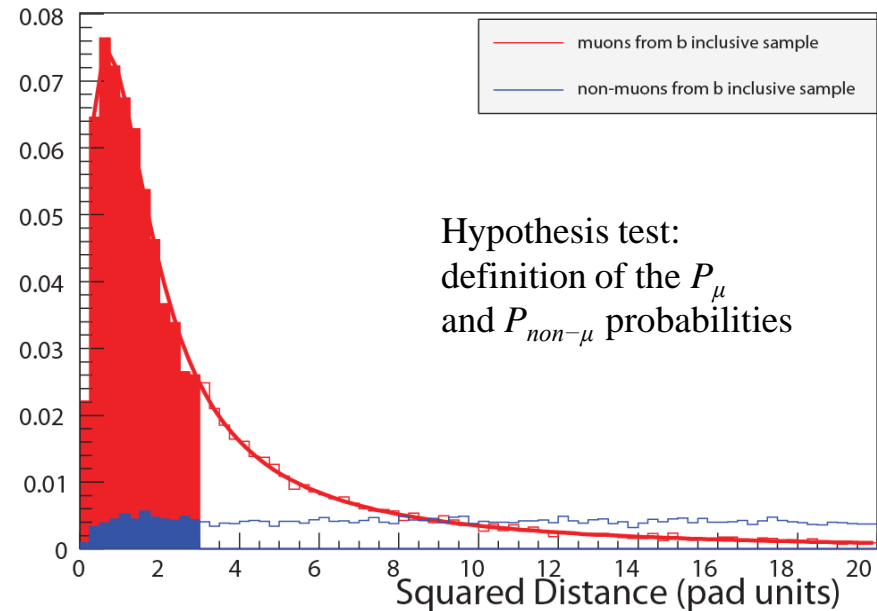
Is-Muon: P_{μ}

Is-non-Muon: $P_{non-\mu}$

the Delta Log Likelihood

$$DLL = \log(P_{\mu} / P_{non-\mu})$$

The distributions obtained from a *b-inclusive sample* are overlaid with the ones obtained from the calibration samples $J/\Psi \rightarrow \mu\mu$ and $\Delta \rightarrow p\pi$.



Add a magnet for better discrimination:

dipole magnets in fixed target or solenoid magnets in colliders:

- some m^3 in volume
- field $\sim 2\text{T}$

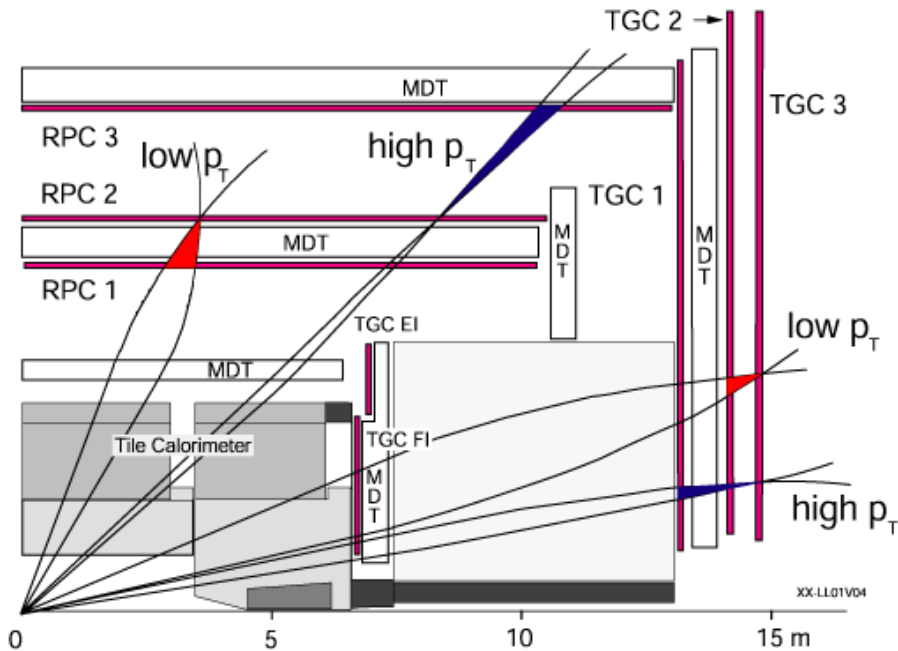
magnetized iron toroids:

- hundreds m^3 volume
- saturation at $\sim 2\text{T}$

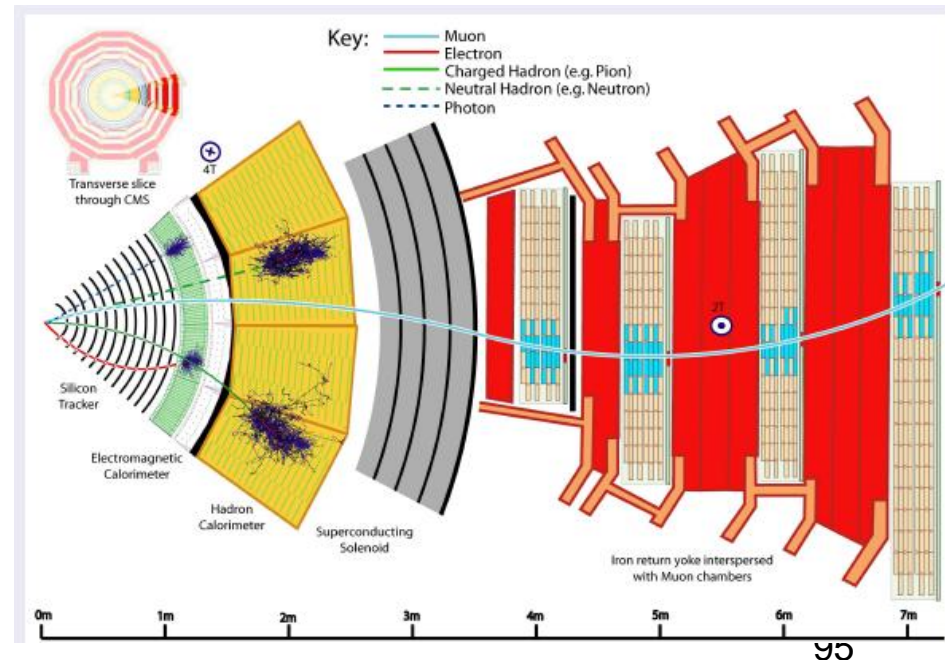
air core super conducting magnets:

- field similar to iron magnets
- no multiple scattering

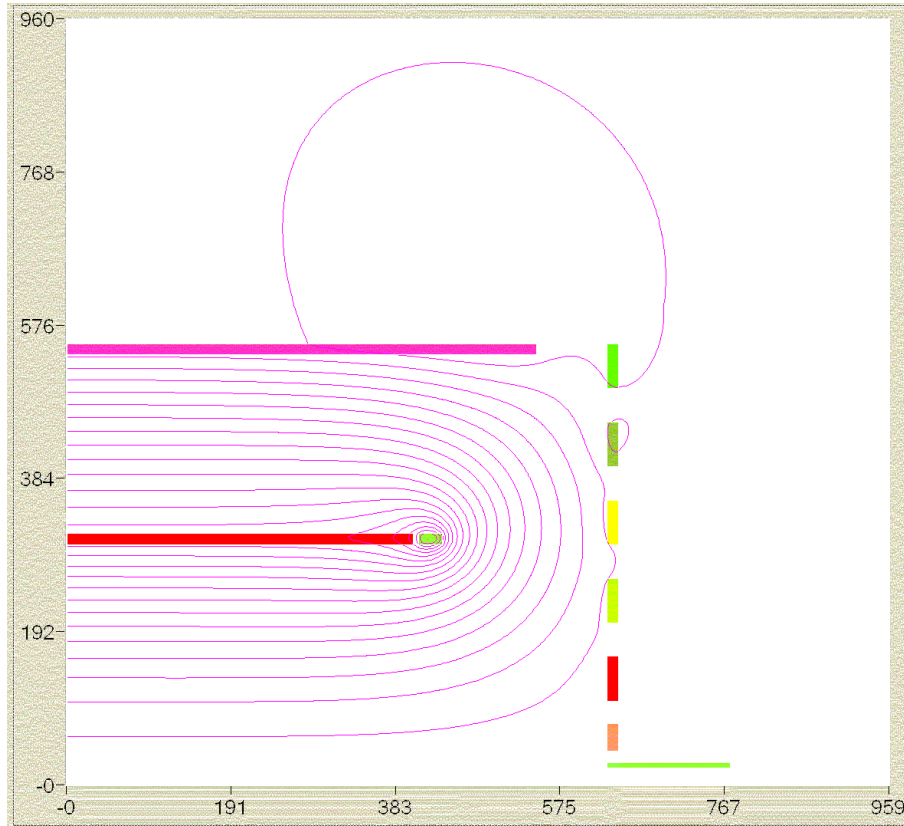
ATLAS: Toroidal magnetic Field



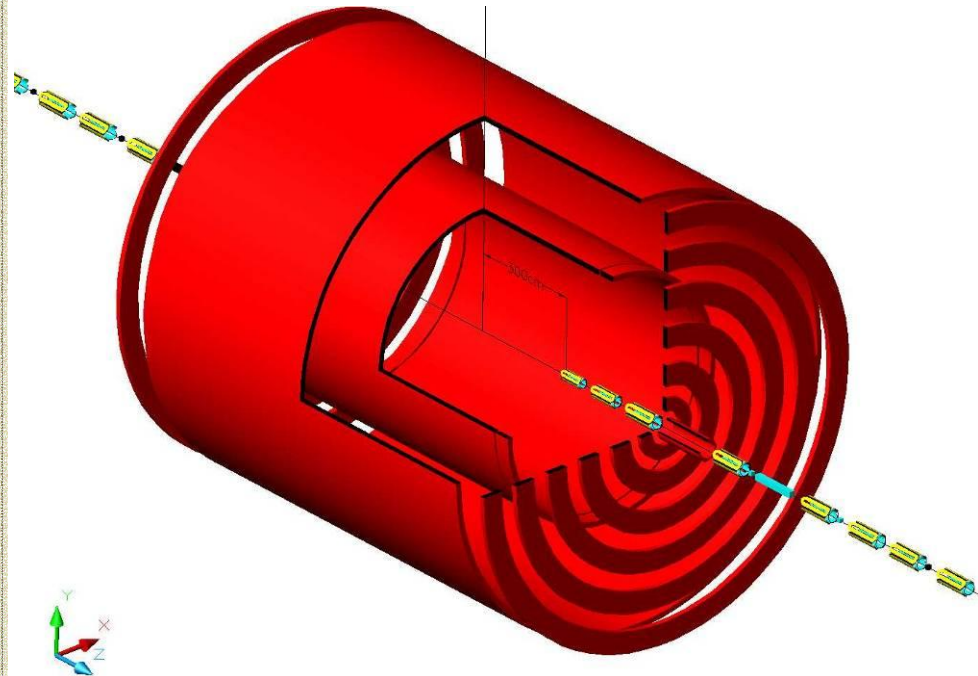
CMS: Solenoidal magnetic Field



Or - throw out the muon arm altogether and work with high resolution calorimeters and trackers which will/(might) give the required separation power.



4th Concept detector showing the dual solenoids. The annulus between the solenoids is filled with cluster counting wires inside precision tubes.



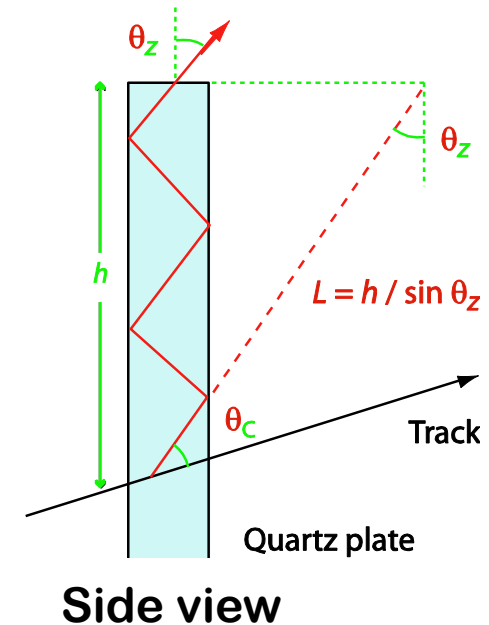
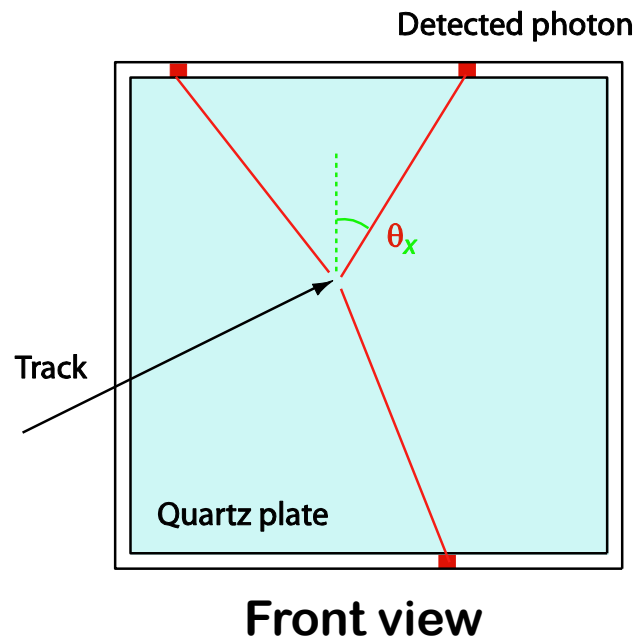
J. Hauptman, *Muon Identification without Iron*, LCWS/ILC2007

Test beam data for the calorimeter and calculations for the magnetic fields and the track reconstruction. For isolated tracks, the rejection of pions against muons ranges from 10^3 at 20 GeV/c to 10^5 at 300 GeV/c.

<http://www.4thconcept.org/>

TORCH concept

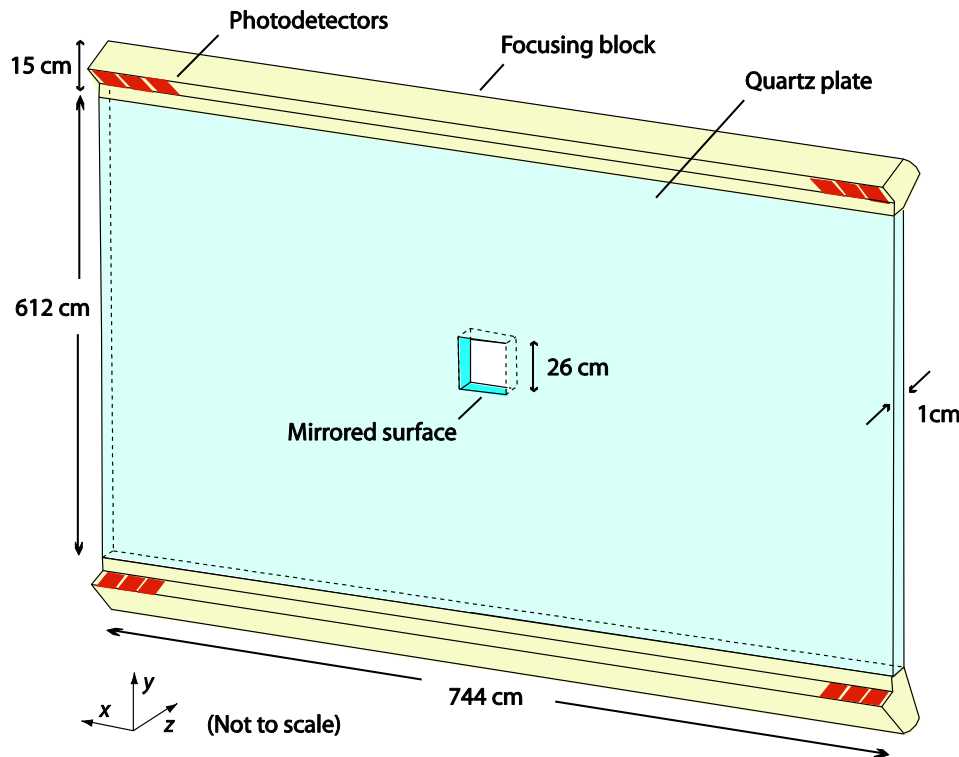
- I am currently working on the design of a new concept for Particle ID for the upgrade of LHCb (planned to follow after ~ 5 years of data taking)
- Uses a large plate of quartz to produce Cherenkov light, like a DIRC
But then identify the particles by measuring the photon arrival times
Combination of **TOF** and **RICH** techniques \rightarrow named TORCH
- Detected position around edge gives photon angle (θ_x)
Angle (θ_z) out of plane determined using focusing
Knowing photon trajectory, the track arrival time can be calculated



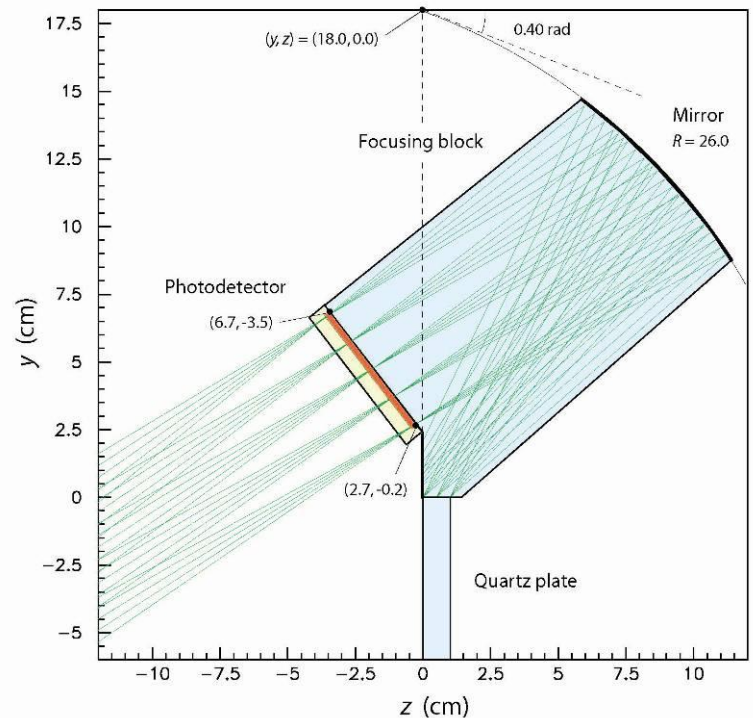
Proposed layout

- Optical element added at edges to focus photons onto MCP detectors
It converts the angle of the photon into a position on the detector

Schematic layout

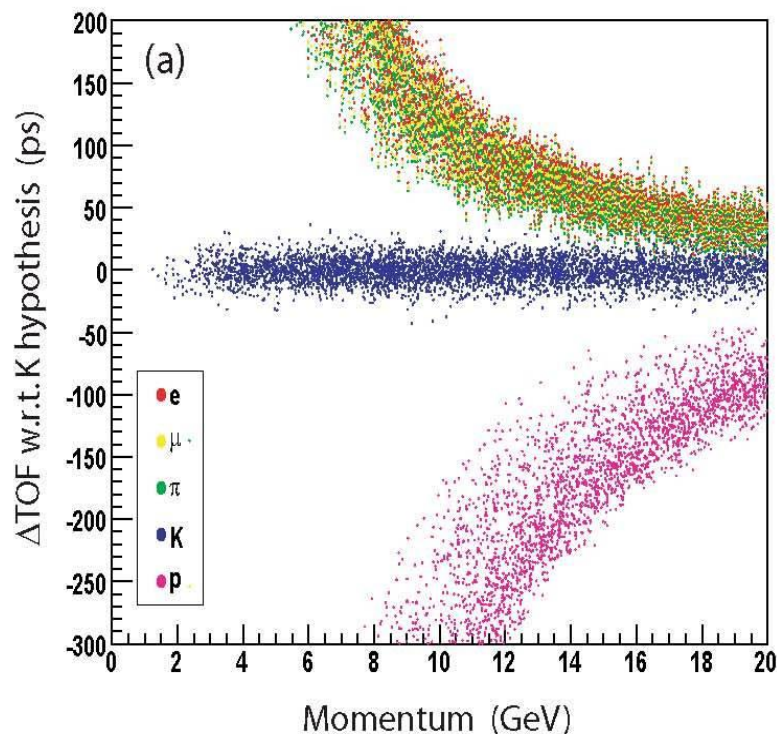
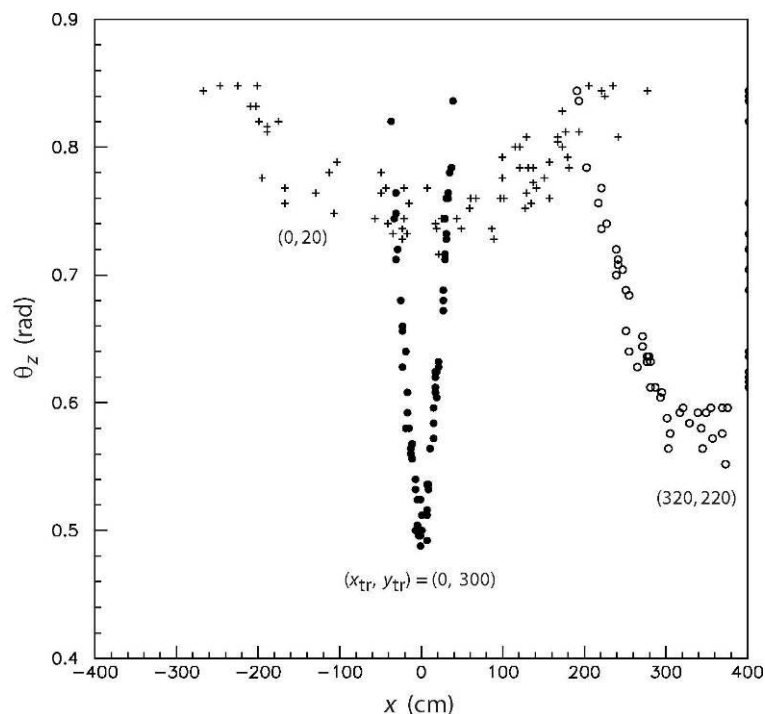


Focusing element

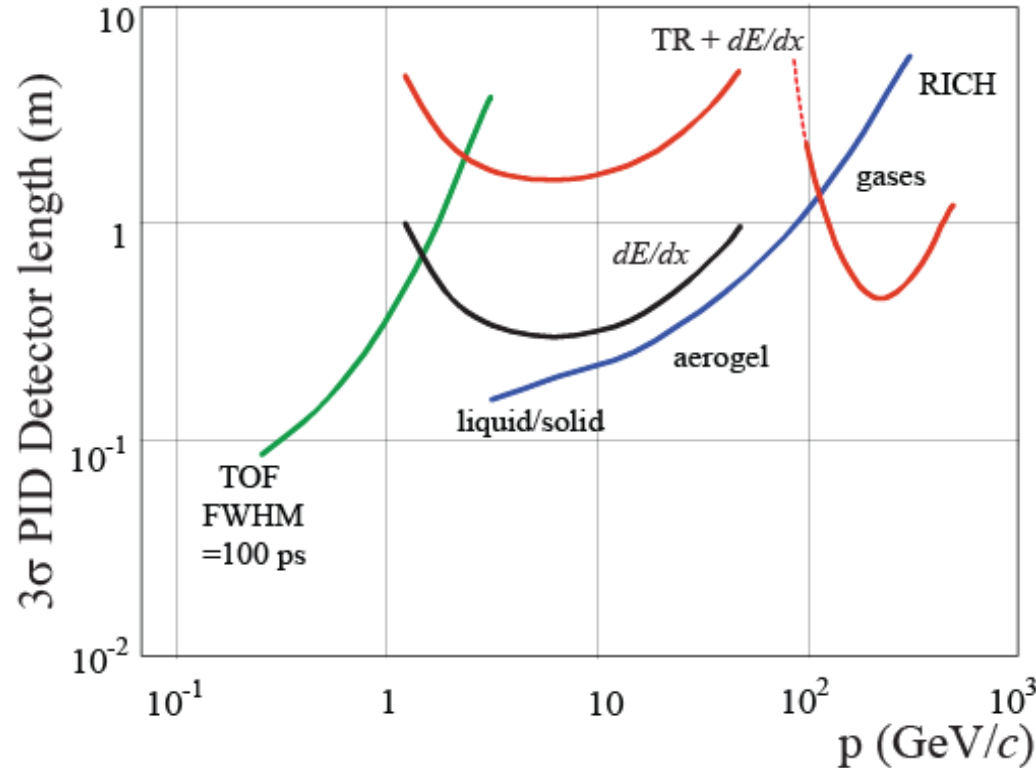


Predicted performance

- Pattern recognition will be a challenge, similar to a DIRC
- Assuming a time resolution per detected photon of 50 ps, the simulated performance gives 3σ K- π separation up to > 10 GeV
Will need to be confirmed with an R&D program using test detectors



Conclusion



Pion-Kaon separation by different PID methods: the length of the detectors needed for 3 sigma separation.

B. Dolgoshein, Complementary particle ID: transition radiation and dE/dx relativistic rise, Nucl. Instrum. Methods Phys. Res., A : 433 (1999) 533

Particle Identification over a large momentum range is possible, but might require the use of all the tools in the box.

Some ingenuity in addition will always be helpful.

A little thinking might also come in handy, (to quote Einstein).



©2007 by King Features Syndicate, Inc. World rights reserved.

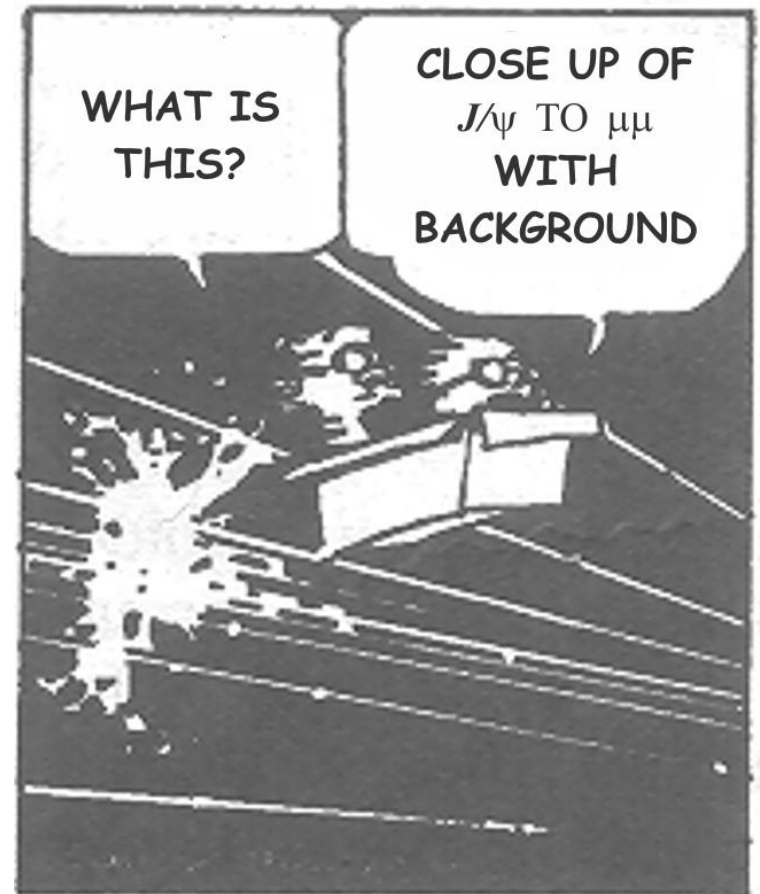


This is **THE END** of the lecture.

Thank you for your attention!

at least I have had a good time.

Spare slides and back-ups



Kolmogorov-Smirnov tests

There is more to it than what is written here!

Frodesen et al., probability and statistics in particle physics, 1979

Assume a sample of n uncorrelated measurements x_i . Let the series be ordered such that $x_1 < x_2 < \dots$. Then the cumulative distribution is defined as:

$$S_n(x) = \begin{cases} 0 & x < x_1 \\ i/n & x_i \leq x < x_{i+1} \\ 1 & x \geq x_n \end{cases}$$

The theoretical model gives the corresponding distribution $F_0(x)$

The null hypothesis is then $H_0: S_n(x) = F_0(x)$

The statistical test is: $D_n = \max |S_n(x) - F_0(x)|$

Example

In 30 events measured proper flight time of the neutral kaon in $\bar{K}^0 \rightarrow \pi^+ e^- \nu$

which gives: $D_{30} = \max |S_{30}(t) - F_0(t)| = 0.17$

or ~50% probability

The same observations by χ^2 method.

n observations of x belonging to N mutually exclusive classes. $H_0: p_1 = p_{01}, p_2 = p_{02}, \dots, p_N = p_{0N}$ for $\sum p_{0i} = 1$

Test statistic:

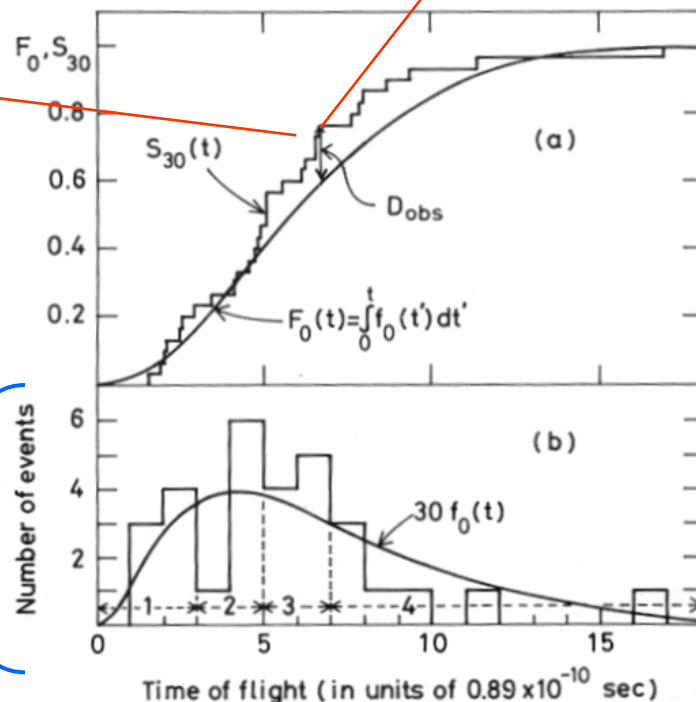
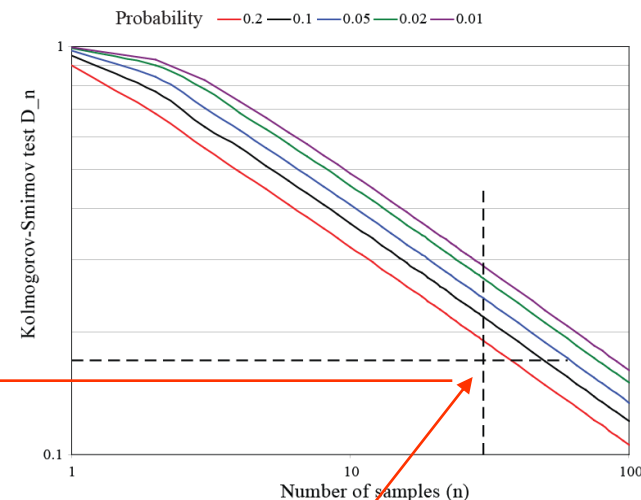
$$X^2 = \sum_{i=1}^N \frac{(n_i - np_{0i})^2}{np_{0i}} = \frac{1}{n} \sum_{i=1}^N \frac{n_i^2}{p_{0i}} - n$$

when H_0 is true, this statistic is approximately

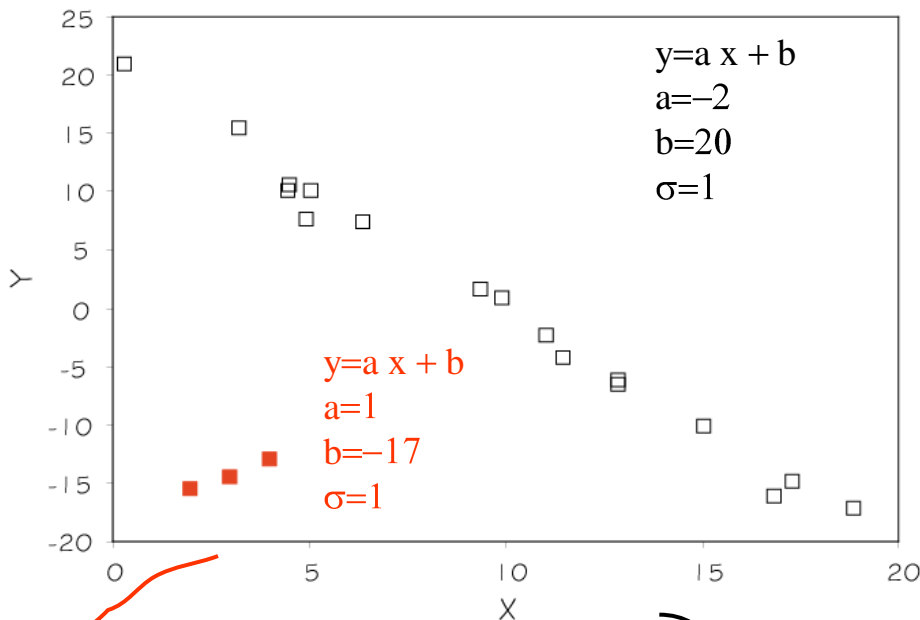
χ^2 distributed with $N-1$ degrees of freedom.

$\chi^2(obs) = 3.0$ with 3 degrees of freedom

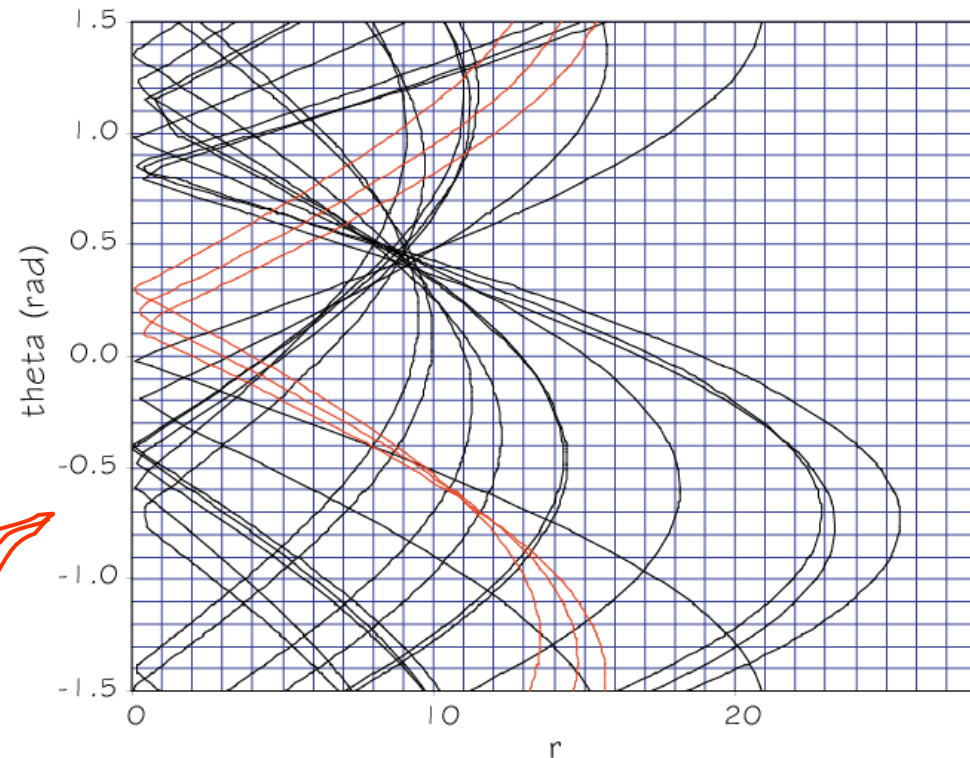
or probability of about 0.40



The Hough transform is a technique which can be used to isolate features of a particular shape within an image. The Hough technique is particularly useful for computing a global description of a feature(s) (where the number of solution classes need not be known *a priori*), given (possibly noisy) local measurements. The motivating idea behind the Hough technique for line detection is that each input measurement (*e.g.* coordinate point) indicates its contribution to a globally consistent solution (*e.g.* the physical line which gave rise to that image point).



$x \cos\Theta + y \sin\Theta = r$
 This *point-to-curve*
 transformation is the
 Hough transformation
 for straight lines



Ring Finding with a Markov Chain. ---

Sample parameter space of ring position and size by use of a Metropolis Metropolis-Hastings Markov Chain Monte Carlo (MCMC)

Interested people should consult:

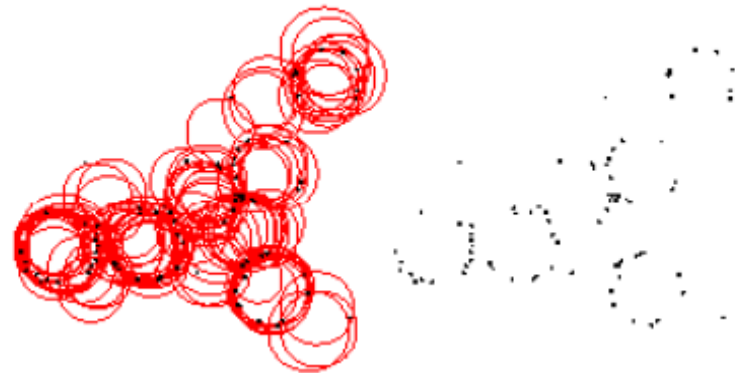
C.G. Lester, *Trackless ring identification and pattern recognition in Ring Imaging Cherenkov (RICH) detectors*, NIM A 560(2006)621-632

<http://lhcb-doc.web.cern.ch/lhcb-doc/presentations/conferencetalks/postscript/2007presentations/G.Wilkinson.pdf>

G. Wilkinson, *In search of the rings: Approaches to Cherenkov ring finding and reconstruction in high energy physics*, NIM A 595(2008)228

W. R. Gilks et al., *Markov chain Monte Carlo in practice*, CRC Press, 1996

Example of 100 new rings *proposed* by the “three hit selection method” for consideration by the MHMC for possible inclusion in the final fit. The hits used to seed the proposal rings are visible as small black circles both superimposed on the proposals (left) and on their own (right).



It is not about Markov chain, but have a look in

M.Morháč et al., Application of deconvolution based pattern recognition algorithm for identification of rings in spectra from RICH detectors, Nucl.Instr. and Meth.A(2010),doi:10.1016/j.nima.2010.05.044

Kalman filter

The Kalman filter is a set of mathematical equations that provides an efficient computational (recursive) means to estimate the state of a process, in a way that minimizes the mean of the squared error.

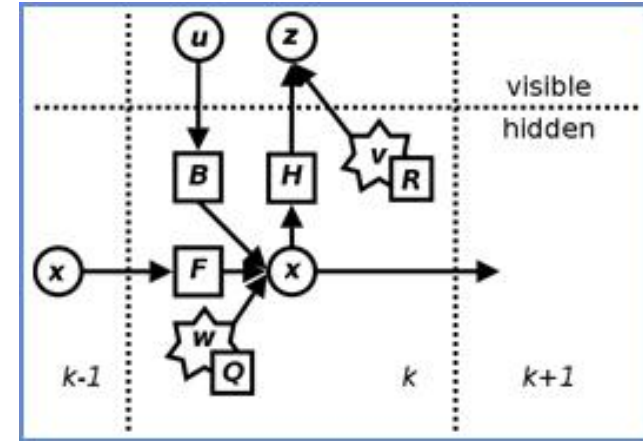
The filter is very powerful in several aspects:

it supports estimations of past, present, and even future states, and it can do so even when the precise nature of the modelled system is unknown.

http://www.cs.unc.edu/~welch/media/pdf/kalman_intro.pdf

iweb.tntech.edu/fhossain/CEE6430/Kalman-filters.ppt

R. Frühwirth, M. Regler (ed), Data analysis techniques for high-energy physics, Cambridge University Press, 2000



07/10/2009

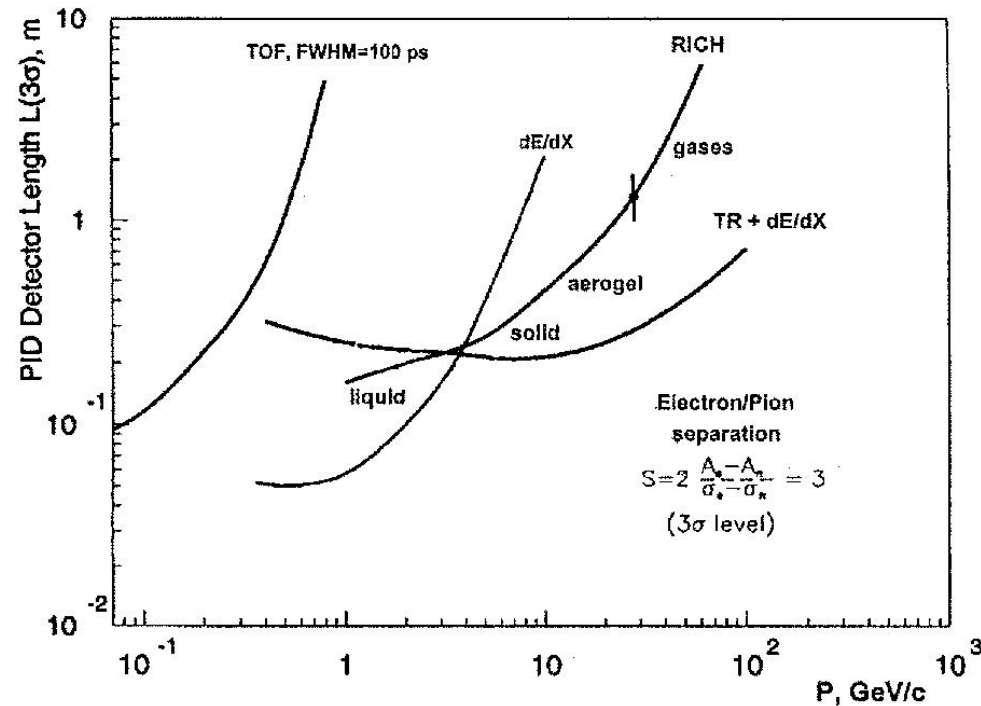
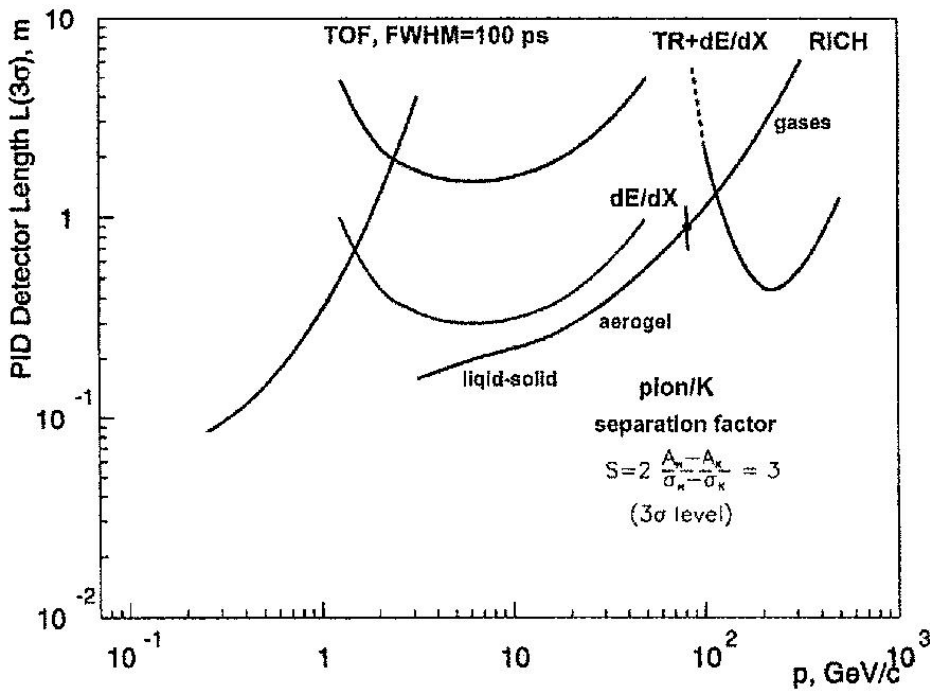
US President Barack Obama presents the National Medal of Science to **Rudolf Kalman** of the Swiss Federal Institute of Technology in Zurich during a presentation ceremony for the 2008 National Medal of Science and the National Medal of Technology and Innovation October 7, 2009 in the East Room of the White House in Washington, DC.

2008

Academy Fellow **Rudolf Kalman**, Professor Emeritus of the Swiss Federal Institute of Technology in Zurich, has been awarded the Charles Stark Draper Prize by the National Academy of Engineering. The \$500,000 annual award is among the engineering profession's highest honors and recognizes engineers whose accomplishments have significantly benefited society. Kalman is honored for "the development and dissemination of the optimal digital technique (known as the Kalman Filter) that is pervasively used to control a vast array of consumer, health, commercial, and defense products."

106

Pion-Kaon separation for different PID methods.
The length of the detectors needed for
 3σ separation.



The same as above, but for
electron-pion separation.

